Dissertation

with the aim of achieving the degree

doctor rerum naturalium

Structural requirements for transport and subunit interactions of the GlcNAc-1-phosphotransferase complex

submitted by

Raffaella De Pace

from Mottola (TA) Italy

at the Department of Biology,

Faculty of Mathematics, Informatics and Natural Sciences,

University of Hamburg

2014 in Hamburg

Academic advisor:	Prof. Dr. rer. nat. Thomas Braulke
Co-advisor:	Prof. Dr. rer. nat. Matthias Kneussel
Date of disputation:	12. December 2014

To my family

1 Introduction 1
1.1 Protein synthesis and modifications in the ER 1
1.2 Protein trafficking from the ER to the Golgi apparatus 2
1.3 Protein trafficking from the Golgi apparatus to lysosomes 3
1.4 The GlcNAc-1-phosphotransferase complex 5
1.4.1 Function of the GlcNAc-1-phosphotransferase 5
1.4.2 Structure of the GlcNAc-1-phosphotransferase complex 6
1.4.3 Synthesis and posttranslational modifications of the GlcNAc-1-phosphotransferase 7
1.4.4 Transport of the GlcNAc-1-phosphotransferase to the Golgi apparatus and proteolytic activation 10
1.4.5 GlcNAc-1-phosphotransferase-related diseases 11
1.5 Aims of the study 13
2 Materials and Methods 14
2.1 Materials 14
2.1.1 Chemicals, equipments and consumables 14
2.1.2 Expression constructs 17
2.1.3 DNA ladders and protein standards 19
2.1.4 Kits 19
2.1.5 Enzymes 19
2.1.6 Oligonucleotides 20
2.1.7 Antibodies 21
2.1.8 Cell lines 22
2.1.9 Media and solutions for cell culture 22
2.1.10 Electronic data processing 22
2.2 Cell biology methods 23
2.2.1 Cell culture 23
2.2.2 Double immunofluorescence microscopy 24
2.2.3 [^{35}S] Methionine metabolic labeling 25
2.3 Biochemical methods 25
2.3.1 Protein extraction 25
2.3.2 Protein quantification 25
2.3.3 Enzymatic protein deglycosylation 25
2.3.4 Enzymatic activity of β-hexosaminidase measurement 26
2.3.5 Enzymatic activity of GlcNAc-1-phosphotransferase measurement 26
2.3.6 SDS-PAGE 27
2.3.7 Western blot 28
2.3.8 Immunoprecipitation of ^{35}S-labelled proteins 29
2.3.9 Fluorography 30

2.3.10 Pull-down assay 30

2.4 Molecular biology methods 33
2.4.1 Transformation of E. coli cells 33
2.4.2 Plasmid-DNA extraction from E. coli 33
2.4.3 Glycerol stocks preparation 33
2.4.4 Photometric measurements of DNA and RNA solutions 33
2.4.5 DNA agarose gels 34
2.4.6 DNA extraction 34
2.4.7 Digestion of DNA with restriction enzymes 34
2.4.8 Generation of construct by nucleotide synthesis and TOPO® cloning 34
2.4.9 Site-directed mutagenesis 35
2.4.10 Megaprimer mutagenesis 35
2.4.11 Plasmid DNA sequencing 36
2.4.12 RNA extraction 37
2.4.13 Synthesis of cDNA 37
2.4.14 Realtime PCR 37
2.4.15 Statistical analysis 38

3 Results 39

3.1 Dimerization and degradation of the α/β-precursor protein of the GlcNAc-1-phosphotransferase 39
3.1.1 Expression analysis of monomeric and dimeric α/β-precursor 39
3.1.2 Enzymatic activity of monomeric and dimeric α/β-precursor 42
3.1.3 Degradation of monomeric and dimeric α/β-precursor 44

3.2 Structural requirements for subunit interactions of the GlcNAc-1-phosphotransferase 47
3.2.1 Interaction between γ- and α-subunits of GlcNAc-1-phosphotransferase 48
3.2.2 Interaction between γ- and β-subunits of GlcNAc-1-phosphotransferase 50
3.2.3 Interaction between γ-subunit and α/β-precursor of GlcNAc-1-phosphotransferase 51
3.2.4 Interaction between α- and β-subunits of GlcNAc-1-phosphotransferase 53
3.2.5 Role of N-glycosylations in the interaction between the γ- and α-subunits of the GlcNAc-1-phosphotransferase 54
3.2.6 Role of γ-subunit and α-subunit dimerization for subunits interaction of the GlcNAc-1-phosphotransferase 56
3.2.7 Identification of α-subunit region required for interaction with γ-subunit 58

3.3 Analysis of mucolipidosis II- and III-related mutations 61
3.3.1 Generation of mutant GNPTAB cDNA constructs 62
3.3.2 Expression and localization of α*/β-mini precursor mutants of GlcNAc-1-phosphotransferase 63
3.3.3 Expression and localization of full length α/β-subunit mutants of the phosphotransferase 68
3.3.4 Enzymatic activity of wild-type and mutants of α/β-subunits of the GlcNAc-1-phosphotransferase 71

4 Discussion 75

4.1 Subunit interactions of the GlcNAc-1-phosphotransferase 75
4.1.1 Interactions between the α-, β- and γ-subunits 76
4.1.2 Role of post-translational modifications for the interaction between α- and γ-subunits 77
4.1.3 Identification of the α-subunit domain required for the interaction with the γ-subunit . 78

4.2 Molecular and biochemical analysis of disease-related mutations in GNPTAB . 80
4.2.1 Analysis of GNPTAB frameshift and nonsense mutations 82
4.2.2 Analysis of MLIII alpha/beta-associated GNPTAB missense and deletion mutations .. 84

4.2.3. Analysis of MLII-associated GNPTAB missense and deletion mutations 87

4.3 Degradation of GlcNAc-1-phosphotransferase 89

5 Summary 91

6 References 93

7 Publications and conference contributions 104

7.1 Publications 104

7.2 Conference contributions 104
7.2.1 Oral presentations 104
7.2.2 Poster presentations 105
7.2.3 Conference (attendance only) 106

8 Abbreviations 107

9 Acknowledgement 110

1 Introduction

Eukaryotic cells are characterized by a nucleus and membrane enclosed organelles. These organelles provide microenvironments containing different compositions of ions, lipids, proteins and glycan structures. The functional homeostasis and metabolism of the whole cell requires a finely tuned communication between all organelles that comprises (among others) the transport of macromolecules across membranes through vesicular trafficking pathways. The secretory and endocytic pathways are used for the delivery of a variety of proteins to their proper cellular location (Bonifacino & Glick, 2004).

1.1 Protein synthesis and modifications in the ER

The endoplasmic reticulum (ER) is an interconnected network of tubules and cisternae, surrounding the nucleus and extending in the entire cytoplasm of eukaryotic cells (Voeltz *et al*, 2002). Its membranes constitute more than half of the total membranes of an average eukaryotic cell. In the ER, soluble secretory proteins, many membrane proteins, and endosomal/lysosomal proteins as well as various lipids are synthesized. The ER represents the entry point into the biosynthetic/secretory pathway. To deliver nascent proteins to the ER, signal recognition particles (SRP) bind the N-terminal signal peptide of nascent polypeptides synthesized at the ribosomes and arrest the protein biosynthesis. The hydrophobic signal peptide is composed of 20 to 25 amino acids (Walter *et al*, 1984). The SRP protein complex is recruited by the SRP receptor to ER membranes followed by transfer to the Sec61 translocon. Subsequently protein synthesis is restarted and the nascent chain is translocated through the pore into the ER lumen (Nyathi *et al*, 2013). Once the signal peptide is cleaved by signal peptidases, the nascent proteins undergo different modifications prior to folding. One modification is the transfer of a preformed oligosaccharide core, $Glc_3Man_9GlcNAc_2$, by the oligosaccharyltransferase to selected asparagine residues which are part of a consensus sequence (N-X-S/T) (X can be any amino acid except proline) of the polypeptide chain (Ruddock & Molinari, 2006). *N*-glycosylations stabilize the folding of proteins and prevent aggregation. To catalyse the correct folding and assembly of synthesized proteins many chaperones and other modifying enzymes like calnexin (CNX), calreticulin (CRT), binding immunoglobulin protein (BiP) and protein disulfide isomerases (PDI) are required in the ER lumen (Caramelo & Parodi, 2008).

Trimming of *N*-glycans of newly synthesized proteins by glucosidase I and II is prerequisite for binding to the ER lectin chaperones CNX and CRT. The newly synthesized protein is thereby exposed to the PDI family member ERp57 that binds to both CNX and CRT (Leach *et al*, 2002; Oliver *et al*, 1999). ERp57 catalyses the formation of short-lived disulfide bonds, which serve as intermediates in oxidation and isomerization reactions and lead to the formation of correctly paired disulfide bonds (Molinari & Helenius, 1999). After the removal of the remaining third glucose residue by glucosidase II, the complexes dissociate form the CNX/CRT cycle, the correctly folded protein is released, and it can exit the ER (Helenius & Aebi, 2001). Moreover, if the protein is only partially folded and still exposing hydrophobic patches, an ER-resident glycoprotein, glucosyltransferase, adds again a glucose residue to high mannose-type glycans keeping the protein in the CNX/CRT cycle (Parodi, 2000), until correct folding or the decision for degradation.

1.2 Protein trafficking from the ER to the Golgi apparatus

Membrane trafficking between the ER and the Golgi apparatus is bidirectional and mediated by interaction between cytosolic sorting signals on transmembrane cargo receptors and coat protein complex (COP) I and II (Schmid, 1997) (Fig. 1.1). The anterograde exit of folded proteins from the ER occurs at ER exit sites (Lee *et al*, 2004), followed by COPII vesicles formation (Bonifacino & Glick, 2004). Two main classes of ER export motifs have been identified in the C-terminal domains of type I and type III membrane proteins: diacidic motifs with the consensus sequence D-E-X-D-E (where X can be any amino acid) (Votsmeier & Gallwitz, 2001), and short dihydrophobic motifs, such as L-L, I-L, F-Y, Y-Y-M or F-F (Barlowe, 2003). A third class of ER export motif, R-K-X-R-K, was identified, for example, in Golgi-resident type II membrane proteins glycosyltransferases (Giraudo & Maccioni, 2003). Several membrane proteins contain combinatorial signals composed by any of the sorting signals described above (Sato & Nakano, 2007). Some transmembrane proteins and most soluble cargo proteins are integrated into the COPII coated vesicles through binding to transmembrane export receptors. After fission from ER membranes, the COPII coat is released and the vesicles fuse with membranes of the ER-Golgi intermediate compartment (ERGIC).

Once in the ERGIC, cargo receptors are sorted to the Golgi apparatus by COPI coated vesicles (Zanetti *et al*, 2012). The COPI vesicles also mediate the retrograde signal-dependent transport of proteins back to the ER and the sorting within the Golgi apparatus (Fig. 1.1).

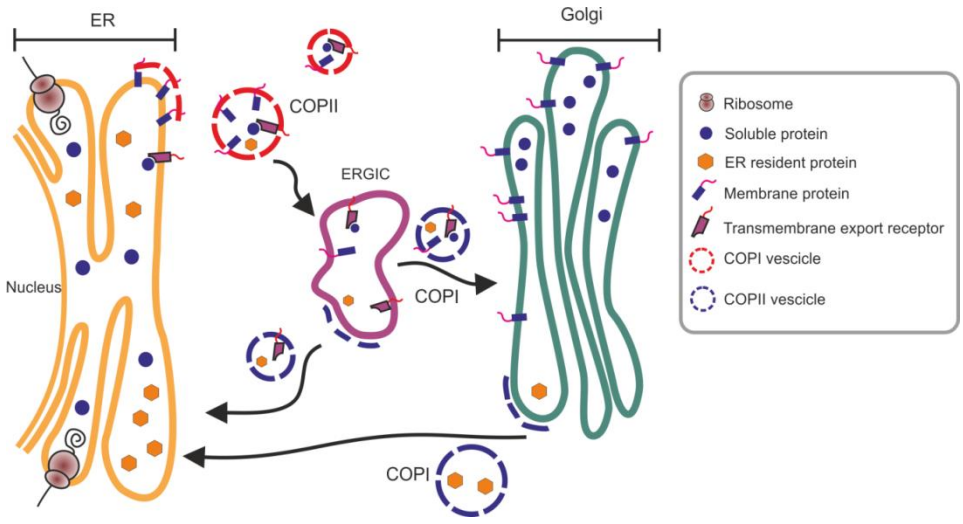

Fig. 1.1 Schematic representation of protein trafficking between ER and Golgi apparatus. Soluble and transmembrane proteins are synthesized in the ER and incorporated in COPII vesicle by direct recognition or via transmembrane export receptors. COPII vesicles then fuse with the ERGIC compartment. ER-resident proteins transported to the Golgi apparatus are recycled back via COPI vesicles.

1.3 Protein trafficking from the Golgi apparatus to lysosomes

Lysosomes contain about 60 different soluble lysosomal enzymes, also called acid hydrolases, like nucleases, proteases, glycosidases, lipases, phosphatases, sulfatases, and phospholipases as well as about 140 lysosomal membrane proteins (Lübke *et al*, 2009). Lysosomes require lysosomal enzymes for their proper degradative function. Newly synthesized lysosomal enzymes have to be transported from the ER through the Golgi apparatus to endosomes/lysosomes. Almost all newly synthesized soluble lysosomal enzymes contain mannose 6-phosphate (M6P) residues that are recognized in the *trans*-Golgi network (TGN) by two distinct M6P receptors called MPR46 and MPR300 (Ghosh *et al*, 2003).

MPR-ligand complexes are packed in the Golgi apparatus into clathrin-coated vesicles, which then fuse with endosomal compartments (Fig. 1.2). Due to the lower pH in endosomes, the complexes dissociate and the lysosomal enzymes are further sorted to lysosomes, whereas the MPRs recycle back to the Golgi apparatus to mediate further rounds of transport (Braulke & Bonifacino, 2009) (Fig. 1.2). Small amounts of lysosomal enzymes (5 - 10 %) escape the binding to MPRs in the Golgi and are secreted into the extracellular space. Here they can be caught up by cell surface-localized MPR300 allowing re-internalization and delivery to lysosomes (Braulke & Bonifacino, 2009) (Fig. 1.2). Upon arrival in lysosomes, the M6P residues are removed from lysosomal enzymes by the action of lysosomal acid phosphatases Acp2 or Acp5 (Makrypidi *et al*, 2012).

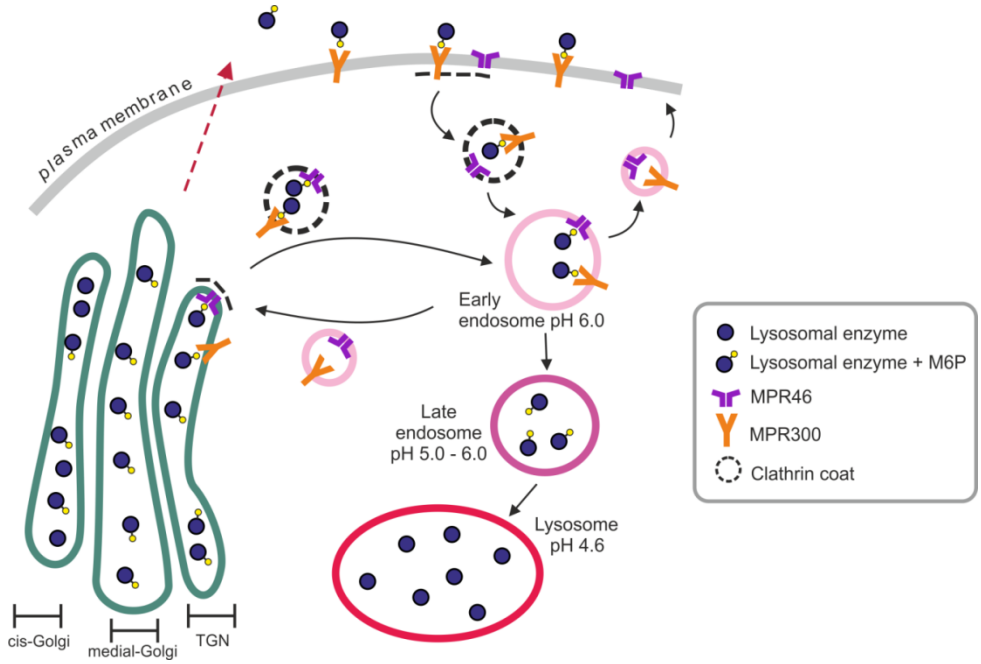

Fig. 1.2 Schematic representation of the M6P-dependent transport of soluble lysosomal proteins along the secretory and endocytic pathways. M6P-containing lysosomal enzymes are recognized by M6P receptors (MPR46 and MPR300) in the TGN. The dissociation of receptor ligand complexes in late endosomes allows the receptors to be recycled to the TGN, whereas the lysosomal proteins reach the lysosomes. At the plasma membrane, MPR300 may internalize M6P-containing lysosomal enzymes that were secreted and transport them to early endosomes.

Unlike soluble lysosomal enzymes, the transport of newly synthesized lysosomal membrane proteins from the TGN to the lysosomes does not require binding to MPRs. They can be sorted either directly from the TGN to lysosomes or indirectly via the plasma membrane followed by internalisation and final delivery to lysosomes (Bonifacino & Traub, 2003). The sorting of membrane proteins to late endosomes and lysosomes is mediated by sorting signals localized in their cytoplasmic domains, that are recognized by cytosolic clathrin-adaptor protein complexes on the TGN exit sites. Most lysosomal targeting signals belong to either (D/E-X-X-X-L-L/I) dileucine-based or Y-X-X-Ø tyrosine-based motifs (where X is any amino acid and Ø is a bulky hydrophobic amino acid) (Robinson, 2004).

1.4 The GlcNAc-1-phosphotransferase complex

1.4.1 Function of the GlcNAc-1-phosphotransferase

Soluble lysosomal enzymes require mannose 6-phosphate (M6P) markers for their efficient receptor-mediated transport to lysosomes (Fig. 1.2). M6P residues on lysosomal enzymes are generated in the Golgi apparatus in a two step reaction. In the first step, the *cis*-Golgi-resident GlcNAc-1-phosphotransferase transfers *N*-acetyl-glucosamine (GlcNAc) 1-phosphate from the phosphate donor UDP-GlcNAc to hydroxyl groups at position C6 of selected terminal mannose residues of high mannose-type oligosaccharides on lysosomal enzymes (Fig. 1.3), generating a phosphodiester intermediate (Lazzarino & Gabel, 1989; Reitman & Kornfeld, 1981). In the second step, the GlcNAc residue is hydrolysed by the GlcNAc-1-phosphodiesterase *N*-acetylglucosaminidase (also called uncovering enzyme) (Kornfeld *et al*, 1982), localized in the trans-Golgi apparatus, and the M6P residue is exposed (Fig. 1.3).

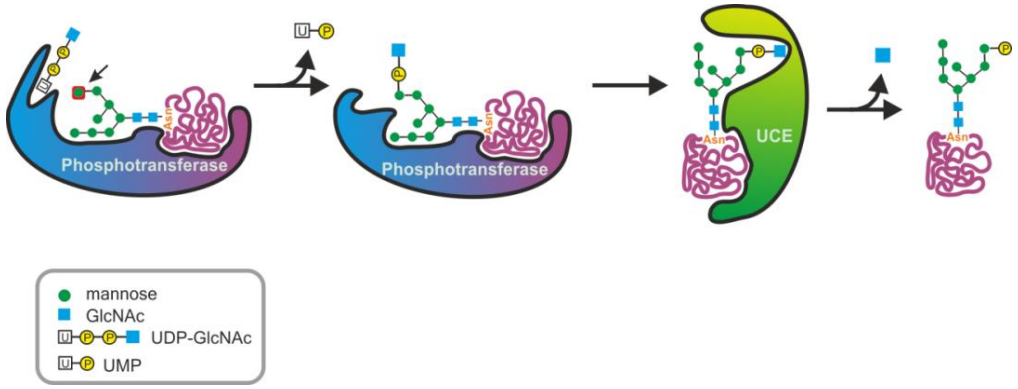

Fig. 1.3 Schematic representation of M6P formation on lysosomal enzymes. Upon arrival of newly synthesized soluble lysosomal proteins, their high mannose-type oligosaccharides are subjected to the action of the GlcNAc-1-phosphotransferase and uncovering enzyme (UCE) in the Golgi apparatus. The GlcNAc-1-phosphotransferase transfers GlcNAc-1-phosphate from UDP-GlcNAc to hydroxyl groups at position C6 of selected terminal mannose residues on high mannose-type oligosaccharides on lysosomal enzymes, generating a phosphodiester intermediate. Afterwards, the GlcNAc residue is hydrolysed by UCE and mannose-6 phosphate (M6P) residue is exposed. The GlcNAc-1-phosphotransferase contains three binding sites for UDP-GlcNAc, lysosomal proteins, and their high mannose type oligosaccharides.

1.4.2 Structure of the GlcNAc-1-phosphotransferase complex

The GlcNAc-1-phosphotransferase was first partially purified from rat liver and from amoeba (Couso *et al*, 1986; Lang *et al*, 1986). The purification of the whole enzymatic complex was obtained from lactating bovine mammary glands, and the subunit structure was finally determined using size exclusion chromatography and N-terminal protein sequencing (Bao *et al*, 1996). It was found that the GlcNAc-1-phosphotransferase represent a 540 kDa complex composed of disulfide-linked homodimers of 166 kDa α-subunits and 51 kDa γ-subunits, and two non-covalently associated 56 kDa β-subunits. To clone the human γ-subunit, the sequence of bovine γ-subunit was determined by automated Edman degradation followed by BLAST database searches (Raas-Rothschild *et al*, 2000). The α/β-subunit precursor of the human GlcNAc-1-phosphotransferase was identified by affinity chromatography using the recombinant human γ-subunit as affinity matrix (Tiede *et al*, 2005b). These studies resulted in a model that describe the GlcNAc-1-phosphotransferase as a hexameric complex composed by two α- and two γ-subunits disulfide-linked homodimers and two β-subunits. The complex assembly of the subunits takes place in the ER (Encarnação *et al*, 2011).

However, the interactions between the different subunits and the structural requirements for these interactions are not known.

1.4.3 Synthesis and posttranslational modifications of the GlcNAc-1-phosphotransferase

The human α/β-subunit precursor is synthesized as a 190 kDa type III membrane protein consisting of 1256 amino acids (Fig. 1.4 A) (Tiede *et al*, 2005b). The precursor protein is proteolytically cleaved between K928 and D929 into mature 145 kDa α-subunit and 45 kDa β-subunit (Marschner *et al*, 2011). The α- and β-subunits are *N*-glycosylated and contain 17 and 3 potential *N*-glycosylation sites, respectively. All three *N*-glycosylation sites of the β-subunit are used *in vivo* and seem to be important for folding and stability of the α/β-subunit precursor (PhD thesis, K. Marschner 2011). The α-subunits form disulfide linked homodimers (Bao *et al*, 1996) which require cysteine residue C70 (PhD thesis, K. Marschner 2011).

The mature α-subunit represents a type II membrane protein with an N-terminal cytoplasmic tail of 22 amino acids, a transmembrane domain of 21 amino acids, and a large luminal domain of 886 amino acids (Fig. 1.4 A). Sequence comparisons showed that the luminal domain has a complex, preserved, modular structure, comprising at least six domains (Tiede *et al*, 2005b) (Fig. 1.4 A). The exact homology domains alignment changed in the time as new alignment software became available and new databases were created. Sequence comparison using the NCBI database leads to the identification of a region with homology for a protein of unknown function (DUF 3184, amino acids 318 - 429) (Fig. 1.4 A). Amino acids 433-469 as well as 500-535 comprise Notch-repeat like domains. The Notch protein is a transmembrane receptor for intercellular signaling, processed in the ER and Golgi apparatus that leads to the generation of a calcium-stabilized heterodimer and acts as a transcriptional factor after proteolytic cleavage at the plasma membrane (Guruharsha *et al*, 2012). The Notch-repeat like domains in the α-subunit of GlcNAc-1-phosphotransferase contain corresponding calcium-binding residues of the Notch receptor but the role of these domains for the GlcNAc-1-phosphotransferase is not clear. This region exhibit also a high content of cysteine residues, 12 of the total 19 in the α/β-subunit precursor, suggesting a complex secondary structure.

Another domain (amino acids 699-814) exhibits similarities to the domain that binds the transcriptional co-repressor DNA methyltransferase 1 (DMAP1) (Fig. 1.4 A). The DMAP homology domain has been recently identified as a binding region for two lysosomal enzymes, cathepsin D and α-iduronidase (Qian *et al*, 2013), suggesting that this region plays a role as binding site of lysosomal proteins.

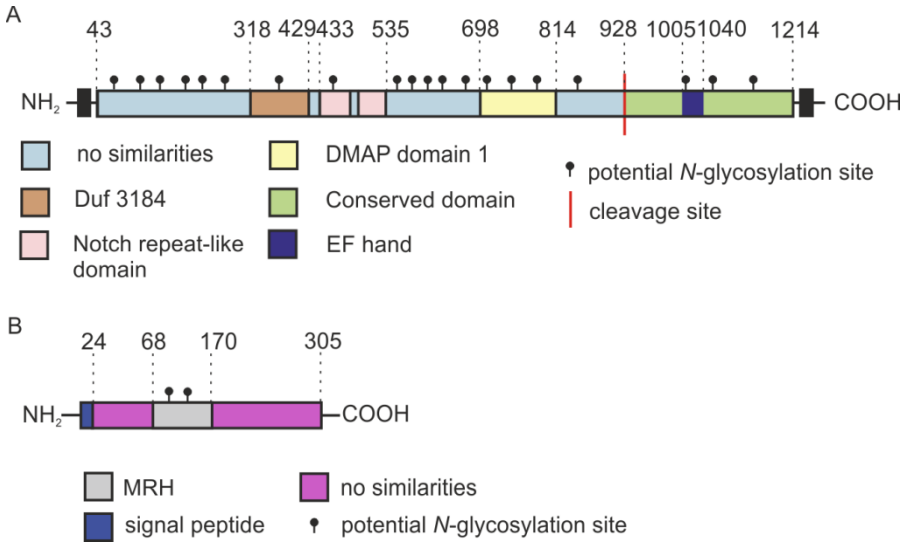

Fig. 1.4 Schematic representation of the human α/β-subunit precursor and γ-subunit. Schematic representation of the human α/β-subunit precursor membrane protein (A) and the human soluble γ-subunit (B). The different homology domains were described according to the homology domain alignment from NCBI database (reference NM_024312.4). Potential *N*-glycosylation sites (•) are indicated. Transmembrane domains are represented as black rectangles. The numbering starts at the first methionine of the coding sequence. The cleavage site (aa 928/929) is marked by the red line.

The mature human β-subunit is a type I membrane protein and contains cytoplasmic, transmembrane and luminal domains of 21, 23 and 286 amino acids, respectively (Fig. 1.4 A). The sequence comprising the mature luminal region of the β-subunit is highly conserved but does not present any homology with other proteins. The amino acid residues 1005 to 1040 exhibit an EF hand structure. The EF hand is a helix-loop-helix structural domain or motif found in a large family of calcium-binding proteins. Although the enzyme reaction catalysed by the GlcNAc-1-phosphotransferase is calcium dependent, it is not known whether Ca^{2+} binds to the EF hand residues of the β-subunit.

In addition, there are four so called stealth regions, two in the α-subunit and two in the β-subunit (Braulke T, 2013; Sperisen *et al*, 2005) of the GlcNAc-1-phosphotransferase. The stealth protein family is conserved from bacteria to eukaryotes, and is involved in the synthesis of extracellular polysaccharides for protection against the host innate immune defence (Sperisen *et al*, 2005). The stealth regions in the α-subunit have homologies to the N-terminal domain of the bacterial capsule biosynthesis proteins XcbA involved in the biosynthesis of α-1,4-linked GlcNAc-1-phosphate capsule of *Neisseria meningitidis* (Tzeng *et al*, 2003), suggesting that this region may comprise the UDP-GlcNAc binding site (Tiede *et al*, 2005b). The impact of all these homology domains on catalytic activity of the GlcNAc-1-phosphotransferase, oligomerization of subunits or interactions with other proteins is not clear.

The human γ-subunit is a soluble 35 kDa protein composed of 305 amino acids residues, comprising a signal peptide of 24 amino acids followed by a 281 amino acids constituting the mature protein (Raas-Rothschild *et al*, 2000) (Fig. 1.4 B). The cysteine residue 245 is responsible for disulfide-linked homodimer formation of the γ-subunit (Encarnação *et al*, 2011). The γ-subunit is *N*-glycosylated at asparagine residues N88 and N115 (Fig. 1.4 B) (Encarnação *et al*, 2011). The γ-subunit contains an M6P receptor homology (MRH) domain from amino acid 68 to 170 (Fig. 1.4 A) (Castonguay *et al*, 2011). Many MRH domains act as lectins and bind specifically phosphorylated or non-phosphorylated high mannose-type *N*-glycans. The role of this domain for the GlcNAc-1-phosphotransferase is not known. Whereas the α/β-precursor contains the catalytic center (Kudo & Canfield, 2006), the function of the γ-subunits is matter of debate. M6P proteomic data from mouse fibroblasts lacking the γ-subunit suggest that the γ-subunit enhances the recognition and phosphorylation of distinct lysosomal enzymes by the α/β-subunits (Lee *et al*, 2007; Qian *et al*, 2010), whereas Biacore and sorting experiments failed to show direct interactions with lysosomal enzymes (Pohl *et al*, 2009; Tiede *et al*, 2005b). In addition, the level of γ-subunits seems to regulate the expression of the α/β-subunit precursor in a compensatory manner (Pohl *et al*, 2009).

1.4.4 Transport of the GlcNAc-1-phosphotransferase to the Golgi apparatus and proteolytic activation

After synthesis and *N*-glycosylation in the ER, the α/β-subunit precursor is transported to the Golgi compartment. A combinatorial sorting motif, composed of a dileucine signal (L-L) at amino acid position 5 and 6 in the N-terminal cytoplasmic tail and a dibasic (R-I-R) motif (amino acids 1253 and 1255) located in the C-terminal cytoplasmic tail, is required for the ER export of the α/β-subunit precursor protein and the COPII-mediated transport to the Golgi apparatus (Franke *et al*, 2013) (Fig. 1.5). Since overexpressed single α- and β-subunits are retained in the ER, these observations demonstrated that the type III membrane topology of the α/β-subunit precursor is a prerequisite for ER exit. Upon arrival in the *cis*-Golgi apparatus, the α/β-subunit precursor is proteolytically cleaved between amino acids K928 and D929 into the mature α- and β-subunits (Kudo & Canfield, 2006). Alanine scanning experiments showed that R925, L927, and K928 are the most critical residues for the cleavage. These residues were homologous to the consensus recognition motif of the Golgi-resident site-1 protease (S1P) (Marschner *et al*, 2011). S1P is a membrane-bound serine protease and is located in *cis*- and *medial*-Golgi compartments (Sakai *et al*, 1998; Seidah *et al*, 1999). Prototypical membrane-bound substrates of S1P are the sterol regulatory element-binding proteins SREBP1 and 2, which play a major role in lipid metabolism and cholesterol homeostasis (Brown & Goldstein, 1999). The S1P-mediated cleavage α/β-subunit precursor protein in the Golgi apparatus is a prerequisite for the catalytic activity of the GlcNAc-1-phosphotransferase, and therefore plays an important role for the biogenesis of lysosomes (Kudo & Canfield, 2006; Marschner *et al*, 2011) (Fig. 1.5).

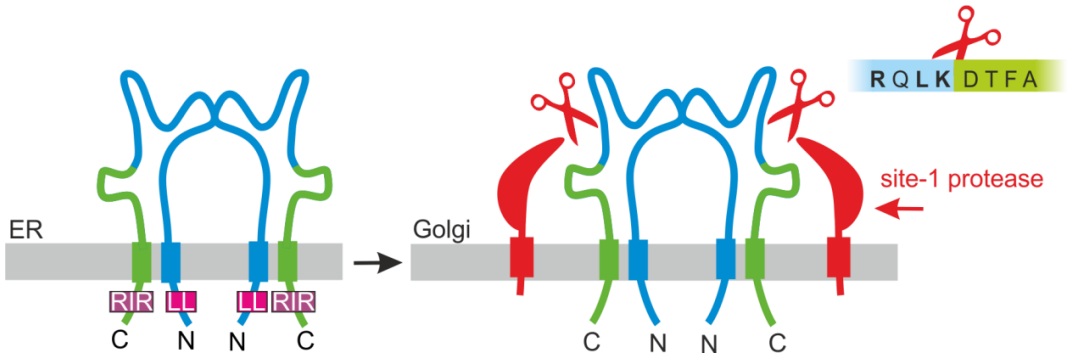

Fig. 1.5 Signal-dependent transport and S1P-mediated proteolytic activation of α/β-subunit precursor in the Golgi. The ER exit of the α/β-subunit precursor protein is mediated by a combinatorial signal, composed of an N-terminal (N) dileucine (L-L) and a C-terminal (C) dibasic (R-I-R) motif. In the Golgi apparatus, the α/β-subunit precursor is proteolytically cleaved in the luminal portion between amino acids K928 and D929 into the mature α- and β-subunits by the site-1-protease recognising the consensus sequence (R-X-L-K) (where X is any amino acid).

The γ-subunit is one of the few soluble Golgi-resident proteins known so far. How this protein is retained in the Golgi apparatus is not clear. It has been described that the γ-subunit is partially secreted in the serum and was found in the medium of γ-subunit overexpressing cells (Encarnação *et al*, 2011). *N*-glycans at N88 and N115 are required for ER exit and trafficking of the γ-subunit along the secretory route as well as for stability of the protein (Encarnação *et al*, 2011).

1.4.5 GlcNAc-1-phosphotransferase-related diseases

The α/β-subunit precursor of the human GlcNAc-1-phosphotransferase is encoded by the *GNPTAB* gene localized at chromosome 12q23.3, which spans 85 kb and contains 21 exons (Tiede *et al*, 2005b). The *GNPTG* gene encodes the γ-subunit (Raas-Rothschild *et al*, 2000), which is located on chromosome 16p13.3 and is composed of 11 exons. Mutations in both *GNPTAB* and *GNPTG* lead to a group of autosomal recessive lysosomal storage diseases. Mucolipidosis (ML) type II (MIM #252500) and MLIII alpha/beta (MIM #252600) are caused by *GNPTAB* mutations whereas *GNPTG* mutations result in the MLIII gamma (MIM#252605) disease. Biochemically, these diseases are characterized by complete or partial loss of the GlcNAc-1-phosphotransferase activity, leading to missorting and hypersecretion of multiple lysosomal enzymes.

The subsequent lysosomal deficiency of multiple lysosomal enzymes results in the accumulation of non-degraded storage material in lysosomes (Kollmann *et al*, 2010). MLII, formerly called I-cell disease, is a fatal disease with death occurring in early childhood, usually in the first decade of life. MLII patients show coarse facial features, gingival hypertrophy, shorten neck and bowed limbs, and a general short stature. They present joint contractures, thoracal asymmetry and osteopenia. The children suffer from severe psychomotor retardation, and the death occurs due to cardiopulmonary complications (Braulke *et al*, 2013; Spranger *et al*, 2002). The symptoms of MLIII alpha/beta and MLIII gamma patients are more slowly progressive than in MLII patients and present a milder clinical picture. These patients are mainly affected in the skeleton with progressive joint stiffness, claw hands, carpal and tarsal tunnel syndrome, scoliosis and decreased mobility of knees and hip joints (Braulke *et al*, 2013). The clinical diagnosis can be confirmed by elevated activities of lysosomal enzymes (like β-hexosaminidase, β-glucuronidase, β-galactosidase) in the serum of the patients or in the medium of cultured patients fibroblasts. In addition, the GlcNAc-1-phosphotransferase activity can be directly determined in cultured fibroblasts or leukocytes using [^{32}P]UDP-GlcNAc or [^{3}H]UDP-GlcNAc substrates (Ben-Yoseph *et al*, 1984) to complete the diagnosis. Moreover, the generation of a recombinant single-chain antibody fragment against M6P allowed the specific and non-radioactive detection of M6P-containing lysosomal proteins by western blotting, and can be used as a rapid supplementary diagnostic tool for MLII and MLIII (Müller-Loennies *et al*, 2010). In all cases, the bidirectional sequencing of the *GNPTAB* and *GNPTG* coding regions is necessary to detect disease-causing mutations and to verify GlcNAc-1-phosphotransferase activity measurement or M6P western blot analysis. There is no specific or definitive treatment for MLII or MLIII and patients are treated symptomatically.

1.5 Aims of the study

The Golgi-resident hexameric GlcNAc-1-phosphotransferase complex (α_2, β_2, γ_2) plays a key role in the formation of M6P-residues on lysosomal enzymes, required for their efficient targeting to lysosomes. The experiments performed in this thesis are focused on the structural requirements for assembly of subunits and intracellular transport and activity of wild-type and mutant GlcNAc-1-phosphotransferase.

- In the first part, the turnover, intracellular localization and degradation mechanisms of wild-type and mutant α/β-subunit precursor forms of the GlcNAc-1-phosphotransferase were studied.
- The second part of this work aimed to determine the direct interaction sites between the different subunits of the GlcNAc-1-phosphotransferase complex *in vitro*.
- In the third part, mutations found in MLII and MLIII patients were analysed. In particular, their effect on mRNA and protein stability, ER export, and activity of the GlcNAc-1-phosphotransferase were investigated.

2 Materials and Methods

2.1 Materials

2.1.1 Chemicals, equipments and consumables

Unless otherwise stated, all general chemicals and solvents were purchased from Serva, Sigma, Merck and JT Baker.

Table 2.1 Chemicals

Chemical	Company
[^{35}S]methionine (activity 1 mCi/mmol)	Hartmann Analytik
[^{3}H]uridine diphosphate N-acetyl glucosamine (UDP-GlcNAc) (activity 20 Ci/mmol)	ARC
2,5-Diphenyloxazole (PPO)	Roth
2-Mercaptoethanol (β-ME)	Sigma
4',6-Diamino-2-phenylindol (DAPI)	Roth
4-Nitrophenyl-N-acetyl-β-D-glucosaminide	Sigma
Acrylamide/bisacrylamide	Roth
Adenosine 5'-triphosphate disodium salt (ATP)	Sigma
Agar	Roth
Albumin standards	Thermo Scientific
Ammonium persulfate (APS)	Bio-Rad
Aqua-Poly/Mount®	Polysciences
Bovine serum albumin (BSA)	Serva
Carbenicillin	Roth
Coomassie® Brilliant Blue R250	Serva
Cycloheximide	Sigma
Dimethylsulfoxide (DMSO)	Roth
Dithiothreitol (DTT)	Sigma
DNA loading dye	Thermo Scientific
Ethidium bromide	Sigma
Ethylenediaminetetraacetate (EDTA)	Fluka
GFP-Trap® beads	ChromoTek
Glycerol	Roth
Glycine	Roth
JetPEI® PolyPlus Transfection™	PeqLab
Kanamycin	Roth
Liquid Rotiszint® eco plus	Roth
L-methionine	Roth
Luminol	Roth

Maxima® probe qPCR master mix	Thermo Scientific
Methyl α-D-mannoside (α-MM)	Sigma
Milk powder non-fat dry	Roth
NNN'N'-Tetramethylethylenediamine (TEMED)	Sigma
Nonidet P40	Roche
Paraformaldehyde (PFA)	Sigma
p-Cumaric acid	Sigma
Protamine sulfate	Sigma
QAE Sephadex A-25	GE Healthcare
Roti®-Quant protein assay	Roth
Saponin	Fluka
Sodium dodecyl sulfate (SDS)	Sigma
TaqMan® assays	Life Technologies
Tris-(hydroxymethyl)-aminomethane	Sigma
Triton X-100	Sigma
Tryptone/peptone	Roth
Tween 20	Roth
UDP-GlcNAc	Sigma
Yeast extract	Roth

Table 2.2 Equipments

Equipment (Model)	**Company**
Balances (AC100, TE2101)	Mettler Toledo, Sartorius
Block heater (MHR23)	HLC
Centrifuges (5424, 5415R and 5804R, MC6)	Eppendorf, Sarstedt
Confocal microscope (TCS SP5)	Leica Camera
Cryogenic freezing unit (CoolCell® alcohol-free)	Biocision
Developing machine (Curix 60)	Agfa
Electrophoresis chambers (Agagel Midi Wide, SE600)	PeqLab, GE Healthcare
Gel documentation (E Box V2)	PeqLab
Gel dryer (GelAir Dryer)	Bio-Rad
Imager (Chemi Doc XRS)	Bio-Rad
Incubators (Gasboy C20A, Innova 4230)	Labotect, Thermo Scientific
Inverted microscope (Axiovert 25)	Zeiss
Liquid nitrogen container (Airpege 55)	Air Liquide
Magnetic stirrer (MSH-basic)	IKA-Werke
Microwave (Promicro)	Whirlpool
pH meter (Five Easy™ FE20)	Mettler-Toledo
Photometer (Multiscan GO)	Thermo Scientific

Pipette controller (Pipetus®)	Hirschmann
Pipettes	Eppendorf
Scanner (GT-9600)	Epson
Scintillation counter (Tri-carb 2900TR)	Perkin Elmer
Shaker	GFL
Spectrophotometer (Nanodrop ND-1000)	PeqLab
Steril bench (Hera Safe)	Thermo Scientific
Thermocyclers (Tpersonal, Mastercycler, Gradient)	Biometra, Eppendorf
Thermocycler Realtime PCR (MxPro3000)	Agilent
Transfer chamber (TE62 & TE22)	GE Healthcare
Vacuum pump (Miniport)	SMT
Vortex (Genie1™)	Scientific Industries
Water bath	Schütt Labortechnik

Table 2.3 Consumables

Consumable	**Company**
Blotting paper	Roth
Coverslips	Glaswarenfabrik Hecht-Assistent
Cryovials	Sarstedt
Cuvettes	Sarstedt
Disposable material for cell culture	BD Falcon, Sarstedt, Nunc
Disposable scraper	Sarstedt
Film cassettes	Rego
Gel electrophoresis combs	GE Healthcare
Gel glass plates	Glasgerätebau OCHS
Lens paper MN 10 B	Zeiss
Micro slides SuperFrost® (glass slides)	Glaswarenfabrik Karl Hecht
Nitrocellulose membrane	GE Healthcare
nUView Tris-Glycine NN8-16%	NuSep
Pipette tips	Sarstedt, Eppendorf
Reaction tubes (0.2, 1.5 and 2 ml)	Sarstedt, Eppendorf
Scalpels	Braun
Scintillation tubes	Perkin-Elmer
Sterile syringe filter (0.22 µm)	VWR
Syringes	Braun
UV-cuvettes	Sarstedt
X-ray films	GE Healthcare

2.1.2 Expression constructs

The plasmids containing human cDNAs used for protein expression in *E. coli* and mammalian cells are listed in the following tables. The empty vectors pcDNA3.1 (+/-) and pEGFP-N1 were obtained from Life Technologies and ClonTech, respectively.

Table 2.4 Wild-type constructs

GNPTAB* and *GNPTG	**Tag**	**Reference**
α/β-precursor (aa 1-1256)	-	Marschner *et al*, 2011
α/β-precursor (aa 1-1256)	C-term myc	Franke *et al*, 2013
α/β-precursor (aa 1-1256)	C-term GFP	generated in this lab
γ-subunit (aa 1-305)	-	generated in this lab
γ-subunit (aa 1-305)	C-term myc	Pohl *et al*, 2009
γ-subunit (aa 1-305)	C-term GFP	Encarnação *et al*, 2011
α-subunit (aa 1-928)	-	generated in this thesis
α-subunit (aa 1-928)	C-term myc	Franke *et al*, 2013
β-subunit (aa 929-1256)	-	generated in this thesis
β-subunit (aa 929-1256)	N-term HA	Franke *et al*, 2013
GalNAc-4OST (aa 1-424)	C-term myc	generated in this lab

aa: amino acids; term: terminal

Based on the wild-type *GNPTG* construct the sequences were mutated. The obtained mutants constructs are listed in Table 2.5.

Table 2.5 GNPTG mutant constructs

***GNPTG* mutations (cDNA/protein)**	**Tag**	**Reference**
c.262_264AAC>CAA, p.N88Q	C-term myc	Encarnação *et al*, 2011
c.262_264AAC>CAG, p.N88Q	C-term GFP	generated in this thesis
c.343_345AAC>CAA, p.N115Q	C-term myc	Encarnação *et al*, 2011
c.343_345AAC>CAA, p.N115Q	C-term GFP	Encarnação *et al*, 2011
c.262_264AAC>CAG; 343_345AAC>CAA, p.N88,115Q	C-term myc	Encarnação *et al*, 2011
c.262_264AAC>CAG; 343_345AAC>CAA, p.N88,115Q	C-term GFP	Encarnação *et al*, 2011
c.733_735TGC>TCC, p.C245S	C-term GFP	Encarnação *et al*, 2011

Based on the full length wild-type *GNPTAB* construct C-terminally myc-tagged the sequences were mutated. The obtained mutants constructs are listed in Table 2.6.

Table 2.6 full length GNPTAB mutant constructs

***GNPTAB* mutations cDNA/protein**	**Tag**	**Reference**
c.209G>C, p.C70S	C-term myc	generated in this lab
c.1290_2545del, p.L431_K848del	-	Marschner *et al*, 2011
c.2068_2457del, p.Q690_E819del	-	generated in this lab
c.1196C>T, p.S399F	C-term myc	generated in this thesis
c.3707A>T, p.K1236M	C-term myc	generated in this thesis
c.242G>T, p.W81L	C-term myc	generated in this thesis
c.2956C>T, p.R986C	C-term myc	generated in this thesis
c.3145insC, p.G1049R*fs*X16	C-term myc	generated in this thesis
c.3503_3504delTC, p.L1168Q*fs*X5	C-term myc	De Pace *et al*, 2014
c.1208T>C, p.I403T	C-term myc	generated in this lab
c.1514G>A, p.C505Y	C-term myc	generated in this lab
c.1723G>A, p.G575R	C-term myc	generated in this lab
c.1931_1932CA>TG, p.T644M	C-term myc	generated in this lab
c.2808A>G, p.Y937_M972del	C-term myc	generated in this lab
c.3668_3670delCTA, p.T1223del	C-term myc	generated in this lab
c.1759C>T, p.R587X	C-term myc	generated in this lab
c.2269_2273delGAAAC, p.E757K*fs*X1	C-term myc	generated in this lab

Based on the mini *GNPTAB* construct (c.1290_2545del, p.L431_K848del) the sequence was mutated. The obtained mutants constructs are listed in Table 2.7.

Table 2.7 mini GNPTAB mutant constructs

***GNPTAB* mutations cDNA/protein**	**Tag**	**Reference**
c.1196C>T, p.S399F	-	De Pace *et al*, 2014
c.3707A>T, p.K1236M	-	De Pace *et al*, 2014
c.242G>T, p.W81L	-	De Pace *et al*, 2014
c.2956C>T, p.R986C	-	De Pace *et al*, 2014
c.3145insC, p.G1049R*fs*X16	-	De Pace *et al*, 2014
c.3503_3504delTC, p.L1168Q*fs*X5	-	De Pace *et al*, 2014

Based on the wild-type *GAL3ST2* construct the sequences were mutated. Part of the α-subunit was fused to *GAL3ST2* C-terminally. The obtained mutants constructs are listed in Table 2.8.

Table 2.8 GAL3ST2 mutant constructs

***GAL3ST2* mutations cDNA/protein**	**Tag**	**Reference**
c.1272insNI, p.423insNI	C-term myc	generated in this lab
c.1272insNII, p.423insNII	C-term myc	generated in this lab

NI: amino acids 428-539 of α-subunit; NII: amino acids 366-565 of α-subunit

2.1.3 DNA ladders and protein standards

The FastRuler™ DNA Ladders (middle or low range) and GeneRuler™ 1 kb were purchased from Termo Scientific. The molecular mass marker PageRuler™ Prestained, Spectrin™, and Rainbow™ Full-Range were purchased from Fermentas and GE Healthcare, respectively.

2.1.4 Kits

Table 2.9 Kits

Kit	**Company**
GeneJet PCR purification kit	Thermo Scientific
GeneJet plasmid miniprep kit	Thermo Scientific
GeneJet RNA purification kit	Thermo Scientific
High-Capacity cDNA reverse transcription Kit	Life Technologies
KAPA HiFi™ PCR kit	PeqLab
pcDNA™ 3.1 directional TOPO® expression Kit	Life Technologies
QIAquick® gel extraction kit	QIAGEN
QIAquick® plasmid midi kit	QIAGEN

2.1.5 Enzymes

Table 2.10 Enzymes

Enzyme	**Activity**	**Company**
Benzonase®	100 U/µl	Merck
FastDigest® Restriction enzymes	10 U/µl	Thermo Scientific
KAPA HiFi™	1 U/µl	PeqLab
MultiScribe™ reverse transcriptase	50 U/µl	Life Technologies
Peptide-*N*-glycosidase F (PNGase F)	1 U/µl	Roche

2.1.6 Oligonucleotides

To insert mutations in the wild-type full length and mini construct *GNPTAB*, in the *GNPTG,* and *GAL3ST2* cDNAs the primers listed in Table 2.11 were used. All nucleotides used for PCR, mutagenesis and sequencing were purchased from MWG Biotech.

Table 2.11 Primers list

Primer	5'-3' Sequence	Tm [°C]
α/β-W81L for	CGTTGTTTACACCT**T**GGTGAATGGCACAGATCTTG	63.3
α/β-W81L rev	CAAGATCTGTGCCATTCACC**A**AGGTGTAAACAACG	63.4
α/β-S399F for	CGCATCGAAGGGCTGT**T**CCAGAAGTTTATTTACC	63.2
α/β-S399F rev	GGTAAATAAACTTCTGG**A**ACAGCCCTTCGATGCG	63.2
α/β-R986C for	CGTCATTTCACAAAGTG**T**GCCATTCTGAGGATATGC	63.1
α/β-R986C rev	GCATATCCTCAGAATGGC**A**CACTTTGTGAAATGACG	63.1
α/β-G1049R for	GTTTGCAGGATTTGACA**C**GGTCTGGAACACATGC	62.7
α/β-G1049R rev	GCATGTGTTCCAGACC**G**TGTCAAATCCTGCAAAC	62.8
α/β-L1168Q for	CAGACAGTGAAGGCTGTT**C**AGGGACTTCTATG	62.6
α/β-L1168Q rev	CATAGAAGTCCCT**G**AACAGCCTTCACTGTCTG	62.6
α/β-I403T for	GCTGTCCCAGAAGTTTA**C**TTACCTAAATGATGATG	75.6
α/β-I403T rev	CATCATCATTTAGGTAA**G**TAAACTTCTGGGACAGC	75.6
α/β-T644M for	CAAAACTGAATTCTA**TG**GCCCAGAAGGGTTAC	72.4
α/β-T644M rev	GTAACCCTTCTGGGC**CA**TAGAATTCAGTTTTG	72.4
α/β-T1223del for	CATTGATTATGTTT**AT**ATTCTCATTTTTTG	69.2
α/β-T1223del rev	CAAAAAATGAGAAT**AT**AAACATAATCAATG	69.2
α/β-G575R for	GAAGTAGCCAAAAGA**A**GAGTTGAAGGTGCC	75.3
α/β-G575R rev	GGCACCTTCAACTC**T**TCTTTTGGCTACTTC	75.3
α/β-R587X for	GTGACAATCCAATAATT**T**GACATGCTTCTATTGC	73.0
α/β-R587X rev	GCAATAGAAGCATGTC**A**AATTATTGGATTGTCAC	73.0
α/β-C505Y for	CAGTGTCTCTTACT**A**TAATCAGGGATGTG	72.0
α/β-C505Y rev	CACATCCCTGATTA**T**AGTAAGAGACACTG	72.0
α/β-E757K*fs*X1 for	CTATAATAACAGA**TA**AATGACAGTTTGG	72.9
α/β-E757K*fs*X1 rev	CCAAACTGTCATT**TA**TCTGTTATTATAG	72.9
α/β-Y937_M972 del for	GATACATTTGCAGATTCCCTCAG/ GTTCCCTGAAGAATTTGACAAGACG	73.7
α/β-Y937_M972 del rev	CGTCTTGTCAAATTCTTCAGGGAAC/ CTGAGGGAATCTGCAAATGTATC	73.7
γ-N88Q for	TGCCCGTTCCAC**C**A**G**GTGACCCAGC	71.2
γ-N88Q rev	GGTCAC**C**T**G**GTGGAACGGGCAGAAC	69.5

ST-NI for	GCCCAACTCTCGGCCCTGCAAAGGGTTTATTTGACA TGGCCTGTGCCA	75.0
ST-NI rev	CAAGCTTGGTACCGAGCTCGGATCCATGATCTTGCC CACAGTCGCCAGCA	75.0
ST-NII for	GCCCAACTCTCGGCCCTGCAAAGGATAGTAACACAC CAGGATGTTTTTCG	75.0
ST-NII rev	AAGCTTGGTACCGAGCTCGGATCCATAAGGCAGGC ATTCACCTTTTGGAA	75.0
Stop α-subunit for	GGCATACTTCACTGATAGCAAAAATACTGGGAGGC AA**TA**AGAACA	71.3
Stop α-subunit rev	TGTTCT**TA**TTGCCTCCCAGTATTTTTGCTATCAGTGA AGTATGCC	70.3
HA tag removal from β-subunit	GGGTTCCAGGTTCCACTGGTGAC/ GGGGCCCAGCCGGCCAGATCTCCCGGG	75.0

for: forward; rev: reverse; Tm: melting temperature. Substituted amino acids are indicated by bold nucleotides. / indicates a missing region; α/β: α/β-precursor; γ: γ-subunit.

2.1.7 Antibodies

Primary and secondary antibodies used for western blotting (WB), immunofluorescence microscopy (IF) and immunoprecipitation (IP) are listed in tables Table 2.12 and 2.13.

Table 2.12 Primary antibodies

Primary antibodies	Host species	Dilution	Company/reference
c-myc	mouse, monoclonal	WB 1:10,000	Cell Signalling
GFP tag	mouse, monoclonal	WB 1:1,500	Roche
GM130	mouse, monoclonal	IF 1:100	BD
HA tag	rat, monoclonal	WB 1:500	Roche
human γ-subunit PT	rabbit, polyclonal	WB 1:250	Pineda
LAMP1 (H4A3)	mouse, monoclonal	IF 1:250	Hybridoma Bank
human α-subunit PT	rat, monoclonal	WB, IP 1:250, IF 1:250	De Pace *et al*, 2014
human β-subunit PT	rabbit, polyclonal	WB 1:500	Marschner *et al*, 2011
PDI	mouse, monoclonal	IF 1:500	Assays Design
β-tubulin	mouse, monoclonal	WB 1:2,000	Sigma

Table 2.13 Secondary antibodies

Secondary antibodies	Dilution	Company
HRP-conjugated goat anti-rabbit IgG	WB 1:5,000	Dianova
HRP-conjugated goat anti-rat IgG	WB 1:3,000	Dianova
HRP-conjugated goat anti-mouse IgG	WB 1:3,000	Dianova
Alexa Fluor® 488 goat anti-rat IgG	IF 1:1,000	Life Technologies
Alexa Fluor® 546 goat anti-rabbit IgG	IF 1:1,000	Life Technologies
Alexa Fluor® 546 goat anti-mouse IgG	IF 1:1,000	Life Technologies

HRP: horse radish peroxidase

For immunoprecipitation anti-rat IgG-agarose beads antibody and monoclonal anti-HA-agarose antibody was obtained from Sigma.

2.1.8 Cell lines

HEK 293 (human embryonic kidney cells) and HeLa (human cervical carcinoma cells) were purchased from the American Type Culture Collection (ATCC).

2.1.9 Media and solutions for cell culture

Dulbecco's modified Eagle's medium (DMEM), GlutaMAX™ (100 x), trypsin/EDTA, Opti-MEM®, Penicillin/Streptomycin (10000 U/ml Pen and 10 mg/ml Strep), and phosphate-buffered saline (PBS) for cell culture (calcium- and magnesium-free) were obtained from Life Technologies. Fetal calf serum (FCS) and DMEM without methionine and glutamine were from PAA and MP Biomedicals, respectively.

2.1.10 Electronic data processing

Table 2.14 Software

Software	Company/Institution
Adobe Photoshop 7.0	Adobe
Corel Draw	Corel
ECapt, ND-1000 V3.5.2	PeqLab
Endnote X3	Thomson Reuter
Finch TV 1.4.0	Geospiza
Image Lab 3.0.1, Quantity One-4.6.7	Bio-Rad
Microsoft Office	Microsoft
MxPro-QPCR software	Agilent
Quanta Smart, Volocity Demo 6.1.1	Perkin Elmer
Skanit software 3.2	Thermo Scientific

Table 2.15 Online programs and databases

Online Programs/databases	Web site
Blast	http://www.ncbi.nlm.nih.gov/blast/Blast.cgi
Expasy	http://www.expasy.org
Human Mutation Database	http://www.hgmd.org
NCBI Database	http://www.ncbi.nlm.nih.gov/

2.2 Cell biology methods

2.2.1 Cell culture

The cells used in this project were cultured at 37 °C and 5 % CO_2 in prewarmed culture medium (DMEM media supplemented with 10 % FCS, 1 x Pen/Strep and 1 x GlutaMAX^{TM}-100).

2.2.1.1 Trypsinization

Adherent cells were washed once with PBS and incubated for 5 min with trypsin/EDTA solution at 37 °C. The protease activity of trypsin was stopped with culture medium. The cells were resuspended in culture media and seeded in the respective plates or flasks.

2.2.1.2 Cryoconservation and revitalization

To prepare long-term stocks, cells were frozen in liquid nitrogen. The cells were washed once with PBS and then trypsinated for 5 min at 37 °C. The cells were afterwards resuspended in freezing medium (DMEM, 10 % FCS, 10 % DMSO). The cells were transferred to cryovials and left at -80 °C overnight in a cryogenic freezing unit that allows a slower drop of temperature (1 °C/min). After 3 days the cells were transferred to a liquid nitrogen container.

For revitalization, the cells were resuspended in 1 ml prewarmed culture medium and transferred from the cryovial to a falcon tube. The cells were centrifuged at 900 × g for 5 min and the medium was removed. The cells were resuspended in culture medium and seeded in a cell culture flask. After 6 h the medium was replaced with fresh culture medium.

2.2.1.3 Transient transfection

The cells were cultivated until a confluence of 80-90 % and transiently transfected using jetPEI® reagent (Table 2.16).

Table 2.16 Transient transfection with JetPEI®

Plate/well	DNA (µg)	NaCl 150 mM (µl)	JetPEI® (µl)	NaCl 150 mM (µl)	Culture medium (µl)
24-well	1	until 50	2	until 50	400
35 mm	3	until 100	6	until 100	1,600
60 mm	5	until 250	10	until 250	4,000
100 mm	10	until 250	20	until 250	8,000

Each mixture in tube 1 (DNA diluted in 150 mM NaCl) and tube 2 (JetPEI® diluted in 150 mM NaCl) was incubated for 5 min. Afterwards the contents of tubes 1 and 2 were mixed and incubated for 25 min at RT.

Media was replaced by fresh culture media and the DNA mixtures were added drop by drop to each plate/well. The cells were incubated for 24 h at 37 °C.

2.2.2 Double immunofluorescence microscopy

HeLa cells were grown on coverslips and transiently transfected for 24 h. Afterwards the cells were treated with 100 µg/ml cycloheximide for 40 min. Cells were washed twice with PBS and fixed with 500 µl of 4 % PFA (in PBS) for 20 min at RT. Cells were washed twice with 50 mM NH_4Cl (in PBS) and incubated in 50 mM NH_4Cl for 5 min at RT. The preparates were permeabilized with 0.1 % saponin (in PBS) for 10 min and blocked for 30 min with 3 % BSA, 0.1 % saponin (in PBS). The cells were incubated with the primary antibodies in 3 % BSA, 0.1 % saponin (in PBS) for 1 h at RT and washed twice with 0.1 % saponin (in PBS). The cells were incubated 1 h with secondary antibodies conjugated to Alexa Fluor® 546 or 488 and washed twice with 0.1 % saponin (in PBS). DAPI (2 µg/ml) staining was performed for 5 min. The cells were washed twice with PBS and once in dH_2O. The coverslips were embedded in Aqua-Poly/Mount® and dried over night. Fluorescence was detected and images were obtained using a Leica TCS SP5 digital scanning confocal microscope. Images were processed with Volocity Demo 6.1.1 software.

2.2.3 [^{35}S] Methionine metabolic labeling

- Starvation media: DMEM without L-glutamine and L-methionine
- ^{35}S-labeling media: starvation media, 400 µCi/ml [^{35}S]methionine
- Chase media: DMEM, 1 x GlutaMAX^{TM}-100, 25 µg/ml L-methionine, 4 % heat-inactivated and dialyzed FCS

HeLa cells grown on 35 mm plates were starved for 2 h at 37 °C in starvation media and then incubated with 750 µl labeling media for 1 h. After removing the labeling media, the cells were either washed once with cold-PBS and lysed or incubated with 750 µl chase media for different time points. The cells were washed, lysed, and processed for immunoprecipitation.

2.3 Biochemical methods

2.3.1 Protein extraction

Cells grown on 60 mm or 100 mm plates were harvested and resuspended in 200 or 500 µl PBS containing 1 % Triton-X100 and 1 x protease inhibitor cocktail. After 30 min incubation on ice, the samples were centrifuged at 20,000 × g for 15 min at 4 °C. The supernatants were transferred to new tubes.

2.3.2 Protein quantification

Protein quantification was carried out using the Roti®-Quant protein assay. A standard series of BSA (0, 5, 10, 15 and 20 µg/µl concentration) was prepared. From the cell extract 2 µl in a total volume of 800 µl were prepared. Afterwards 200 µl of Roti®-Quant protein assay was added and the tubes were mixed by inversion. After 5 min the standards and the samples were measured at 595 nm wavelength in a photometer.

2.3.3 Enzymatic protein deglycosylation

To cleave off all types of *N*-linked oligosaccharides from glycoproteins, the enzyme peptide-*N*-glycosidase F (PNGase F) was used. The reaction was prepared as follows:

- 50-75 µg cell lysate in 100 µl water
- add 10 % SDS to a final concentration of 0.2 % and incubate at 95 °C for 10 min
- add 10 % Nonidet P40 to a final concentration of 1 %
- add 2 µl PNGase F

Incubation was performed for 60 min at 37 °C.

2.3.4 Enzymatic activity of β-hexosaminidase measurement

- Substrate buffer (2 x): 10 mM 4-nitrophenyl-N-acetyl-β-D-glucosaminide, 0.2 M Na-citrate (pH 4.6), 0.2 % Triton X-100, 0.4 % BSA
- Stop buffer: 0.4 M glycine/NaOH (pH 10.4)

For the reaction 50 µl cell extract and 50 µl water were mixed. Afterwards 100 µl of 2 x substrate buffer was added and the reaction was incubated at 37 °C for 45 min. The reaction was stopped by adding 800 µl stop buffer. The absorption of the sample was measured at 405 nm.

2.3.5 Enzymatic activity of GlcNAc-1-phosphotransferase measurement

- Buffer A: 50 mM Tris/HCl (pH 7.4), 10 mM $MgCl_2$, 10 mM $MnCl_2$, 2 mg/ml BSA, 2 mM ATP, 100 mM α-methylmannoside (α-MM), 75 µM UDP-GlcNAc, 1 µCi [^{3}H]UDP-GlcNAc
- Buffer B: 2 mM Tris/HCl (pH 8.0)
- Buffer C: 30 mM NaCl, 2 mM Tris/HCl (pH 8.0)

To measure the enzymatic activity of GlcNAc-1-phosphotransferase, [^{3}H]UDP-GlcNAc was used as phosphate donor whereas α-methylmannoside (α-MM) was used as phosphate acceptor (Fig. 2.1) (Ben-Yoseph *et al*, 1984; Qian *et al*, 2013).

HEK cells were grown on 10 mm plates and were transfected with cDNAs of different full length α/β-precursor constructs of the phosphotransferase for 24 h. The cell pellets were harvested in cold PBS and the proteins were extracted in 400 µl lysis buffer. After quantification 100 µg cell extract was diluted in a total volume of 25 µl lysis buffer. Afterwards 25 µl buffer A was added and the reaction incubated at 37 °C for 1 h. The samples were passed through the QAE sephadex A-25 column (1 ml of resins equilibrated in buffer B). The anion exchanger QAE binds the [^{3}H] GlcNAc-P reaction product. The column was washed with 5 ml of buffer B. The column was eluted twice with 2 ml and once with 1 ml of buffer C. Each elution was collected and measured in 5 volumes of scintillation liquid.

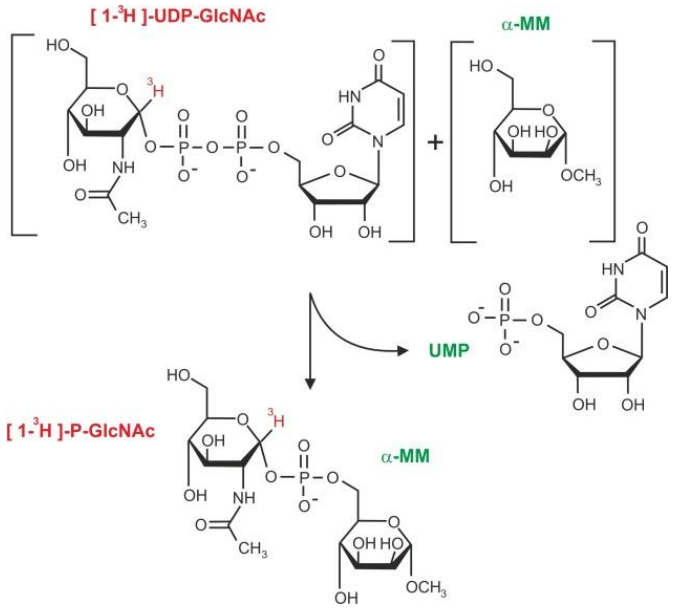

Fig. 2.1 Enzymatic reaction of the GlcNAc-1-phosphotransferase. Representation of phosphorylation of α-methylmannoside (α-MM). [^{3}H]UDP-GlcNAc was used as phosphate donor. During the reaction UMP and α-MM bound to [^{3}H]GlcNAc-P are produced.

2.3.6 SDS-PAGE

- Anode buffer: 192 mM glycine, 25 mM Tris/HCl (pH 6.8)
- Cathode buffer: 192 mM glycine, 25 mM Tris/HCl (pH 6.8), 0.1% SDS
- Sample buffer: 125 mM Tris/HCl (pH 6.8), 1 % SDS, 10 % glycerin, Coomassie® Blue R (for reducing conditions: 10 mM DTT, 0.1 mM β-mercaptoethanol)

Gel electrophoresis was performed using a vertical slab gel unit. Running gels (30 ml) and stacking gels (10 ml) were prepared as described in the Table 2.17. Depending on the experiment, samples (50-100 µg of total protein) were solubilized in reducing or non-reducing sample buffer. After incubation at 95 °C for 5 min the samples were loaded on a polyacrylamide gel. The electrophoresis was performed for 3 h at 50 mA per gel at RT.

Table 2.17 Running and stacking gels for SDS-PAGE

Chemicals, buffers	**running gel 8 %**	**running gel 10 %**	**running gel 12,5 %**	**stacking gel 4 %**
Acrylamide (30 %), bisacrylamide (0.8 %)	7.8 ml	9.8 ml	14.6 ml	1.3 ml
1.5 M Tris/HCl (pH 8.8)	7.5	7.5 ml	7.5 ml	-
1.5 M Tris/HCl (pH 6.8)	-	-	-	2.5 ml
dH_2O	14.1 ml	12.2 ml	9.8 ml	6 ml
10 % APS	250 µl	250 µl	250 µl	100 µl
10 % SDS	300 µl	300 µl	300 µl	100 µl
TEMED	25 µl	25 µl	25 µl	10 µl

2.3.7 Western blot

Buffers:

- 10 x TBS (Tris-buffered saline): 1.37 M NaCl, 27 mM KCl, 250 mM Tris/HCl (pH 7.4)
- Transfer buffer: 25 mM Tris/HCl (pH 7.4), 192 mM glycine, 20 % methanol
- TBS-T: 0.05 % Tween 20 in TBS
- Blocking solution: 5 % non-fat dry milk powder in TBS-T

Enhanced chemiluminescence (ECL) reactions:

- Solution 1: 5 ml 0.1 M Tris/HCl (pH 8.5), 100 µl 250 mM luminol/DMSO, 50 µl 90 mM p-cumaric acid/DMSO
- Solution 2: 5 ml 0.1 M Tris/HCl (pH 8.5), 12 µl 30 % H_2O_2

A transfer sandwich (fiber pad, 2 sheets of paper, nitrocellulose membrane, running gel, 2 sheets of paper, fiber pad) kept together by a plastic cassette was assembled in transfer buffer. The cassette was inserted in a transfer buffer tank and the transfer was performed at 900 mA for 120 min. After protein transfer the membrane was incubated with blocking solution for 20 min at RT. The membrane was washed 3 x for 10 min with TBST and incubated for 1 h at RT with the respective primary antibodies (Table 2.11) diluted in blocking solution. The membrane was washed 3 x for 10 min with TBST and incubated with the HRP-coupled secondary antibody for 1 h at RT. Afterwards the membrane was washed 3 x for 10 min with TBST and the immunoreactive bands were detected by ECL. Therefore solution 1 and 2 were prepared and mixed shortly before detection.

The membrane was incubated with both solutions for 1 min and chemiluminescence was detected on an Imager ChemiDocXRS with exposure times between 15 sec and 5 min. Prior to detection of a second protein on the same blot primary and secondary antibodies were removed by incubation for 5 min with 0.2 M NaOH.

2.3.8 Immunoprecipitation of ^{35}S-labelled proteins

- Lysis buffer: 0.4 % Triton X-100, 0.2 % Na-deoxycholate, 0.2 % SDS, 0.8 % BSA, 1 x protease inhibitor cocktail in PBS (pH 7.4)
- Neufeld buffer: 10 mM Tris/HCl (pH 8.5), 0.6 M NaCl, 0.1% SDS, 0.05 % Nonidet P-40
- IMM: 1 % Triton X-100, 0.5 % Na-deoxycholate in PBS

The cells were harvested by scraping with 1,200 µl lysis buffer. To remove the DNA, samples were incubated for 10 min at RT with 0.5 µl benzonase® (50 U) and 12 µl of 3 % freshly prepared protamine sulfate was added. The samples were centrifuged at 12,000 × g for 10 min at 4 °C and the supernatants were transferred to new tubes. To reduce non-specific binding, the protein extracts were incubated with 50 µl anti rat IgG agarose beads (50 % slurry) for 1 h at 4 °C on a rotating wheel. After centrifugation, the supernatants were collected and the beads discarded.

The collected supernatants were incubated with the monoclonal α-subunit antibody over night at 4 °C on a rotating wheel. For precipitation of the antibody-antigen complexes, 50 µl anti rat IgG agarose beads were added to the samples and incubated for 1 h at 4 °C on a rotating wheel. The samples were centrifuged at 1,000 × g for 1 min, the supernatants were stored at -20 °C and the beads were washed as follows: once with 1 ml Neufeld buffer; once 1 ml IMM; 1 ml IMM + 2 M KCl and twice with 1 ml 0.1 x PBS. After each washing step, the samples were centrifuged at 1,000 × g for 0.5 min at 4 °C and the supernatant was discarded. The precipitates on beads were subjected to PNGase F to cleave off all types of *N*-linked oligosaccharides. The reaction was prepared as follows:

- add 50 µl dH_2O to the washed beads
- add 10 % SDS to a final concentration of 0.2 % and incubate at 95 °C for 10 min
- add 10 % Nonidet P40 to a final concentration of 1 %
- add 4 µl PNGase F

The beads that were not subjected to PNGase F treatment were identically prepared but the PNGase F was omitted. Incubation was performed for 90 min at 37 °C. The samples were mixed with sample buffer, boiled for 5 min at 95 °C and subjected to SDS-PAGE followed by fluorography.

2.3.9 Fluorography

The gel containing ^{35}S-labelled proteins was incubated 3 x 20 min at RT in DMSO while shaking. After that the gel was incubated over night at RT in 20 % PPO/DMSO solution. After three washes in water, the gel was dried, placed between two films and stored at -80 °C for 2 days. Afterwards the films were developed. The β-emitting isotope-labelled molecules present in the gel emit radiation that excites the PPO fluorophore (Bonner & Laskey, 1974). The visible light emitted by the molecules was detected by photographic film. Fluorography allows a high sensitivity to detect samples labelled with ^{35}S. After fluorography the radiolabelled polypeptides were evaluated by densitometry.

2.3.10 Pull-down assay

GFP-Trap® beads:

- Lysis buffer: 10 mM Tris/HCl (pH 7.4), 150 mM NaCl, 0.5 mM EDTA, 0.1 % Nonidet P40, 1 x protease inhibitor cocktail
- Wash buffer: 10 mM Tris/HCl (pH 7.4), 150 mM NaCl, 0.5 mM EDTA, 1 x protease inhibitor cocktail

Pull-down experiments allow the identification of interacting proteins or protein complexes present in cell extracts. GFP-Trap® beads contain heavy chain antibodies produced in *Camelidae*, so-called nanobodies, that recognizes and binds GFP via a single variable domain (Pichler *et al*, 2012). This antibody is coupled to agarose beads for biochemical analysis of GFP fusion proteins and their interacting partners.

To perform pull-down of the subunits of phosphotransferase, HEK cells overexpressing different constructs were used. At first the overexpressed GFP-fusion proteins from HEK cell extracts were caught up with GFP-Trap® beads. Afterwards the preformed complexes were incubated with the second cell extract overexpressing the interacting proteins (Fig. 2.2).

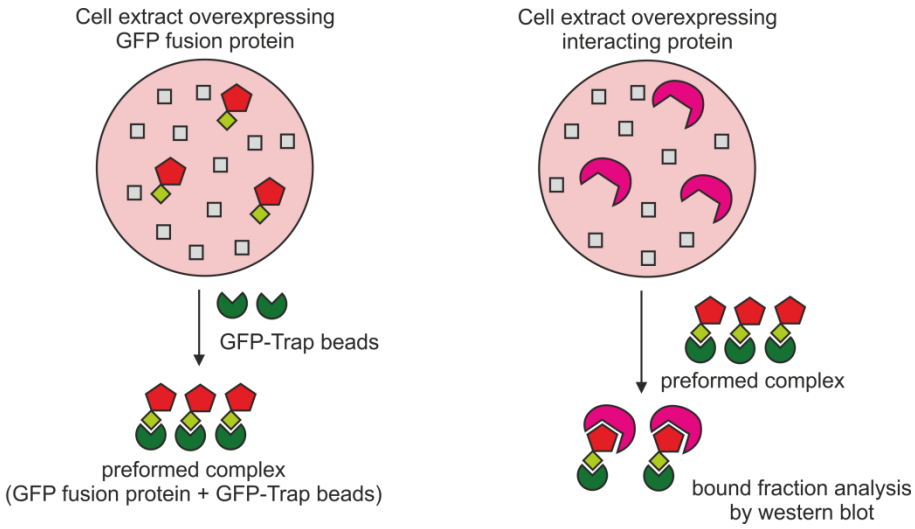

Fig. 2.2 Schematic representation of pull-down procedure. Extracts from HEK cells overexpressing GFP fusion proteins were incubated with GFP-Trap® beads. After wash, the preformed complexes were incubated with extracts from HEK cells overexpressing the protein of interest. The bound material was then analysed by western blotting.

Cells grown on 60 mm plates were transiently transfected for 24 h and harvested in PBS. Cell pellets were collected by centrifugation (900 × g for 5 min at 4 °C) and resuspended in 400 µl lysis buffer. After incubation for 30 min on ice with extensive pipetting every 15 min lysates were cleared by centrifugation at 20,000 × g for 10 min at 4 °C. Protein content was quantified and 50 µg of total cell extract were separated for western blot analysis (input). From the remaining supernatant, 500 µg protein extract of cells overexpressing GFP-fusion protein was added to 25 µl of GFP trap® beads equilibrated in wash buffer. The cell extract and the beads were filled to a total volume of 500 µl with wash buffer. The sample was incubated with gentle end-over-end mixing for 2 h at 4 °C and centrifuged at 1,700 × g for 1 min. 50 µl of the supernatant was collected and referred as flow through. After three washes with 500 µl wash buffer, 50 µl from the last wash was collected and referred as wash. 500 µg of the second cell extract containing the overexpressed protein of interest was incubated with the preformed complex with gentle end-over-end mixing for 2 h at 4 °C. 50 µg of the second cell extract was separated (input). The tubes were centrifuged at 1,700 × g for 1 min. 50 µl of the supernatant was collected and referred as flow through. After three washes with 500 µl wash buffer, 50 µl from the last wash were collected and referred as wash.

The beads were boiled in 100 µl sample buffer with reducing reagent and referred as bound fraction. All collected fractions were subjected to western blot analysis.

Anti rat IgG agarose beads:

- Lysis buffer: 1 % Triton X-100, 1 x protease inhibitor cocktail in PBS (pH 7.4)
- Wash buffer: 0.5 M NaCl, 2.8 mM NaH_2PO_4, 7.2 mM Na_2HPO_4 (pH 7.2)

To perform pull-down assays of the α-subunit and interacting partners of GlcNAc-phosphotransferase that do not contain a GFP-tag, the antibody raised against the α-subunit was used. HEK cells grown on 60 mm plates were transiently transfected for 24 h and harvested in PBS. Cell pellets were collected by centrifugation (900 × g for 5 min at 4 °C) and resuspended in 400 µl lysis buffer. After incubation on ice for 30 min lysates were cleared by centrifugation at 20,000 × g for 10 min at 4 °C. Protein content was quantified and 50 µg of total cell extract were separated for western blot analysis (input). From the remaining supernatant, 500 µg of each extract from overexpressing HEK cells were mixed and incubated in a total volume of 1 ml wash buffer for 2 h at 4 °C. Afterwards 50 µl of anti α-subunit antibody was added and the sample was incubated over night at 4 °C with gentle end-over-end mixing. The immunocomplexes were incubated with 25 µl anti rat IgG agarose beads to pull-down the preformed complexes. The beads were first equilibrated in wash buffer and then incubated with the immunocomplexes with gentle end-over-end mixing for 1 h at 4 °C. The tubes were centrifuged at 1,700 × g for 1 min. 50 µl of the supernatant was collected and referred as flow through. After three washes with 500 µl wash buffer, 50 µl from the last wash were collected and referred as wash. The beads were boiled in 100 µl sample buffer with reducing reagent and referred as bound fraction. All collected fractions were subjected to western blot analysis.

2.4 Molecular biology methods

2.4.1 Transformation of *E. coli* cells

- LB medium: 10 g Tryptone/peptone, 5 g Yeast extract, 10 g NaCl, ad 1 l dH_2O (pH 7.0)
- LB agar plates: 7.5 g Agar in 1 l LB medium

TOP10 *E. coli* competent cells were thawed. After adding the Plasmid-DNA to the cells, the mix was incubated for 30 min on ice. To provoke a heat shock, the bacteria were incubated for 45 sec at 42 °C followed by incubation on ice for 5 min.

LB media (1 ml) was added and the cells were incubated at 37 °C for 40 min with shaking. The bacteria were centrifuged for 5 min at 4,500 × g . The pellet was resuspended in 50 µl of LB-media and plated on LB agar plates containing the respective antibiotics (100 µg/ml carbenicillin or 50 µg/ml kanamycin) and incubated over night at 37 °C. Colonies from the LB agar plate were selected and inoculated in 5 ml LB medium with the appropriate antibiotic. The mini cultures were incubated over night with shaking. Mini-preps were prepared from 2 ml of cell suspension.

2.4.2 Plasmid-DNA extraction from *E. coli*

Plasmid preparations were made using the GeneJet plasmid miniprep kit and QIAquick® plasmid midi kit according to the manufacturer's instructions.

2.4.3 Glycerol stocks preparation

For storage of transformed *E. coli*, glycerol stocks were prepared in a cryovial using 500 µl of bacterial culture and 500 µl of glycerol. Glycerol stocks were stored at -80 °C.

2.4.4 Photometric measurements of DNA and RNA solutions

DNA and RNA concentration was measured in a spectrophotometer. The concentration was calculated automatically in base of the absorbance at 260 nm (OD_{260}). The absorbance ratio at 260 and 280 nm ($OD_{260/280}$) was used to assess the purity of nucleic acids.

2.4.5 DNA agarose gels

- 50 x TAE buffer: 2 M Tris/HCl (pH 8.3), 1 M acetic acid, 100 mM EDTA

Agarose gels were prepared by boiling the required agar amount in 1 x TAE buffer in a microwave. After cooling down to about 55 °C, ethidium bromide was added to a final concentration of 0.5 µg/ml. The solution was poured into a gel form. The DNA samples were mixed with 6 x MassRuler™ loading dye and loaded on the solid agarose gel together with a DNA loading ladder. Electrophoresis was performed at 120 V for 20 min and the DNA bands were detected with UV illumination.

2.4.6 DNA extraction

DNA was extracted from agarose gel using the QIAquick gel extraction kit, or purified from PCR products using the GeneJet™ PCR purification kit according to the manufacturer's instruction.

2.4.7 Digestion of DNA with restriction enzymes

To digest PCR products and vectors FastDigest® enzymes were used as follow:

- 2 µl 10 x FastDigest® buffer
- 1 µl Restriction enzyme(s) (10 U/µl)
- x µl DNA (0.1-1 µg)
- x µl Nuclease-free water (20 µl final volume)

2.4.8 Generation of construct by nucleotide synthesis and TOPO® cloning

A synthetic cDNA was generated by GeneArt (Life Technologies) in order to generates the α-subunit lacking the Notch homology domain. The translated protein is missing the amino acids P434 to C535. The codon usage was optimized for expression in eukaryotic cells. The insert was cloned into the prokaryotic expression vector pMK-RQ vector. To clone the insert into an eukaryotic expression vector the construct was amplified with specific primers required for Topo® cloning. The amplified insert was purified by agarose gel extraction and inserted into the pcDNA™ 3.1 D/TOPO® vector according to the manufacturer's instructions.

2.4.9 Site-directed mutagenesis

To substitute nucleotides in expression vectors, the KAPA HiFi PCR kit was used. Two complementary oligonucleotides with the desired mutation were used to amplify a template plasmid. The oligonucleotides were diluted with water to obtain a 100 µM stock solution or a 10 µM working solution. PCR reaction and cycling condition for site-directed mutagenesis:

- 5 µl 5 x KAPA HiFi Buffer
- 0.75 µl dNTP-Mix (10 mM)
- 0.75 µl 10 µM mutagenic forward primer
- 0.75 µl 10 µM mutagenic reverse primer
- 1 µl KAPA HiFi polymerase
- x µl Template (50 ng)
- x µl Nuclease-free water (25 µl final volume)

	Temperature	**Time**	
1.	98 °C	5 min	
2.	98 °C	45 sec	
3.	60 °C	30 sec	
4.	72 °C	260 sec	[2 to 4] x 18 cycles
5.	72 °C	30 min	

PCR product was digested with restriction enzyme *Dpn*I to remove the methylated, non-mutated DNA template. The mixture was incubated for 20 min at 37 °C

- 5 µl PCR product
- 2 µl 10 x FastDigest^{TM} buffer
- 1 µl *Dpn*I
- 12 µl H_2O

2.4.10 Megaprimer mutagenesis

To delete a DNA region from a plasmid insert, megaprimers were used. The primers were designed to have a complementary sequence flanking the deletion (Fig. 2.3). After the annealing of the megaprimers, the deletion region loops out and is excluded from the PCR (Soderberg & Lang, 2006). The megaprimers were incorporated in the newly synthesized plasmid lacking the loop region.

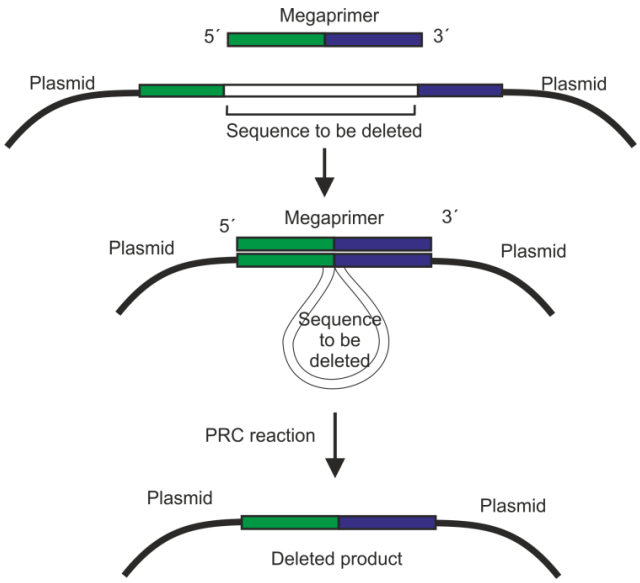

Fig. 2.3 Mutagenesis of cDNA using the megaprimers method. Complementary flanking sequences are represented in green and blue. After the annealing of megaprimer the deletion sequence loops out. The megaprimers were incorporated in the newly synthesized plasmid lacking the loop region.

To perform the PCR reaction the KAPA HiFi PCR kit was used.

- 5 µl 5 x KAPA HiFi Buffer
- 0.75 µl dNTP-Mix (10 mM)
- 0.75 µl 10 µM megaprimer
- 1 µl KAPA HiFi polymerase
- x µl Template (50 ng)
- x µl Nuclease-free water (25 µl final volume)

	Temperature	**Time**	
1.	98 °C	5 min	
2.	98 °C	45 sec	
3.	60 °C	30 sec	
4.	72 °C	260 sec	[2 to 4] x 18 cycles
5.	72 °C	30 min	

2.4.11 Plasmid DNA sequencing

For sequencing of constructs the samples were sent to SEQLAB, Göttingen. The reaction mixture for sequencing was prepared as follows:

- 3 µl 10 pM primer
- x µl Template (1.2 µg plasmid)
- x µl Nuclease-free water (15 µl final volume)

2.4.12 RNA extraction

RNA was extracted from HEK cells using GeneJet RNA purification kit according to the manufacturer's instructions. The RNA quality was tested afterwards by agarose gel. The RNA was stored at - 80 °C.

2.4.13 Synthesis of cDNA

The cDNA was synthesized from 1 µg RNA using the High-Capacity cDNA reverse transcription kit. PCR reaction and cycling condition for cDNA-synthesis:

- 2 µl 10 x RT-Buffer
- 0.8 µl 25 x dNTP-Mix (100 mM)
- 2 µl 10 x RT random primers
- 1 µl MultiScribe™ reverse transcriptase
- 1 µg RNA
- x µl Nuclease-free water (20 µl final volume)

	Temperature	Time
1.	25 °C	10 min
2.	37 °C	120 min
3.	85 °C	5 min

2.4.14 Realtime PCR

To determine the *GNPTAB* mRNA expression level, the TaqMan® gene expression assays were used. In this assays probes are linked to the 5′ end with a reporter FAM™ dye. A non-fluorescent quencher is at the 3′ end of the same probe. During PCR, the TaqMan® probe anneals specifically to a complementary sequence between the forward and reverse primer sites. When the probe is intact, the proximity of the reporter dye to the quencher dye results in quenching of the reporter fluorescence. When the primer and probe are annealed to the target, the DNA polymerase cleaves the probe during amplification and separate the reporter from the quencher dye. This results in increased reporter fluorescence. Polymerization of the strand continues, but because the 3′ end of the probe is blocked, no extension of the probe occurs during PCR.

Reaction and cycling condition for realtime PCR:

- 1 µl TaqMan® assay (*GNPTAB,* Hs00225647_m1; *ACTB*, Hs99999903_m1)
- 10 µl 2 x Maxima® probe qPCR master mix
- 2 µl cDNA
- 7 µl Nuclease-free water

	Temperature	**Time**	
1.	95 °C	10 min	
2.	95 °C	30 sec	
3.	60 °C	1 min	[2-3] x 40 cycles

For the calculation of $\Delta\Delta C_T$ values, the difference between the CT value of the gene under investigation and the control gene (β-actin) were calculated. The relative expression was determined from the comparison of each group (sample versus control) according to the following equation (Schmittgen & Livak, 2008):

$2^{-\Delta\Delta C_T}$ with $\Delta C_T = C_{T\ gene} - C_{T\ control\ gene}$

$\Delta\Delta C_T = \Delta C_{T\ sample} - \Delta C_{T\ control}$

For the graphical analysis the $\Delta\Delta C_T$ was set equal to 100 %. All PCR were performed in triplicate and detected with the fluorescence detector MX3000P™.

2.4.15 Statistical analysis

The statistical analysis of the obtained data were performed using the Microsoft Excel program 2000, Version 9.0. When the result is obtained form multiple determinations, the arithmetic mean is calculated and the standard deviation is shown. To calculate the differences between two different sets of data Student's t-test was performed. When the P-value < 0.05 the changes were considered significant (*).

3 Results

The GlcNAc-1-phosphotransferase is the key enzyme in the generation of the M6P recognition marker on lysosomal enzymes, which is essential for their transport to lysosomes. The hexameric enzyme complex is composed of three subunits ($\alpha_2\beta_2\gamma_2$). To form an enzymatically active complex, the membrane-bound α/β-subunit precursor has to be transported to the *cis*-Golgi apparatus and cleaved into mature α- and β-subunits by the site-1 protease. Whereas the α- and β-subunits contain the catalytic activity, the function of the soluble γ-subunit is not clear. In the first part of the thesis the dimerization and degradation of the α/β-subunit precursor (3.1) and the structural requirements for subunit interactions (3.2) of the GlcNAc-1-phosphotransferase were studied. For all experiments the cDNAs encoding the human α/β-subunit precursor, the isolated α- and β-subunits, the γ-subunit (Fig. 3.1), and respective mutants, were overexpressed in HEK or HeLa cells.

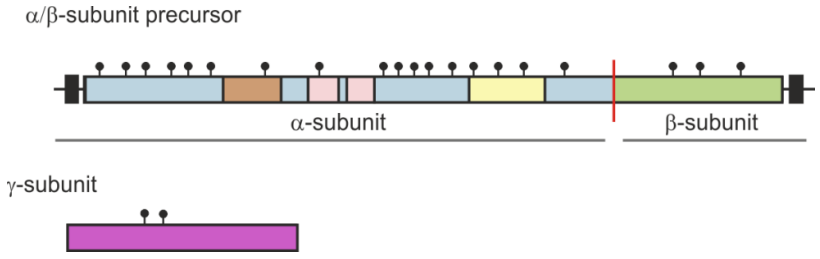

Fig. 3.1 Schematic representation of the GlcNAc-1-phosphotransferase subunits. The full length α/β-precursor containing both N- and C- terminal transmembrane domains and the soluble γ-subunit of the GlcNAc-1-phosphotransferase complex were used in these studies (detailed structural information of α/β-precursor are shown in Fig. 1.4).

3.1 Dimerization and degradation of the α/β-precursor protein of the GlcNAc-1-phosphotransferase

3.1.1 Expression analysis of monomeric and dimeric α/β-precursor

The GlcNAc-1-phosphotransferase complex contains disulfide-linked homodimers of α- and γ-subunits (Bao *et al*, 1996). The cysteine residue C245 is responsible for the dimerization of the human γ-subunit (Encarnação *et al*, 2011), whereas the cysteine residue C70 was found to be important for the dimerization of a shortened α/β-precursor containing amino acids 1 to 430 (PhD thesis, K. Marschner 2011).

Here the role of C70 for the dimer formation of the full length α/β-precursor was investigated. HeLa cells were transiently transfected with the cDNAs encoding wild-type (WT) or mutant (C70S) myc-tagged α/β-precursor protein for 24 h (Fig. 3.2 A). Cell extracts were both subjected and not subjected to PNGase F treatments. The samples were resolved by SDS-PAGE under reducing conditions followed by western blot analysis using a rat monoclonal antibody raised against the human α-subunit and an anti-myc antibody for detection of the β-subunit of the GlcNAc-1-phosphotransferase. The WT and mutant proteins were detectable as a 190 kDa α/β-subunit precursor (Fig. 3.2 B, lane 2 and 4). These immunoreactive bands were not present in extracts of non-transfected cells (lane 1). After complete deglycosylation of *N*-linked oligosaccharides by PNGase F, the molecular masses of both α/β-subunit precursors shifted to 145 kDa (lane 3 and 5).

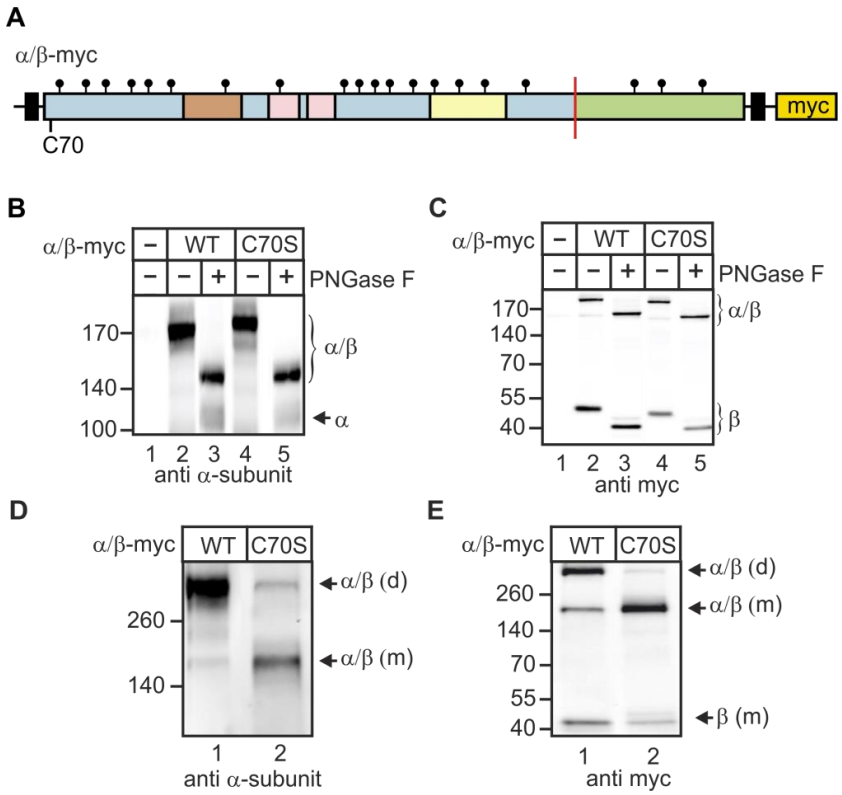

Fig. 3.2 Expression of wild-type (WT) and C70S mutant full length α/β-precursor of the GlcNAc-1-phosphotransferase. A. Schematic representation of the α/β-precursor C70S mutant C-terminally fused with a myc-tag. Lysates from HeLa cells overexpressing the wild-type (WT) or the mutant (C70S) α/β-precursor were treated (+) or not (-) with PNGase F. The samples were resolved by SDS-PAGE under reducing (B and C) or non-reducing conditions (D and E) followed by western blotting using antibodies against α-subunit (B and D) or myc (C and E). For non-reducing conditions gradient gel (8-16%) from NuSep were used. The positions of the molecular mass marker proteins in kDa, dimeric (d) and monomeric (m) α/β-precursor, α- and β-subunits are indicated. α^{dg}: deglycosylated α-subunit.

The monoclonal antibody recognized the deglycosylated α-subunit (α^{dg}) of 130 kDa but not the *N*-glycosylated form. The myc antibody detected both the *N*-glycosylated and non-glycosylated α/β-precursors as well as 45 kDa and 38 kDa cleaved β-subunits, respectively (Fig. 3.2 C). The data showed that the WT and C70S mutant α/β-precursors are highly *N*-glycosylated and transported to the Golgi apparatus where the α/β-precursor is cleaved by site-1 protease (S1P) to mature α- and β-subunits. The same cell extracts were analysed in the absence of reducing reagents to detect disulfide-linked proteins. The dimeric form (d) of α/β-myc WT was detected at a molecular mass higher than 260 kDa with both α-subunit and myc-tag antibodies (Fig. 3.2 D and E, lanes 1). A faint immunoreactive band was detectable at 190 kDa, representing minor amount of monomeric (m) α/β-precursor form. In the extract of cells overexpressing the C70S mutant a minor signal for the dimeric form was detectable, whereas the majority was present as 190 kDa monomeric α/β-precursor (Fig. 3.2 D and E, lanes 2). The myc antibody recognized also monomeric β-subunits at 45 kDa (Fig. 3.2 E). These experiments confirmed the role of cysteine 70 for the α/β-precursor homodimer formation. The presence of dimeric α/β-precursor indicates that the dimer formation takes place in the ER prior to S1P-mediated cleavage in the Golgi apparatus.

To examine the intracellular localization of monomeric and dimeric GlcNAc-1-phosphotransferase, HeLa cells were transiently transfected with wild-type and C70S α/β-myc subunit precursor cDNA followed by immunofluorescence microscopy using monoclonal antibody against the α-subunit of GlcNAc-1-phosphotransferase.

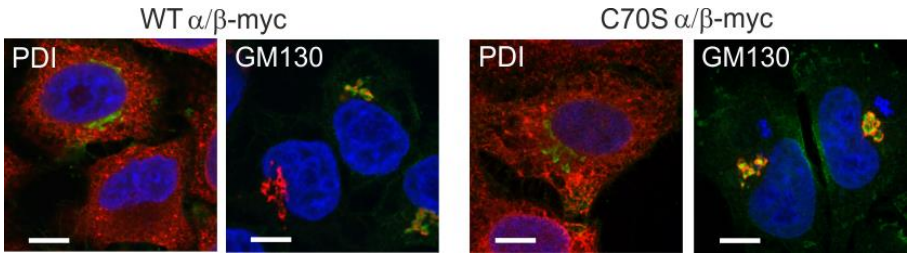

Fig. 3.3 Intracellular localization of wild-type (WT) and C70S mutant α/β-subunit precursor of the GlcNAc-1-phosphotransferase. HeLa cells were transfected with cDNA encoding the wild-type (WT) and the monomeric mutant (C70S) α/β-subunit precursor of GlcNAc-1-phosphotransferase. After 24 h cells were treated with 100 µg/ml cycloheximide for 40 min to block protein translation and release newly synthesized precursor proteins from the ER. The cells were fixed and stained with monoclonal antibodies against the α-subunit (green), the ER marker protein PDI (red) and the *cis*-Golgi marker protein GM130 (red). Nuclei were stained with DAPI (blue). Only the magnified merge images are shown. The yellow color indicates co-localization. Scale bar: 7 µm.

For co-localization analysis, stainings of endogenous organelle marker proteins for the ER and the *cis*-Golgi apparatus were included. Dimeric (WT) and monomeric (C70S) α/β-subunit precursor positive staining were found to co-localize with the *cis*-Golgi marker protein GM130 but not with the ER marker protein disulfide isomerase (PDI) (Fig. 3.3). These experiments confirm that the GlcNAc-1-phosphotransferase is a *cis*-Golgi-resident protein and indicate that the α-subunit dimerization does not influence the correct transport of the GlcNAc-1-phosphotransferase.

3.1.2 Enzymatic activity of monomeric and dimeric α/β-precursor

The α- and β-subunits contain the catalytic center of the GlcNAc-1-phosphotransferase complex (Kudo & Canfield, 2006). To analyse whether the dimer formation of the α-subunit is required for enzymatic activity of the complex, the activity of overexpressed wild-type and C70S mutant GlcNAc-1-phosphotransferase was measured. The GlcNAc-1-phosphotransferase catalyses the transfer of GlcNAc-1-phosphate from the donor UDP-GlcNAc to selected mannose residues on lysosomal enzymes (acceptor). The hydrolysis of the GlcNAc residue from the mannose 6-phosphodiester intermediate is catalysed by the GlcNAc-1-phosphodiesterase (Fig. 3.4 A). For the *in vitro* enzyme reaction ^{3}H-labelled UDP-GlcNAc and α-methylmannoside (α-MM) were used as GlcNAc-1-phosphotransferase donor and acceptor, respectively. To establish the method an initial test was performed to measure the endogenous activity of the GlcNAc-1-phosphotransferase in non-transfected HEK cells using a published protocol (Ben-Yoseph *et al*, 1984; Qian *et al*, 2013). Cell extracts (50 and 100 µg) were incubated with UDP-[^{3}H]GlcNAc as a phosphate donor and α-MM for 30, 60 and 120 min. The incorporated [^{3}H]GlcNAc-P was bound to an ion exchange matrix, washed and eluted. The eluted radioactivity was measured by scintillation counting (Fig. 3.4 B). After 60 min incubation the amonut of [^{3}H]GlcNAc-P generated from the 50 µg reaction and 100 µg reaction were in relation 1:2 as expected by using double amount of cell extracts. The 60 min incubation and 100 µg of cell extract were chosen as conditions for the following experiments since 120 min of incubation may lead to protein degradation *in vitro*. Next, HEK cells were transiently transfected with the cDNAs of WT and C70S mutant α/β-precursor for 24 h.

The GlcNAc-1-phosphotransferase activity in 100 µg cell extracts was measured under the described conditions for 60 min. For each sample an aliquot was analysed by western blotting. The activity measurements were normalised to the immunobands intensity values determined by densitometric evaluation of western blots of the same cell extracts. The activity of overexpressed wild-type GlcNAc-1-phosphotransferase was 13-fold increased compared to the non-transfected HEK cells and was set 100 % (Fig. 3.4 C). The activity of the monomeric mutant C70S was decreased by 5 % and therefore comparable to the wild-type protein. This experiment indicates that the dimer formation is not important for the activity of GlcNAc-1-phosphotransferase.

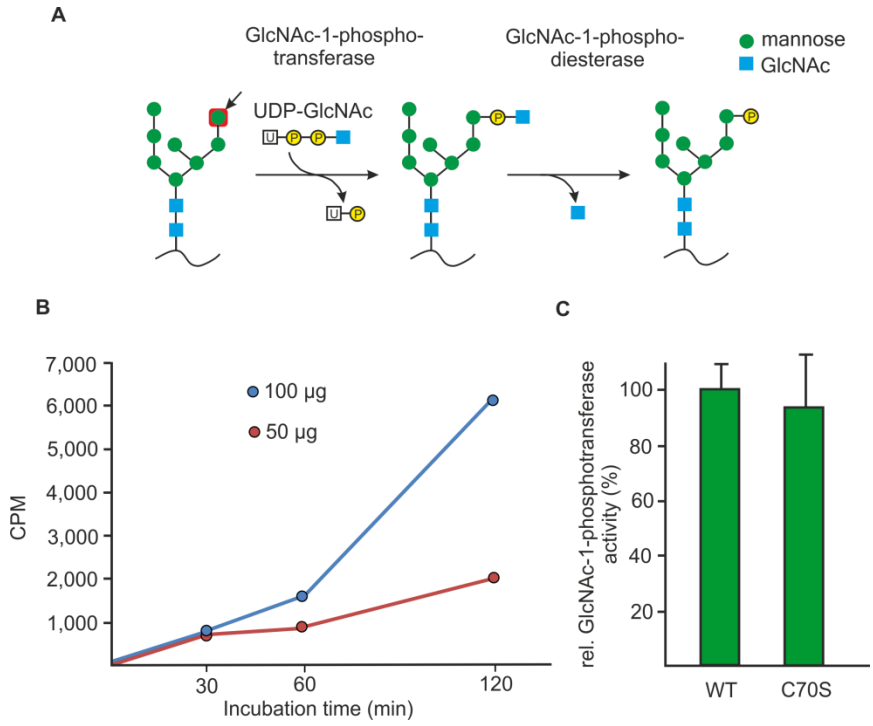

Fig. 3.4 Activity of wild-type and mutant C70S GlcNAc-1-phosphotransferase. A. Schematic representation of enzyme reaction catalysed by the GlcNAc-1-phosphotransferase and GlcNAc-1-phosphodiesterase. B. The activity of endogenous GlcNAc-1-phosphotransferase in HEK cells was determined by incubating 50 or 100 µg of total cell extracts for 30, 60 and 120 min with the reaction components. Each value represents the mean of triplicates. Afterwards the reaction was stopped and the radioactivity eluted from the ion exchange matrix was measured in counts per minutes (CPM) and plotted. C. The GlcNAc-1-phosphotransferase activity corresponding to 100 µg protein extracts of non-transfected, overexpressing wild-type or C70S mutant GlcNAc-1-phosphotransferase HEK cells was measured for 60 min. Each activity value was normalised to the β-subunit immunoband intensities determined by densitometry of western blots using aliquots of the same extracts used for activity measurements. The activity of overexpressed wild-type GlcNAc-1-phosphotransferase was set as 100 % ± the calculated standard deviation.

3.1.3 Degradation of monomeric and dimeric α/β-precursor

To investigate the effect of dimerization on the stability of the α/β-precursor and the cleaved α-subunit of the GlcNAc-1-phosphotransferase [^{35}S]methionine pulse-chase experiments were performed. HeLa cells were transiently transfected with cDNA of α/β-myc subunit precursor and C70S mutant for 24 h. Afterwards the cells were incubated for 1 h with medium containing [^{35}S]methionine.

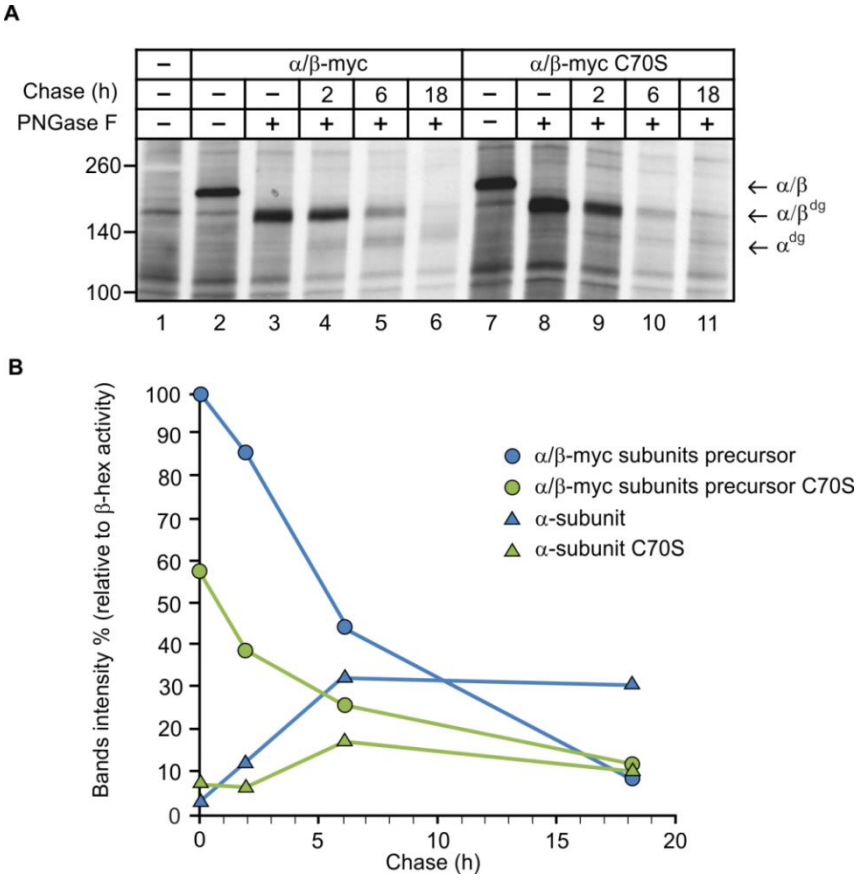

Fig. 3.5 Pulse-chase analysis of wild-type and mutant (C70S) α/β-myc subunit precursor. A. HeLa cells transiently transfected with wild-type and mutant C70S α/β-myc subunit precursor for 24 h were incubated for 1 h with medium containing [^{35}S]methionine (pulse). Afterwards the cells were immediately harvested (- chase) or the medium was replaced with fresh medium containing non-radioactive methionine and incubated for 2, 6 and 18 h (chase). The cell extracts were incubated with the antibody against the α-subunit and the immunocomplexes were precipitated with anti rat IgG agarose beads. After washing the bound proteins were subjected (+) or not (-) to PNGase F treatment. The bound material was resolved by SDS-PAGE and the labelled proteins were detected by fluorography. B. The film was subjected to densitometric analysis. The band intensities of α/β-myc subunit precursor (blue circle), α/β-myc subunit precursor C70S (green circle), α-subunit (blue triangle), and α-subunit C70S (green triangle) are shown. Each intensity value was normalised to the β-hexosaminidase (β-hex) activity in the sample. Afterwards the values were related to the normalized α/β-myc subunit precursor value at 0 h chase after PNGase F treatment (100 %) and plotted.

All newly synthesized proteins were radioactively labelled during this time period (pulse). After the pulse the cells were harvested or chased for 2, 6 and 18 h. The cell extracts were incubated with the monoclonal antibody against the α-subunit and the immunocomplexes were precipitated with anti rat IgG agarose beads. Bound proteins were both subjected and not subjected to PNGase F treatment since the monoclonal antibody recognized the deglycosylated α-subunit of 120 kDa but not the *N*-glycosylated form. All samples were afterwards resolved by SDS-PAGE followed by fluorography. In the precipitated material from extracts of cells overexpressing α/β-myc subunit precursor and mutant C70S, a 190 kDa band that was not present in the non-transfected material was detectable (Fig. 3.5 A, lane 1, 2 and 7). To distinguish between the α/β-precursor and the cleaved α-subunit, protein extracts were deglycosylated with PNGase F. The deglycosylated α/β-myc subunit precursor was detected at 160 kDa (lane 3 and 8). After 2 h of chase the α-subunit was detectable at 130 kDa, indicating that the newly synthesized α/β-myc subunit precursor reached the Golgi apparatus and was cleaved by site-1 protease (lane 4 and 9). Both the wild-type and the mutant α-subunit are still present after 6 h chase (lane 5 and 10), whereas the signal of α/β-myc subunit precursor was decreased during this time. After 18 h chase the wild-type and mutant forms are barely detectable (lane 6 and 11). For densitometric analysis the intensity of the bands were normalised to the β-hexosaminidase activity in the same cell extracts. The intensity of the α/β-myc subunit precursor protein after the pulse was set 100 % and the relative values of the other bands were calculated. After 2 h chase 15 % of the α/β-myc precursor protein is cleaved into the mature α-subunit. After 6 h and 18 h chase 50 % and 8 % of the α/β-myc precursor was detectable, respectively, whereas the α-subunit was increased by 12 % after 2 h reaching 32 % of the wild-type α/β-precursor after 6 h chase (Fig. 3.5 B). The amount of α-subunit remains stable even after 18 h chase (32 % of wild-type protein). The α/β-myc C70S precursor protein synthesized during the pulse period was 58 % compared to the wild-type polypeptide. After 2 h chase one third of the monomeric α/β-myc subunit precursor was cleaved into the mature protein. Half of the newly synthesized C70S precursor remained after 6 h chase and one third after 18 h indicating that the transport to Golgi apparatus was slower compared to the wild-type polypeptide. A low amount of α-subunit C70S was formed during the 6 h chase period, which decreased to 9 % after 18 h chase.

These data demonstrated that the monomeric form of α-subunit is fast degraded compared to the wild-type GlcNAc-1-phosphotransferase. Pulse-chase analysis of α/β-precursor proteins revealed decreased stability of the monomeric C70S mutant in comparison to the wild-type protein (Fig. 3.5). To identify the compartment involved in the degradation of wild-type and mutant α/β-precursor proteins, overexpressing cells were incubated in the absence or presence of bafilomycin A1 (BafA1), that blocks vacuolar H+ ATPase (V-ATPase), leading to inhibition of lysosomal acidification and lysosomal enzyme activities (Yoshimori *et al*, 1991). After treatment the cells were analysed by immunofluorescence microscopy using antibodies against the α-subunit of GlcNAc-1-phosphotransferase and the lysosomal marker protein LAMP1 (Fig. 3.6).

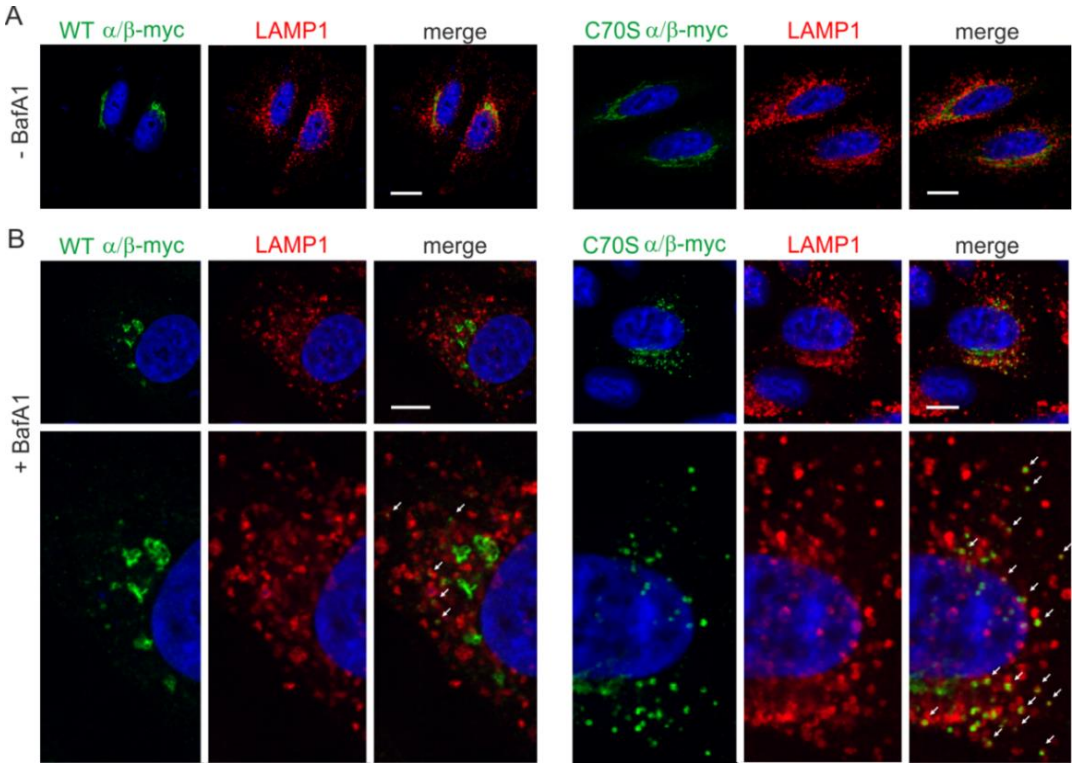

Fig. 3.6 Lysosomal localization of C70S mutant GlcNAc-1-phosphotransferase. HeLa cells were transfected with cDNA encoding the wild-type (WT) and the monomeric mutant (C70S) α/β-subunit precursor of GlcNAc-1-phosphotransferase. After 24 h cells were treated with 100 mM bafilomycin A1 (+ BafA1) (B) or not (- BafA1) (A) for 6 h to block V-ATPases and to inhibit lysosomal acidification. The cells were fixed and stained with monoclonal antibodies against the α-subunit (green) and the lysosomal marker LAMP1 (red). Nuclei were stained with DAPI (blue). Only the magnified merge images are shown.The white arrows indicates co-localization. Scale bar: 10 µm.

In non-treated cells the wild-type α/β-subunit precursor showed a typical juxtanuclear localization, which is characteristic for the Golgi apparatus, whereas the monomeric C70S mutant α/β-subunit precursor was also found in perinuclear structures (Fig. 3.6 A). No co-localizations of wild-type and C70S mutant α/β-subunit precursors were observed with the lysosomal marker protein LAMP1. In BafA1-treated cells both the wild-type and monomeric C70S α/β-subunit precursor were found in LAMP1-positive compartments (Fig. 3.6 B). An increased amount of the C70S mutant compared to the wild-type α/β-subunit precursors were found in lysosomal structures.

In the first part of the thesis the dimerization of the α/β-precursor of the GlcNAc-1-phosphotransferase via cysteine residue C70 was shown. Although the transport of monomeric α/β-precursor to the Golgi apparatus was rather slow compared to the wild-type protein, the mutant C70S is cleaved into mature α- and β-subunits showing the same catalytic activity as the wild-type protein. The mature monomeric α-subunit was degraded faster than the wild-type α-subunit. The decreased acidic pH of lysosomal compartments by BafA1 treatment resulted in an increased amount of the C70S mutant in the lysosomal compartment, suggesting that monomeric α/β-precursor is degraded in the lysosome.

3.2 Structural requirements for subunit interactions of the GlcNAc-1-phosphotransferase

In the second part of the thesis interactions between the subunits of the GlcNAc-1-phosphotransferase were analysed. Therefore different tagged constructs of the membrane-bound α/β-subunit precursor as well as the membrane-bound α- and β-subunits and the soluble γ-subunit of the GlcNAc-1-phosphotransferase (Fig. 3.1) were generated and used for subunit interaction studies by pull-down assays. In overexpressing cells the full length α/β-subunit precursor and the γ-subunit are transported to the Golgi apparatus, whereas the isolated α- and β-subunits cannot exit the ER (Encarnação *et al*, 2011; Franke *et al*, 2013). Because *N*-glycosylation, dimerization and folding are completed in the ER, pull-down assays are suitable to analyse subunit interactions of the GlcNAc-1-phosphotransferase *in vitro*.

3.2.1 Interaction between γ- and α-subunits of GlcNAc-1-phosphotransferase

To precipitate GFP-tagged subunits and their interacting proteins, GFP-Trap® beads were used as tool. GFP-Trap® is a GFP binding protein coupled to agarose beads. To perform pull-down analysis different subunits of the GlcNAc-1-phosphotransferase (Fig. 3.1) were overexpressed in HEK cells for 24 h and 500 µg of protein extracts were used as input. Aliquots (10 %) of the input cell extracts (IN) were separated for western blot analysis as control. GFP alone or GFP-fusion proteins expressed in HEK cells were precipitated using GFP-Trap® beads by incubation for 2 h at 4 °C. Afterwards 10 % of the flow through (FT) was collected. The beads were washed 3 times and 10 % of the last wash fraction (W) was collected. Afterwards the preformed GFP-fusion protein-GFP-Trap® complex was incubated for 2 h with the second cell extract (500 µg) overexpressing the protein of interest. Aliquots (10 %) of the flow through and the last wash fractions were collected. The beads and all the collected fractions were analysed by western blotting. The intensities of the co-precipitated immunoreactive polypeptides of the fractions were determined by densitometry.

As negative control for unspecific binding of proteins to the GFP-Trap® matrix, HEK cells overexpressing GFP were lysed and incubated with GFP-Trap® beads. This preformed complex was also incubated with cell lysates overexpressing the myc-tagged protein of interest. In the starting material of GFP overexpressing cells a 27 kDa band was detectable which was not present in extracts of non-transfected cells (Fig. 3.7 B, lane 1 and 2). A minor part of GFP (< 1 %) was also detectable in the flow through (FT) fraction (lane 3) but not in the last washing fraction (W) (lane 4). In the input and flow through fractions of cell extracts overexpressing the α-subunit (α-myc) a protein of 130 kDa band and a weaker doublet band at 100 kDa were observed which were absent in extracts of non-transfected cells (lanes 5 and 6). Deglycosylation of cell extracts with PNGase F resulted in the disappearance of the doublet band (Fig. 3.7 C, lane 2 and 3). This indicates that the 130 kDa protein represents the *N*-glycosylated form of the α-myc protein and the doublet band the non-glycosylated (α-myc^{dg}) and partially *N*-glycosylated forms. After incubation with GFP-Trap® beads 95 % of α-myc protein was present in the flow through (Fig. 3.7 B, lane 6) but absent in the last wash (lane 7). In the bound fraction (B) 60 % of the loaded GFP was caught up with GFP-Trap® beads but not the α-myc protein indicating that the α-subunit does not bind unspecifically to GFP (lane 8).

The interaction between the γ-subunit (γ-GFP) and the α-subunit (α-myc) was investigated under identical conditions. In the starting material corresponding to lysates of cells overexpressing γ-GFP a 64 kDa band not present in extracts of non-transfected cells was detected (Fig. 3.7 D, lane 1 and 2). Densitometric evaluations revealed that in the flow through fraction ~ 40 % of the loaded γ-GFP protein was detectable (lane 3). In the input of cell extracts overexpressing α-myc the 130 kDa band and the doublet band at 100 kDa were detected (lane 5). In the flow through fraction 80 % of the loaded myc-tagged α-subunit was detectable (lane 6). After washing no proteins were present in the wash fractions (lane 4 and 7). In the bound fraction 60 % of the γ-GFP was detectable. Interestingly, 20 % of the *N*-glycosylated but only 2 % of the non-glycosylated α-subunit were precipitated. This experiment shows the specific interaction between the γ- and the *N*-glycosylated form of the α-subunit of the GlcNAc-1-phosphotransferase *in vitro*.

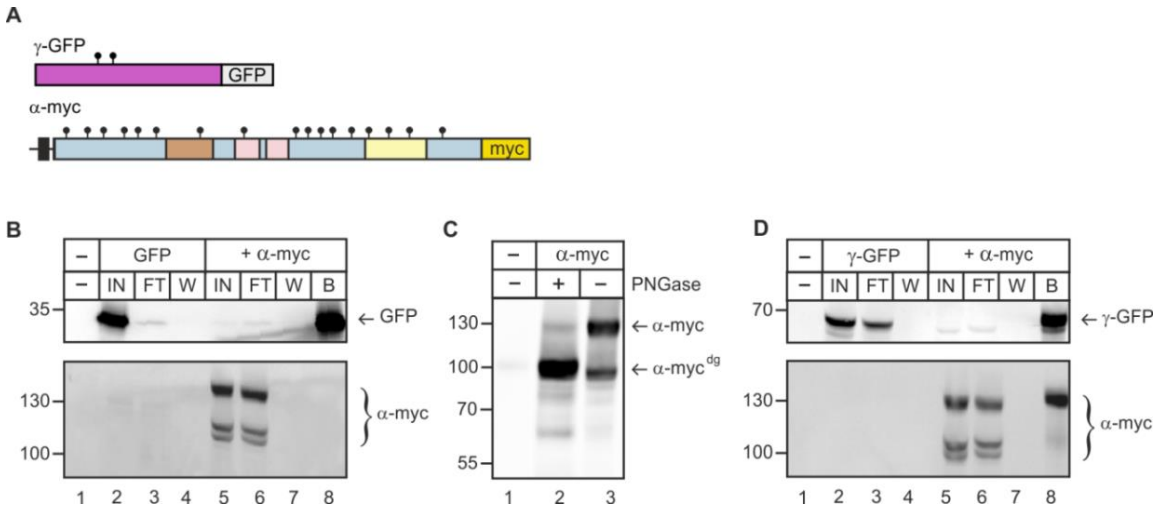

Fig. 3.7 Interaction of γ- and α-subunits of the GlcNAc-1-phosphotransferase. A. Schematic representation of the γ-subunit C-terminally fused to GFP (γ-GFP) and the isolated α-subunit C-terminally fused with a myc-tag (α-myc). Lysates from HEK cells overexpressing GFP (B) or γ-GFP (D) were used. After incubation and washing of the preformed complexes (GFP-GFP-Trap® or γ-GFP-GFP-Trap® beads), extracts from HEK cells overexpressing α-myc subunit were incubated with the beads. Aliquots of the input (IN, 10 %), flow through (FT, 10 %) and last wash (W, 10 %) fractions from the GFP protein incubation as well as the input, flow through, last wash fractions and the bound material (B, 100 %) after the α-myc incubation were resolved by SDS-PAGE followed by western blotting using antibodies against GFP or myc. C. HEK cells overexpressing α-myc subunit were subjected (+) or not (-) to PNGase F treatment. The positions of the molecular mass marker proteins in kDa, GFP, α-myc, α-myc^{dg} and γ-GFP are indicated. α-myc^{dg}: deglycosylated α-subunit.

3.2.2 Interaction between γ- and β-subunits of GlcNAc-1-phosphotransferase

To examine whether the γ-subunit (γ-GFP) interacts with the β-subunit (β-HA) (Fig. 3.8 A) of the GlcNAc-1-phosphotransferase, GFP-Trap® pull-down (PD) analysis was performed under conditions described previously. This experiment was done in parallel with GFP as negative control. Only the immunoprecipitates, along with the starting material, flow through, and the last wash step after the incubation with cell extracts overexpressing the β-subunit are shown in Fig. 3.8 B and C. In the input fraction of cell extract overexpressing β-HA the β-subunit was detectable as a 45 kDa protein (Fig. 3.8 B, lane 1). In the flow through 90 % of the loaded protein was detectable, but not in the last wash fraction (lane 2 and 3). In the bound fraction the GFP was detectable (not shown) but not the β-HA protein (lane 4). In the second experiment γ-GFP was pulled-down and the preformed complex was incubated with extracts from HEK cells overexpressing the β-HA construct. The 45 kDa β-subunit was found in the input and flow through fractions, but not in the last wash (Fig. 3.8 C, lanes 1-3). In the bound material the γ-GFP was observed (not shown) but not the β-HA protein (lane 4). These experiments showed that the γ-subunit does not interact directly with the β-subunit of the GlcNAc-1-phosphotransferase *in vitro*.

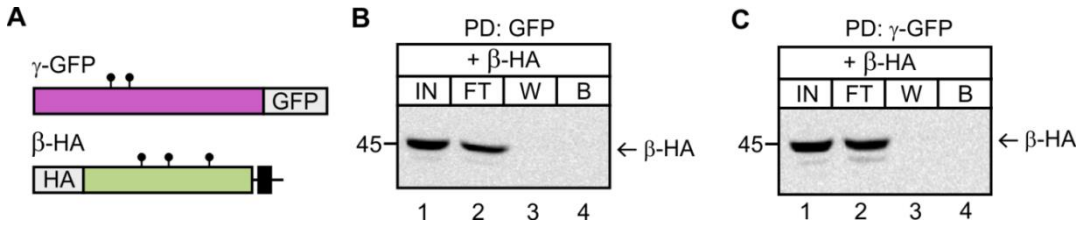

Fig. 3.8 Interaction of γ- and β-subunits of the GlcNAc-1-phosphotransferase. A. Schematic representation of the soluble γ-subunit C-terminally fused to GFP (γ-GFP) and the isolated β-subunit N-terminally fused with an HA-tag (β-HA). Lysates from HEK cells overexpressing GFP (B) or γ-GFP (C) were used. After incubation and washing of the preformed complexes (GFP-GFP-Trap® or γ-GFP-GFP-Trap® beads), extracts from HEK cells overexpressing β-HA subunit were incubated with the beads. Aliquots of the input (IN, 10 %), flow through (FT, 10 %), last wash (W, 10 %) fractions and the bound material (B, 100 %) after the β-HA incubation were resolved by SDS-PAGE followed by western blotting using antibodies against HA. The positions of the molecular mass marker proteins in kDa and β-HA are indicated.

3.2.3 Interaction between γ-subunit and α/β-precursor of GlcNAc-1-phosphotransferase

After the analysis of single subunit interactions, the *in vitro* binding between the γ-GFP and the full length α/β-precursor protein (α/β-myc) of the GlcNAc-1-phosphotransferase was investigated (Fig. 3.9 A). This experiment was done in parallel with GFP as negative control. In the starting material the 190 kDa α/β-precursor and the 45 kDa mature β-subunit were found, which were also detectable in the flow through but not in the wash fraction (Fig. 3.9 B, lanes 1-3). In the bound fraction only the GFP was pulled-down (not shown) and no myc-tagged proteins were found (lane 4), demonstrating that there is no unspecific interaction between α/β-subunit precursor and GFP. For the specific binding, extracts of HEK cells overexpressing the γ-GFP and α/β-myc were used.

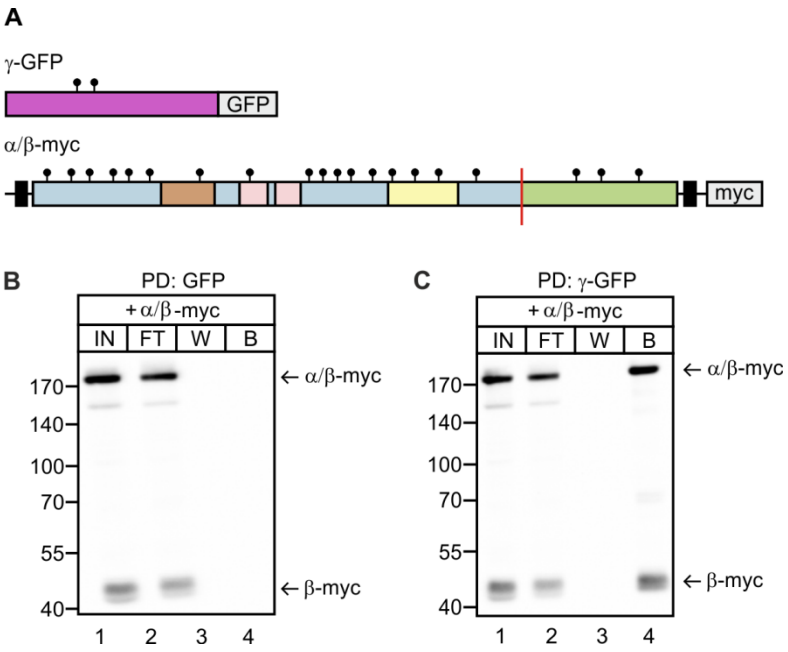

Fig. 3.9 Interaction of γ- and α/β-subunit precursor of the GlcNAc-1-phosphotransferase. A. Schematic representation of the γ-subunit C-terminally fused to GFP (γ-GFP) and full length α/β-precursor containing both membrane domains C-terminally fused with a myc-tag (α/β-myc). Lysates from HEK cells overexpressing GFP (B) or γ-GFP (C) were used. After incubation and washing of the preformed complexes (GFP-GFP-Trap® or γ-GFP-GFP-Trap® beads), extracts from HEK cells overexpressing α/β-myc were incubated with the beads. Aliquots of the input (IN, 10 %), flow through (FT, 10 %), last wash (W, 10 %) fractions and the bound material (B, 100 %) after the α/β-myc incubation were resolved by SDS-PAGE followed by western blotting using antibodies against myc. The positions of the molecular mass marker proteins in kDa, the α/β-myc and β-myc are indicated.

In the input, as well as in the flow through fractions, the α/β-precursor and the mature β-subunit were detected, but not in the last wash fraction (Fig. 3.9 C, lanes 1-3). In the bound fraction, the γ-GFP (not shown), 20 % of the loaded α/β-precursor, and the mature β-subunit were detectable (lane 4).

To confirm the obtained results *vice versa*, α/β-precursor C-terminally fused to GFP (α/β-GFP) was used to pull-down the non-tagged γ-subunit (Fig. 3.10 A). In the starting material from extracts of α/β-GFP overexpressing cells, the approximately 220 kDa α/β-precursor and the 75 kDa mature β-subunit were found (Fig. 3.10 B, lane 2), and they were not detectable in extracts of non-transfected cells (lane 1). In the flow through fraction, 20 % of the loaded α/β-GFP was detectable (lane 3), but not in the wash fraction (lane 4). In the input extracts of cells overexpressing γ-subunit protein, a 35 kDa band was observed, which was absent in lysates of non-transfected cells (lanes 1 and 5).

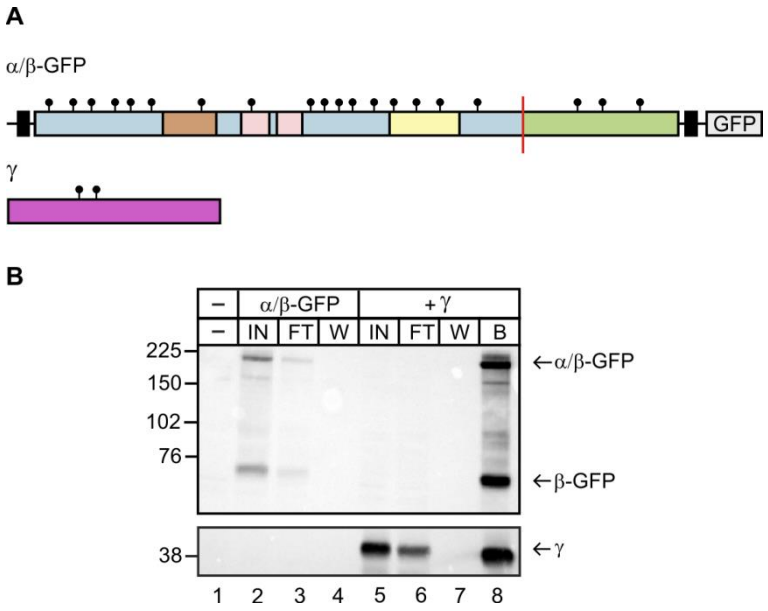

Fig. 3.10 Interaction of γ- and α/β-subunit precursor of the GlcNAc-1-phosphotransferase. A. Schematic representation of the full length α/β-precursor C-terminally fused to GFP (α/β-GFP) and non-tagged γ-subunit (γ). B. Lysate from HEK cells overexpressing α/β-GFP protein were used. After incubation and washing of preformed complexes (α/β-GFP-GFP-Trap® beads), extracts from HEK cells overexpressing the γ-subunit were incubated with the beads. Aliquots of the input (IN, 10 %), flow through (FT, 10 %), last wash (W, 10 %) fractions from the α/β-GFP incubation as well as the input, flow through, last wash fractions and the bound material (B, 100 %) after incubation with the γ-subunit were resolved by SDS-PAGE followed by western blotting using antibodies against GFP or γ-subunit. The positions of the molecular mass marker proteins in kDa, the α/β-GFP, β-GFP, and γ-subunit are indicated.

After incubation with the preformed complex, the γ-subunit was present in the flow through but not in the wash fraction (lane 6 and 7). In the bound fraction, 30 % of the loaded α/β-precursor, the mature β-subunit, as well as 20 % of the loaded γ-subunit were detectable (lane 8). These experiments demonstrated that there is a specific interaction between the γ-subunit and the α/β-precursor of the GlcNAc-1-phosphotransferase *in vitro*.

3.2.4 Interaction between α- and β-subunits of GlcNAc-1-phosphotransferase

To analyse the interaction between α- and β-subunits of the GlcNAc-1-phosphotransferase, overexpressing HA-tagged β-subunit (β-HA) was pulled-down form cell extracts with HA-agarose beads and incubated with extracts of cells overexpressing myc-tagged α-subunit (α-myc). No interaction was detectable between α-myc and β-HA subunits (not shown).

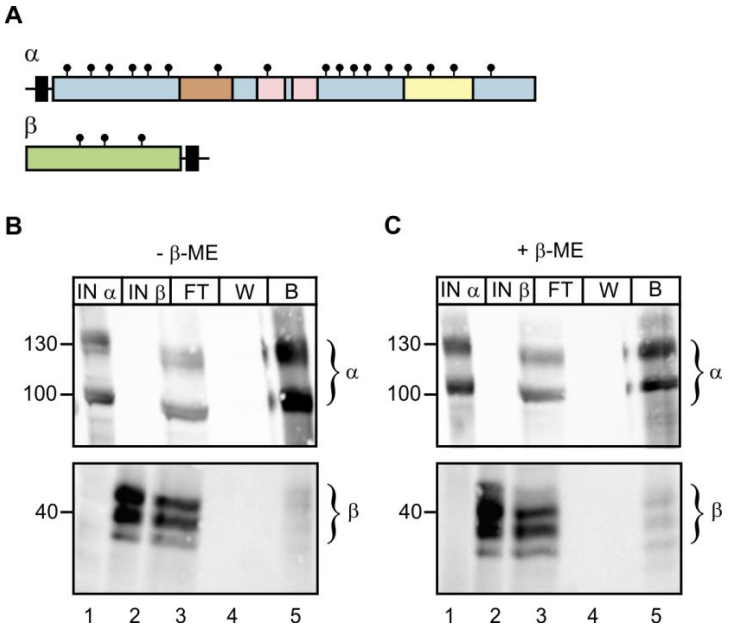

Fig. 3.11 Interaction of α- and β-subunits of the GlcNAc-1-phosphotransferase. A. Schematic representation of the α- and β-subunit (α and β). Extracts from HEK cells overexpressing α- or β-subunits were used. Equal proteins amounts of both cell extracts were incubated with the monoclonal anti α-subunit antibody in the absence (- β-ME) (B) or presence (+ β-ME) (C) of β-mercaptoethanol. The immunocomplexes were pulled-down with anti rat IgG agarose beads. Aliquots of input (IN α and IN β, 10 %), flow through (FT, 10 %), last wash (W, 10 %) fractions and the bound material (B, 100 %) were resolved by SDS-PAGE followed by western blotting using antibodies against the α- or β-subunit. The positions of the molecular mass marker proteins in kDa and the α- and β-subunits are indicated.

To exclude that the terminal tags abolish the binding between the subunits, constructs without tags were generated (Fig. 3.11 A). Equal protein amounts from cells overexpressing the α- and β-subunits were mixed and incubated for 2 h in the presence or absence of β-mercaptoethanol (β-ME). Aliquots (10 %) of each input cell extract (IN α and IN β) were separated for western blot analysis. The mixed extracts were incubated with the monoclonal antibody against the α-subunit to pull-down the complex. After over night incubation the immunocomplexes were pulled-down with anti rat IgG agarose beads. Afterwards, 10 % of the supernatant (FT) was collected. The beads were washed and 10 % of the last wash fraction (W) was separated. The beads and all aliquots of collected fractions were analysed by western blotting using antibodies against the α- or β-subunit. In the starting material of α-subunit overexpressing cells the 130 kDa *N*-glycosylated form of the α-subunit and the non-glycosylated and partially glycosylated doublet bands were detectable (Fig. 3.11 B and C, lane 1). In the starting material of cells overexpressing the β-subunit a 45 kDa band was observed, but also two lower bands indicating a partial *N*-glycosylation of the overexpressed protein (Fig. 3.11 B and C, lane 2). The α- and β-subunits were also observed in the flow through fractions (lane 3), but not in the last wash fractions (lane 4). Under non-reducing conditions (- β-ME) only the α-subunit was detectable in the bound fraction (Fig. 3.11 B, lane 5). In the presence of β-ME the α-subunit was detectable, as well as a faint signal of the β-subunit (Fig. 3.11 C, lane 5). This experiment shows a week interaction between the α- and β-subunits of the GlcNAc-1-phosphotransferase *in vitro*.

3.2.5 Role of *N*-glycosylations in the interaction between the γ- and α-subunits of the GlcNAc-1-phosphotransferase

It was shown that the γ-subunit interacts only with *N*-glycosylated α-subunits (Fig. 3.7). The γ-subunit is *N*-glycosylated at asparagine residues N88 and N115 (Encarnação *et al*, 2011). To analyse the role of *N*-glycosylations for the interaction of α- and γ-subunits, single glycosylated mutants of the γ-subunit (N88Q; N115Q) or non-glycosylated γ-subunit (N88,115Q) fused to GFP were used to pull-down the α-myc subunit. In all input fractions the 130 kDa glycosylated form and the ~100 kDa non-glycosylated doublet of α-myc were detected (Fig. 3.12 B, lane 1).

The proteins were found in the flow through but not in the last wash fraction (lanes 2 and 3). In the solubilized bound material all γ-GFP mutants were detected (not shown) together with the *N*-glycosylated form of α-subunit (lane 4). Densitometric analysis revealed that the binding of the α-myc subunit to the γ-subunit mutant N115Q (20 % of loaded protein) was comparable with the binding of the wild-type γ-subunit (Fig. 3.7).

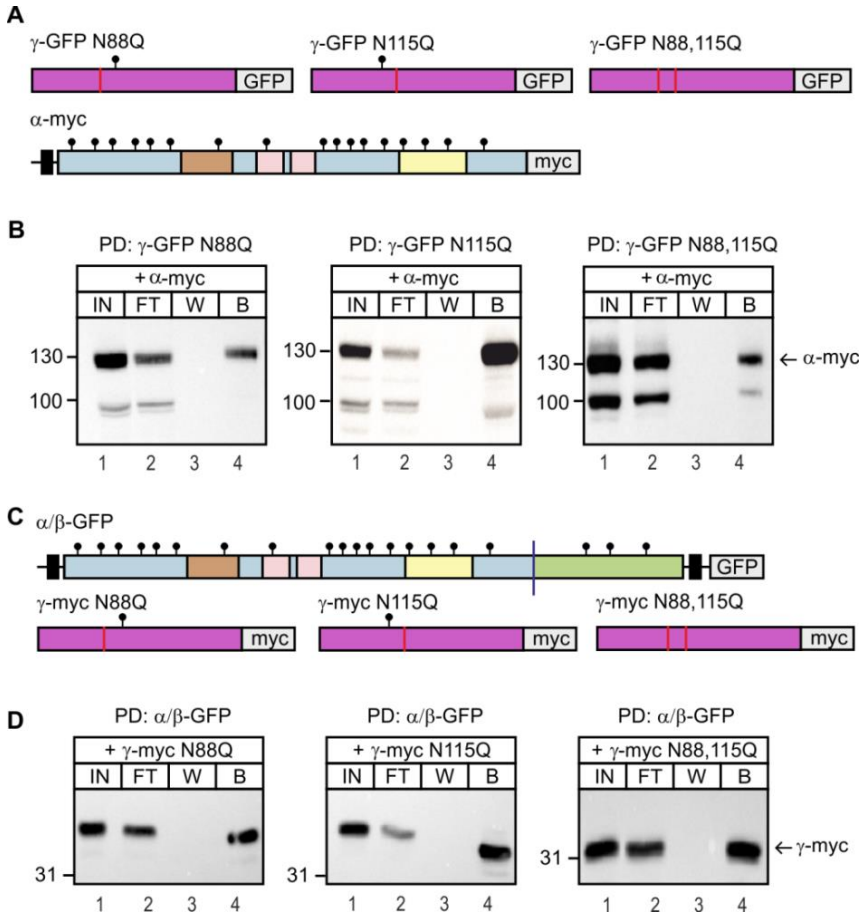

Fig. 3.12 Interaction of *N*-glycosylation mutants of the γ-subunit and the α-subunit or α/β-precursor protein. A and C. Schematic representation of the full length α/β-precursor C-terminally fused to GFP (α/β-GFP) and myc-tagged γ-subunit (γ-myc) as well as the γ-subunit fused GFP (γ-GFP) and the isolated α-subunit fused with a myc-tag (α-myc). Mutants of γ-myc and γ-GFP missing single (N88Q; N115Q) or both (N88,115Q) *N*-glycosylations sites (indicated by a red line) are shown. Lysates from HEK cells overexpressing γ-GFP mutants missing both (N88,115Q) or single (N88Q; N115Q) *N*-glycosylations sites (B) or α/β-GFP (D) were used. After incubation and washing of the preformed complexes, extracts from HEK cells overexpressing α-myc (B) or γ-myc mutants (D) were incubated with the beads. Aliquots of the input (IN, 10 %), flow through (FT, 10 %), last wash (W, 10 % of) fractions and bound material (B, 100 %) after the α-myc (B) or γ-myc mutants (D) incubation were resolved by SDS-PAGE followed by western blotting using antibodies against myc. The positions of the molecular mass marker proteins in kDa, the α-myc, and the γ-myc are indicated.

10 % of the α-myc subunit were found in the binding fraction with the γ-subunit mutants N88Q and N88,115Q. In the *vice versa* experiment the α/β-precursor (α/β-GFP) was used to pull-down the different *N*-glycosylation mutants of the γ-myc subunit. In the input fractions 36 kDa proteins (γ-myc N88Q or N115Q) and 32 kDa (γ-myc N88,115Q) were observed respectively (Fig. 3.12 D, lane 1). After incubation with the preformed complexes, the γ-subunits are present in the flow through but not in the wash fractions (lanes 2 and 3). In the bound material the α/β-GFP was found (not shown) together with the γ-myc mutants (lane 4). Whereas 20 % of the loaded γ-subunit N115Q mutant was present in the bound material, only 5 % of the γ-subunit N88Q and N88,115Q mutants were detected. These experiments suggest that *N*-glycosylations of γ-subunit do not play a role in the subunit interactions of the GlcNAc-1-phosphotransferase.

3.2.6 Role of γ-subunit and α-subunit dimerization for subunits interaction of the GlcNAc-1-phosphotransferase

Both the α- and the γ-subunit form disulfide linked homodimers mediated by cysteine residues C70 (Fig. 3.2) (PhD thesis, K. Marschner 2011) and C245, respectively (Encarnação *et al*, 2011). Single cysteine substitution results in monomeric subunit forms which were used to investigate the role of dimer formation for the interaction of α- and γ-subunits. In the first experiment, γ-GFP was used to pull-down the monomeric α/β-precursor (α/β-myc C70S). In the starting material, bands of approximately 190 kDa (α/β-myc C70S precursor) and 45 kDa (β-myc C70S) were found, which were also detectable in the flow through but not in the wash fraction (Fig. 3.13 B, lanes 1-3). In the bound fraction, the γ-GFP subunit (not shown), 30 % of loaded α/β-myc C70S precursor, and the mature β-myc proteins were detected (lane 4). In the second experimental approach the γ-subunit monomer mutant (γ-GFP C245S) was used to pull-down the α/β-myc precursor protein. In the input fractions, polypeptides of 190 kDa (α/β-myc precursor) and 45 kDa (β-myc) were observed, which were also detectable in the flow through but not in the wash fraction (Fig. 3.13 C, lanes 1-3). In the bound material, the γ-GFP C245S (not shown), 30 % of loaded α/β-myc, and β-myc proteins were detected (lane 4).

To investigate the interaction between the monomeric γ-subunit and the α-subunit, γ-GFP C245S was used to pull-down the α-myc subunit. In the starting material, bands of 130 kDa and a doublet band of 100 kDa were detected (Fig. 3.13 D, lane 1). In the flow through myc-tagged α-subunit was observed, but not in the wash fraction (lanes 2 and 3). In the bound material the γ-GFP C245S (not shown) and 20 % of the glycosylated form of α-myc were found (lane 4). These experiments show that there is a specific interaction between the γ-subunit, the α/β-precursor, and the isolated α-subunit of the GlcNAc-1-phosphotransferase *in vitro* independently of the dimerization state of both the γ- and α-subunits.

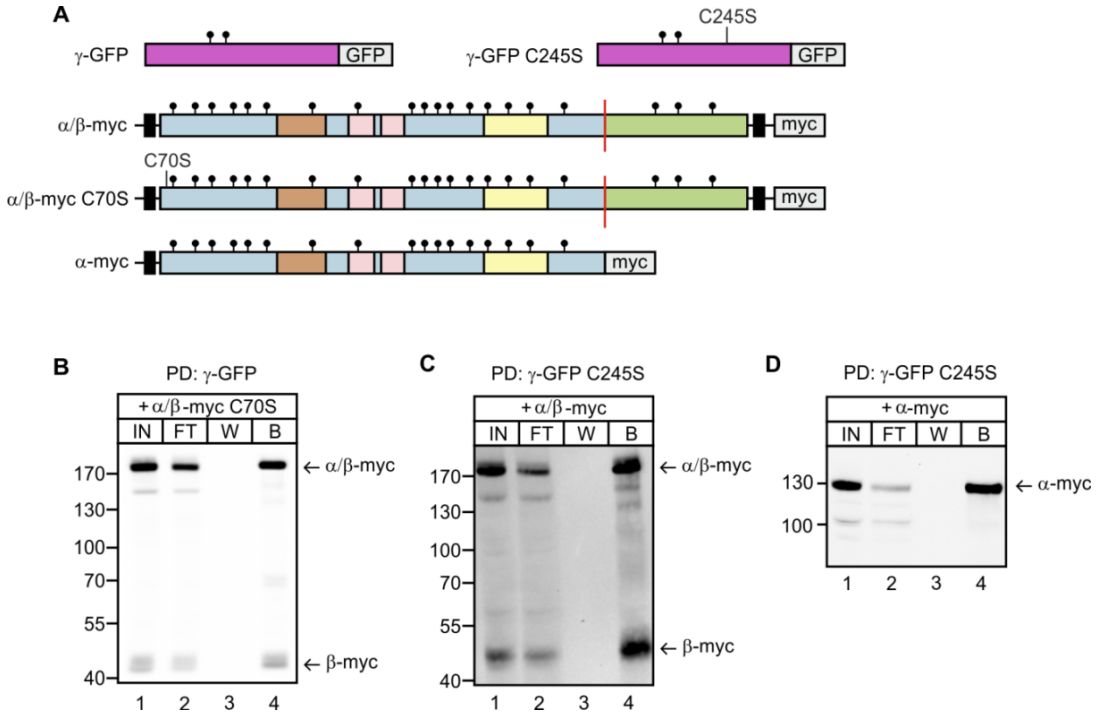

Fig. 3.13 Interaction of monomeric γ-subunit with monomeric α-subunit and α/β-subunit precursor of the GlcNAc-1-phosphotransferase. A. Schematic representation of GFP-tagged γ-subunit (γ-GFP) and γ-GFP mutant (C245) as well as the full length α/β-subunit precursor, α/β-subunit precursor mutant (C70S) and isolated α-subunit C-terminally fused with a myc (α/β-myc, α/β-myc C70S and α-myc). Lysates from HEK cells overexpressing γ-GFP (B) and γ-GFP C245S (C and D) were used. After incubation and washing of preformed complex (γ-GFP-GFP-Trap® or γ-GFP C245S-GFP-Trap® beads), extracts from HEK cells overexpressing α/β-myc C70S (B), α/β-myc (C), and α-myc (D) were incubated with the beads. Aliquots of the input (IN, 10 %), flow through (FT, 10 %), last wash (W, 10 %) fractions as well as the bound material (B, 100 %) were resolved by SDS-PAGE followed by western blotting using antibodies against myc. The positions of the molecular mass marker proteins in kDa, α/β-myc, β-myc, and α-myc are indicated.

3.2.7 Identification of α-subunit region required for interaction with γ-subunit

The α-subunit of the GlcNAc-1-phosphotransferase comprises a complex and preserved modular structure with several domains (Tiede *et al*, 2005b). To define the region of the α-subunit that is responsible for the interaction with the γ-subunit, first an α*/β-mini construct was used (Fig. 3.14 A). The α*/β-mini construct misses the amino acids 431-848 and exhibits i) identical topology, ii) N- and C-terminal ER exit signal sequences and iii) structural requirements for efficient proteolytic cleavage by site-1 protease as the full length α/β-precursor (Marschner *et al*, 2011). To examine whether the γ-subunit interact with the α*/β-mini construct pull-down experiments were performed. In parallel, GFP was used as negative control. In the input fraction the 125 kDa α*/β-mini precursor and the 80 kDa α*-subunit were detectable (Fig. 3.14 B, lane 1), which were also detectable in the flow through but not in the wash fraction (lanes 2 and 3). In the bound fraction only the GFP was pulled-down (not shown) whereas neither α*/β- nor α*-proteins were found (lane 4) demonstrating that there is no unspecific interaction between α*/β-mini and GFP.

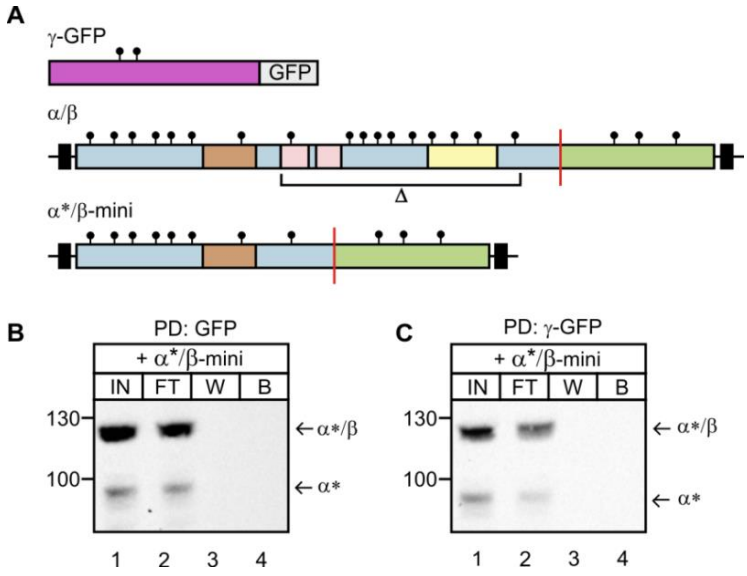

Fig. 3.14 Interaction of γ-subunit and α*/β-mini precursor of the GlcNAc-1-phosphotransferase. A. Schematic representation of GFP-tagged γ-subunit (γ-GFP), the full length α/β-precursor and the α*/β-mini precursor missing the amino acids 431-848 (α*/β-mini). Lysates from HEK cells overexpressing GFP (B) or γ-GFP (C) were used. After incubation and washing of the preformed complexes (GFP-GFP-Trap® or γ-GFP-GFP-Trap® beads), extracts from HEK cells overexpressing α*/β-mini were incubated with the beads. Aliquots of the input (IN, 10 %), flow through (FT, 10 %), last wash (W, 10 %) fractions and bound material (B, 100 %) after the α*/β-mini incubation were resolved by SDS-PAGE followed by western blotting using antibodies against the α-subunit. The positions of the molecular mass marker proteins in kDa, the α*/β, and α* are indicated.

In the second experiment the γ-GFP was used to pull-down the α*/β-mini construct precursor. Both in the input and in the flow through fraction the α*/β-mini precursor and the mature α*-subunit were detected, but not in the wash fraction (Fig. 3.14 B, lanes 1-3). In the fraction of γ-GFP precipitated proteins, the γ-GFP was detected (not shown) but neither the α*/β-mini precursor nor the mature α*-subunit were observed (lane 4). This experiment shows that the γ-subunit does not bind to the α*/β-mini precursor and suggests that the region responsible for the binding of the γ-subunit is located between the amino acids 431 and 848 of the α-subunit.

To further define the region responsible for the interaction between α- and γ-subunits, two constructs missing two homology domains, the Notch-like repeated, and DMAP domains, both absent in the α*/β-mini precursor, were tested. First, the Notch homology domain, spanning a region from amino acid 433 to 535, was deleted from the the α-subunit (α Δ-Notch) (Fig. 3.15 A).

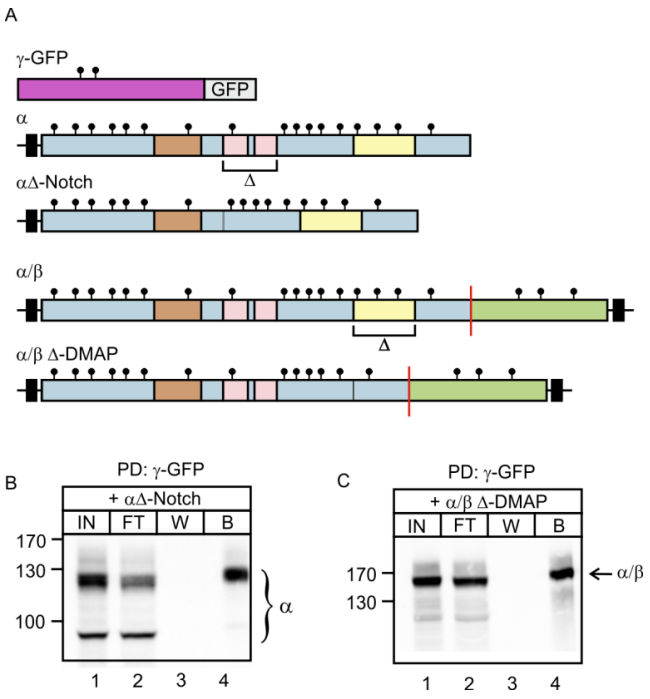

Fig. 3.15 Interaction of γ-subunit with α-subunit Δ-Notch and α/β-precursor Δ-DMAP of the GlcNAc-1-phosphotransferase. A. Schematic representation of GFP-tagged γ-subunit (γ-GFP), the α-subunit missing the amino acids 433-535 (α Δ-Notch) and the α/β-precursor protein missing the amino acids 698-819 (α/β Δ-DMAP). Lysates from HEK cells overexpressing γ-GFP were used. After incubation and wash of the preformed complexes (γ-GFP-GFP-Trap® beads), extracts from HEK cells overexpressing α Δ-Notch (B) or α/β Δ-DMAP (C) were incubated with the beads. The input (IN, 10 %), flow through (FT, 10 %), wash (W, 10 %) and bound material (B, 100 %) were resolved by SDS-PAGE followed by western blotting using antibodies against the α-subunit. The positions of the molecular mass marker proteins in kDa, the α, and the α/β are indicated.

The γ-GFP was used to pull-down the α Δ-Notch protein. In the input fraction the *N*-glycosylated ~125 kDa α Δ-Notch protein was detectable (Fig. 3.15 B, lane 1), which was also present in the flow through, but not in the wash fraction (lanes 2 and 3). In the bound fraction the γ-GFP subunit was found (not shown) together with the *N*-glycosylated form of α Δ-Notch subunit (lane 4), demonstrating that the Notch homology domain of the α-subunit is not responsible for the interaction with the γ-subunit of the GlcNAc-1-phosphotransferase. The DMAP homology domain comprises the amino acids 698-814. As template the cDNA of full length α/β-precursor protein was used to delete this domain (α/β Δ-DMAP) (Fig. 3.15 A). In the input fraction the ~150 kDa α/β Δ-DMAP precursor was detectable (Fig. 3.15 C, lane 1), which was also present in the flow through but not in the wash fraction (lanes 2 and 3). In the bound fraction the γ-GFP was pulled-down (not shown) together with the α/β Δ-DMAP (lane 4). This experiment shows that the binding of the γ-subunit to the α/β-precursor of the GlcNAc-1-phosphotransferase does not depend on the DMAP domain. In parallel, the potential interaction of the γ-subunit with the Notch-like repeat domain of the α-subunit was investigated with a different approach. The region comprising the Notch-like domain from aa 433-535 (NI) and a longer region from aa 366-565 (NII) were inserted into the C-terminal part of the human N-acetylgalactosamine 4-sulfate 6-O-sulfotransferase (ST) (Fig. 3.16 A). This protein is a type II Golgi-resident protein and exhibits the same topology than the α-subunit. The γ-GFP was used to pull-down the ST constructs. In the input fractions the ST (~60 kDa), the ST-NI (~65 kDa), the ST-NII (~70 kDa) as well as the α-subunit, which was used as positive control, were detectable (Fig. 3.16 B, lanes 1-4). In the bound fractions the γ-GFP subunit was found (not shown) but no ST wild-type or fusion proteins were detected (lanes 5-7). The bound fraction from the α-myc pull-down contains both the γ-GFP (not shown) and the α-myc (lane 4), confirming the interaction between γ- and α-subunits (Fig. 3.7). This experiment confirms that the Notch homology domain of the α-subunit is not responsible for the interaction with the γ-subunit of the GlcNAc-1-phosphotransferase.

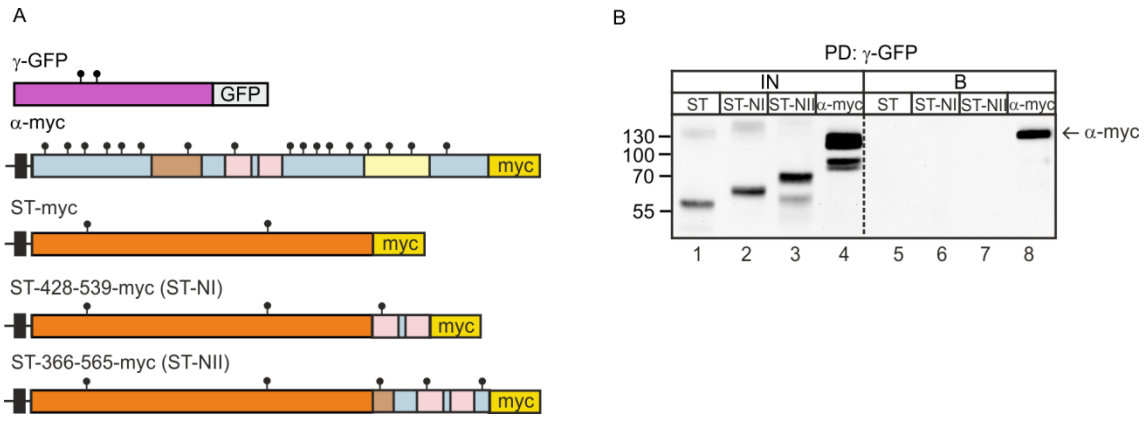

Fig. 3.16 Interaction of γ-subunit with α-subunit, wild-type N-acetylgalactosamine 4-sulfate 6-O-sulfotransferase (ST) and fusion constructs of ST. A. Schematic representation of GFP-tagged γ-subunit (γ-GFP), the α-subunit (α-myc) and the ST protein C-terminally fused with the aa 428-539 (ST-NI), and aa 366-565 (ST-NII). B. Lysates from HEK cells overexpressing γ-GFP were used. After incubation and wash of the preformed complexes (γ-GFP-GFP-Trap® beads), extracts from HEK cells overexpressing α-myc, ST-NI and ST-NII were incubated with the beads. The input (IN, 10 %), flow through (FT, 10 %), wash (W, 10 %) and bound material (B, 100 %) were resolved by SDS-PAGE followed by western blotting using antibodies against the α-subunit. The positions of the molecular mass marker proteins in kDa, and the α-myc are indicated.

Taken together, detailed *in vitro* pull-down analysis showed the direct interaction of the γ-subunit with the α-subunit, but not with the β-subunit of the GlcNAc-1-phosphotransferase. The γ-subunit interacted also with the α/β-precursor, suggesting that the subunits assembly takes place in the ER. The β-subunit was found to interact weakly with the α-subunit. The γ-subunit interacted preferentially with the *N*-glycosylated form of the α-subunit. The dimerization of the α- and γ-subunits do not affect the interaction between both subunits. The region of the α-subunit that is most likely responsible for the binding to the γ-subunit is located in the *N*-glycosylated region comprising amino acids 535 to 698 of the α-subunit.

3.3 Analysis of mucolipidosis II- and III-related mutations

Up to date, more than 125 different mutations of *GNPTAB*, encoding the α/β-subunit precursor of the GlcNAc-1-phosphotransferase, have been described to cause mucolipidosis (ML) type II and III alpha/beta (Human Gene Mutation Database, www.hgmd.org).

In general MLII alpha/beta patients with a more severe course of the disease have nonsense, frameshift or splice-site mutations in *GNPTAB* whereas MLIII alpha/beta patients with a milder course of disease carry missense mutations. In the second part of this thesis, the effects of various mutations in *GNPTAB* that were identified in MLII and MLIII alpha/beta patients from different populations in both homozygous and heterozygous states, on the stability, subcellular localization, proteolytic cleavage, and enzymatic activity of the GlcNAc-1-phosphotransferase were investigated.

3.3.1 Generation of mutant *GNPTAB* cDNA constructs

To examine the effects of disease-causing *GNPTAB* mutations, different constructs were generated.

Table 3.1 Insertion of patient mutations in α/β-full length and α/β-mini construct of GlcNAc-1-phosphotransferase.*

Mutation, cDNA, protein	α/β-full length	α*/β-mini
c.1196C>T, p. S399F	X	X
c.3707A>T, p.K1236M	X	X
c.242G>T, p.W81L	X	X
c.2956C>T, p.R986C	X	X
c.3145insC, p.G1049R*fs*X16	X	X
c.3503_3504delTC, p.L1168Q*fs*X5	X	X
c.1208T>C, p.I403T	X	-
c.1514G>A, p.C505Y	X	-
c.1723G>A, p.G575R	X	-
c.1931_1932CA>TG, p.T644M	X	-
c.2808A>G, p.Y937_M972del	X	-
c.3668_3670delCTA, p.T1223del	X	-
c.1759C>T, p.R587X	X	-
c.2269_2273delGAAAC, p.E757K*fs*X1	X	-

Used (X) or not (-) as template for mutagenesis.

The *GNPTAB* mutations were inserted by site-directed mutagenesis into the cDNA encoding either the wild-type, full length, or α*/β-mini construct. The subsequent changes on the protein level are indicated in Table 3.1 (mutations on cDNA sequence and position of the tag are listed in Table 2.6 and 2.7).

3.3.2 Expression and localization of α*/β-mini precursor mutants of GlcNAc-1-phosphotransferase

Two missense mutations, W81L and R986C, and two frameshift mutations, G1049R*fs*X16 and L1168Q*fs*X5, found in severely affected MLII patients, as well as two missense mutations, S399F and K1236M, associated with a slower progression of the MLIII alpha/beta disease were inserted in the α*/β-mini construct. The studied mutations are not located in the region that is missing in the α*/β-mini precursor. The α*/β-mini construct allows a more efficient and invariable expression than the full length α/β-precursor (Marschner *et al*, 2011). To analyse the effect of these mutations in the α*/β-subunit mini precursor on expression, stability and proteolytic cleavage into mature α*- and β-subunits, HEK cells were transiently transfected with the cDNA encoding wild-type and mutant α*/β-mini precursor (Table 3.1). The cells extracts were analysed by western blotting using specific antibodies against the α- and β-subunits of human GlcNAc-1-phosphotransferase. In cell extracts overexpressing the wild-type mini construct a 120 kDa α*/β-subunit precursor, a 75 kDa α*-subunit, and 45 kDa β-subunit were detectable, which were not present in extracts of non-transfected cells (Fig. 3.17, lanes 1 and 2). The presence of the cleaved α*- and β-subunits demonstrated the correct transport of the α*/β-mini construct to the Golgi apparatus where the α*/β-precursor is cleaved by the site-1 protease into mature subunits. After complete deglycosylation of *N*-linked oligosaccharides by PNGase F, the molecular masses of the α*/β-subunit precursor, α*- and β-subunits shifted to 90, 50 and 38 kDa, respectively (lane 3). In protein extracts of cells overexpressing the missense mutant S399F, only the α*/β-subunit precursor proteins were observed, but not the cleaved α*- and β-subunits (lanes 4 and 5). In protein extracts of cells overexpressing the missense mutant W81L, most of the immunoreactive bands corresponds to the α*/β-subunit precursor protein. Only faint bands were observed for the cleaved α*- and β-subunits (lanes 8 and 9). The amounts of expressed S399F and W81L mutants were comparable to the wild-type protein. The expression levels of the mutant K1236M and R986C precursor were decreased by approximately 60 % and 20 % in comparison to the wild-type polypeptide, respectively. Both mutants were cleaved into mature α*- and β-subunits (lanes 6, 7, 10, and 11). In protein extracts of cells overexpressing the frameshift mutations G1049R*fs*X16 or L1168Q*fs*X5, the *N*-glycosylated α*/β-subunit truncated precursor proteins were shifted to 90 and 110 kDa, respectively.

Neither cleaved α*- nor β-subunits were detectable (lanes 12-15). The expression level of both mutants was decreased by approximately 50 % compared to the wild-type protein.

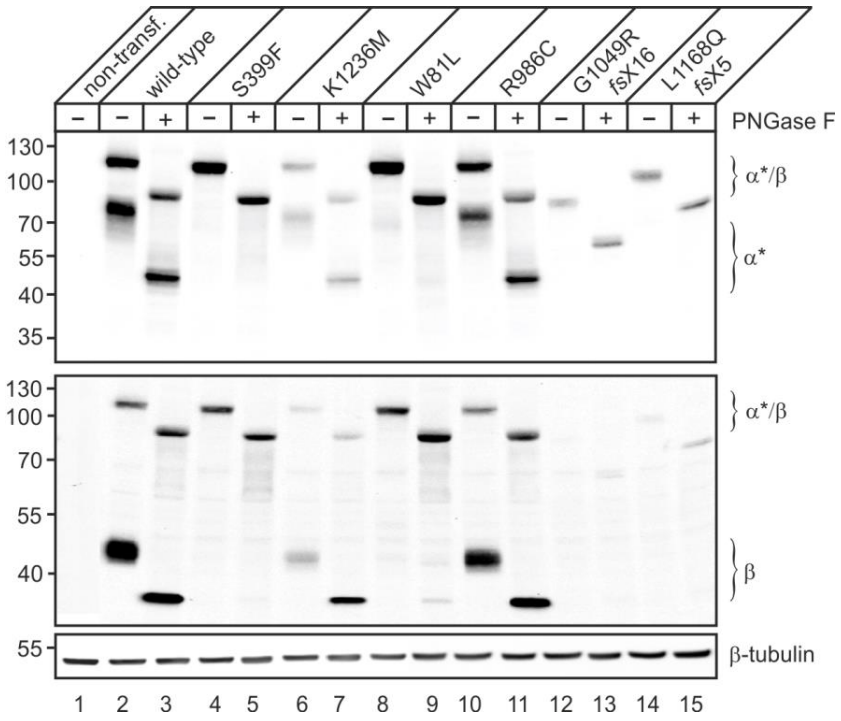

Fig. 3.17 Expression and proteolytic cleavage analysis of wild-type and mutant α*/β-mini constructs. HEK cells were transfected with cDNA encoding wild-type and mutant α*/β-mini constructs of GlcNAc-1-phosphotransferase for 24 h. Cell extracts were prepared and incubated for 1 h in the presence (+) or absence (−) of PNGase F followed by SDS-PAGE (10 % acrylamide) under reducing conditions. Immunoreactive bands were detected with a monoclonal antibody against the α-subunit or a polyclonal antibody against the β-subunit. The expression of the endogenous β-tubulin was used as loading control. Extracts of non-transfected cells were used as negative control. The positions of α*/β-precursor, α*-subunit, β-subunit, and molecular mass marker proteins in kDa are indicated.

To determine whether the variations observed at the protein level between the wild-type and mutant α∗/β-mini construct result from differences in the amounts of transcripts, the *GNPTAB* mRNA levels of the overexpressed constructs were analysed by quantitative real-time PCR. In comparison to the endogenous *GNPTAB* mRNA level in non-transfected HEK cells, the transcript levels of overexpressed wild-type *GNPTAB* was increased 350-fold and was set to 100 % (Fig. 3.18). The mRNA expression levels of overexpressed mutants S399F, W81L and R986C were 65 %, 111 % and 97 % of the wild-type transcript level, respectively.

According to the observations by western blotting (Fig. 3.17), the transcript levels of the mutants K1236M, G1049R*fs*X16 and L1168Q*fs*X5 were only 25 %, 17 % and 14 % compared to the overexpressed *GNPTAB* wild-type mRNA level suggesting that these mutant mRNAs are unstable (Fig. 3.18).

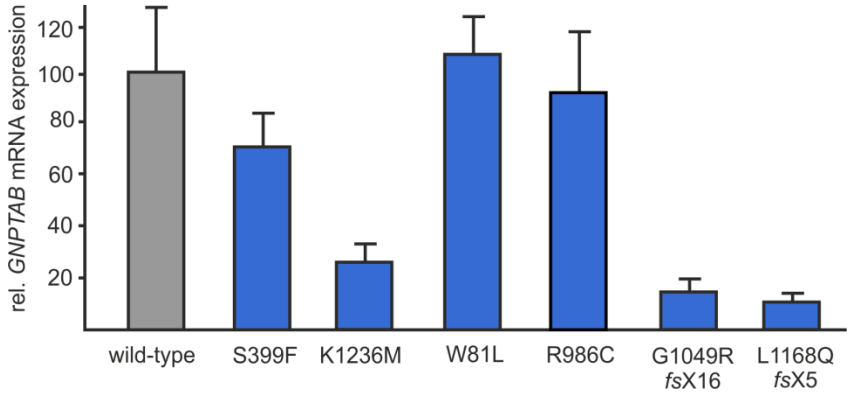

Fig. 3.18 Analysis of mRNA expression of overexpressed wild-type and mutant α*/β-mini precursor in HEK cells. The relative *GNPTAB* mRNA levels of overexpressed wild-type and mutant α*/β-mini constructs were determined 24 h post transfection by real-time PCR and normalized to actin (*ACTB*) mRNA expression (mean ± SD, n = 3). The mRNA expression of the overexpressing wild-type *GNPTAB* in HEK cells was 350-fold increased compared to the endogenous level and was assigned as 100 %.

The mature α- and β-subunits of the full length and mini construct of the GlcNAc-1-phosphotransferase are localized in the Golgi apparatus (Marschner *et al*, 2011; Tiede *et al*, 2005a). To analyse how mutations in the GlcNAc-1-phosphotransferase affect the intracellular localization, HeLa cells overexpressing the wild-type and mutant α*/β-mini precursor constructs were analysed by immunofluorescence microscopy using an antibody against the α-subunit of the GlcNAc-1-phosphotransferase.

Wild-type α*/β-subunit precursors were found to co-localize with the *cis*-Golgi marker protein GM130 but not with the ER marker protein PDI (Fig. 3.19) (Marschner *et al*, 2011). The majority of the S399F mutant co-localized with PDI, but small amounts of the mutant GlcNAc-1-phosphotransferase reached GM130-positive Golgi structures. As expected by the presence of cleaved α*-subunits (Fig. 3.17), the mutants K1236M and R986C were correctly targeted to the Golgi apparatus and showed co-localization with GM130 but not with PDI (Fig. 3.19).

A complete co-localization with the ER marker PDI, but no localization in the Golgi apparatus, was observed in cells overexpressing the mutant W81L, the frameshift mutants G1049R*fs*X16, and L1168Q*fs*X5 (Fig. 3.19), accompanied by the failure of the mutant α*/β-subunit precursors to be proteolytically processed (Fig. 3.17).

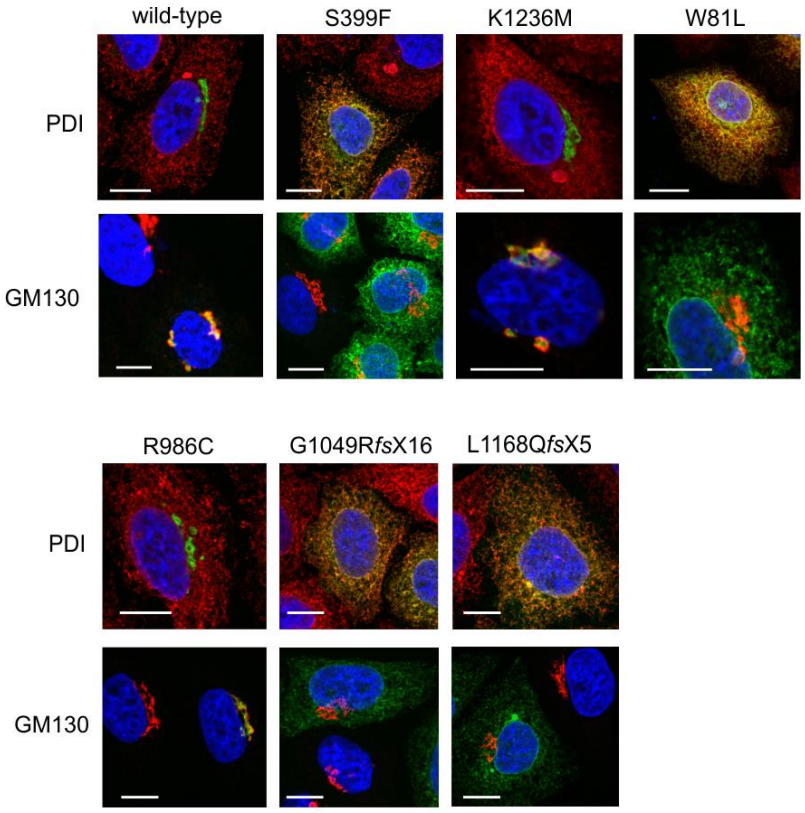

Fig. 3.19 Intracellular localization of wild-type and mutant α*/β-mini precursor of the GlcNAc-1-phosphotransferase. HeLa cells were transfected with cDNAs encoding the wild-type or mutant α*/β-mini precursor for 24 h. Cells were treated with 100 µg/ml cycloheximide for 40 min to block protein translation and release of newly synthesized precursor proteins from the ER. Cells were fixed and stained with monoclonal antibodies against the α-subunit (green), the ER marker protein PDI (red) or the *cis*-Golgi marker protein GM130 (red). Nuclei were stained by DAPI (blue). Only the magnified merge images are shown. The yellow color indicates co-localization. Scale bar: 10 µm.

The MLII mutation affecting the tryptophan at position 81 is located close to cysteine 70, responsible for the dimerization of the α-subunit (Fig. 3.2 and 3.20 A). To investigate whether the mutant W81L is able to form disulfide linked dimers, extracts from HEK cells overexpressing wild-type as well as mutant C70S or W81L α*/β-mini constructs were resolved by SDS-PAGE under non-reducing conditions followed by western blotting.

In extracts from cells overexpressing the wild-type α*/β-mini construct, the α*/β-precursor dimer (d) and monomer (m) were detected at 240 kDa and 120 kDa, respectively (Fig. 3.20 B, lane 1). The dimeric and monomeric α*-subunits were observed at 150 kDa and 75 kDa, respectively. In extracts of cells overexpressing the α*/β-mini C70S mutant, a minor signal for an apparent dimeric form of α*/β-precursor was detectable, whereas the majority was found as 120 kDa monomeric α*/β-precursor and 75 kDa monomeric α*-subunit (lane 2) indicating that C70 is responsible for the dimerization of the α*/β-mini construct as it was shown for the full length α/β-precursor protein (Fig. 3.2). The W81L mutant of the α*/β-mini construct was mostly detectable as monomeric α*/β-precursor protein (lane 3). Minor amounts of the dimeric precursor were observed. These experiments indicate that the mutation W81L also affects the dimer formation of the α-subunit.

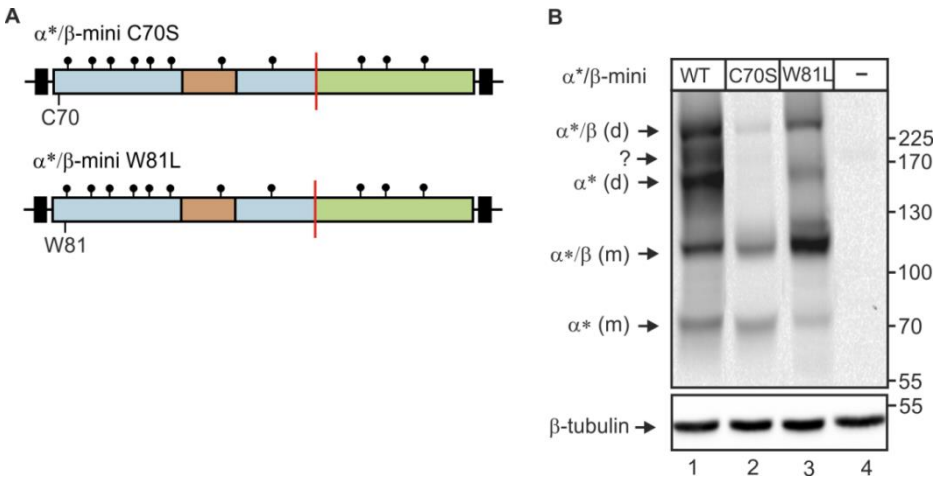

Fig. 3.20 Expression of wild-type, C70S and W81L mutants α*/β-precursor of the GlcNAc-1-phosphotransferase. A. Schematic representation of the α*/β-mini construct precursor C70S (α*/β-mini C70S) and W81L (α*/β-mini W81L) mutants. B. Lysates from HEK cells overexpressing the wild-type (WT) or mutant (C70S and W81L) α*/β-precursor proteins were resolved by SDS-PAGE under non reducing conditions followed by western blotting using antibodies against α-subunit. The endogenous β-tubulin was used as loading control. Extracts of non-transfected cells were used as negative control. The positions of the molecular mass marker proteins in kDa and of dimeric (d) and monomeric (m) α*/β-precursor and α*-subunits are indicated.

The data presented in this chapter have been published recently (De Pace *et al*, 2014).

3.3.3 Expression and localization of full length α/β-subunit mutants of the phosphotransferase

In the group of Prof. I. Schwartz (University FRGS, Brazil) eight *GNPTAB* mutations in Brazilian MLII and MLIII alpha/beta patients have been identified. In cooperation with her group, the corresponding mutant proteins (I403T, C505T, G575R, R587X, T644M, E757K*fs*X1, Y937_M972del and T1223del) were included in this study. For the expression analysis, the mutations were introduced into the α/β-full length constructs fused to a C-terminal myc-tag (Table 2.6) since most of these mutations are located in the region (aa 431-848) that is missing in the α*/β-mini construct. HEK cells were transiently transfected with the cDNAs encoding full length wild-type and mutant α/β-precursor constructs and further analysed by western blotting using antibodies against the α-subunit or myc-tag to detect the β-subunit. No immunoreactive bands were present in extracts of non-transfected cells (Fig. 3.21, lane 1). The wild-type protein was detectable as 190 kDa α/β-precursor, 145 kDa α-subunit and 45 kDa β-subunit (lane 2). After deglycosylation of *N*-linked oligosaccharides by PNGase F, the molecular masses of the α/β-subunit precursor, α-subunit, and β-subunit shifted to 160, 120 and 38 kDa, respectively (lane 3). In protein extracts of cells overexpressing the missense mutants I403T, only the α/β-subunit precursor proteins but no cleaved α- and β-subunit were observed (lanes 4 and 5). The expression levels of both mutant C505Y and G575R precursors were decreased by 40 % in comparison to the wild-type polypeptide and they were cleaved into the mature α- and β-subunits (lanes 6 - 9). In protein extracts of cells overexpressing the nonsense mutant R587X, the truncated *N*-glycosylated α-subunit was detected at 75 kDa, and shifted to 60 kDa after PNGase F treatment (lanes 10 and 11). In protein extracts of cells overexpressing the missense mutant T644M the α/β-subunit precursor was expressed and cleaved into the mature α- and β-subunits, even though the expression of the precursor was reduced by 70 % compared to the wild-type precursor protein (lanes 12 and 13). The frameshift mutant E757K*fs*X1 was present as truncated *N*-glycosylated α-subunit of 120 kDa which shifted to 75 kDa after PNGase F treatment (lanes 14 and 15). In protein extracts of cells overexpressing the deletion mutants Y937_M972del and T1223del the α/β-subunit precursor was expressed in comparable amounts as the wild-type precursor and was cleaved into α- and β-subunits (lanes 16-19).

The mutation Y937_M972del leads to a deletion of 36 aa in the β-subunit, therefore a change of ~4 kDa is expected in the molecular mass. As there are no changes in the molecular mass of the mutant β-subunit, an unusual cleavage process may occur.

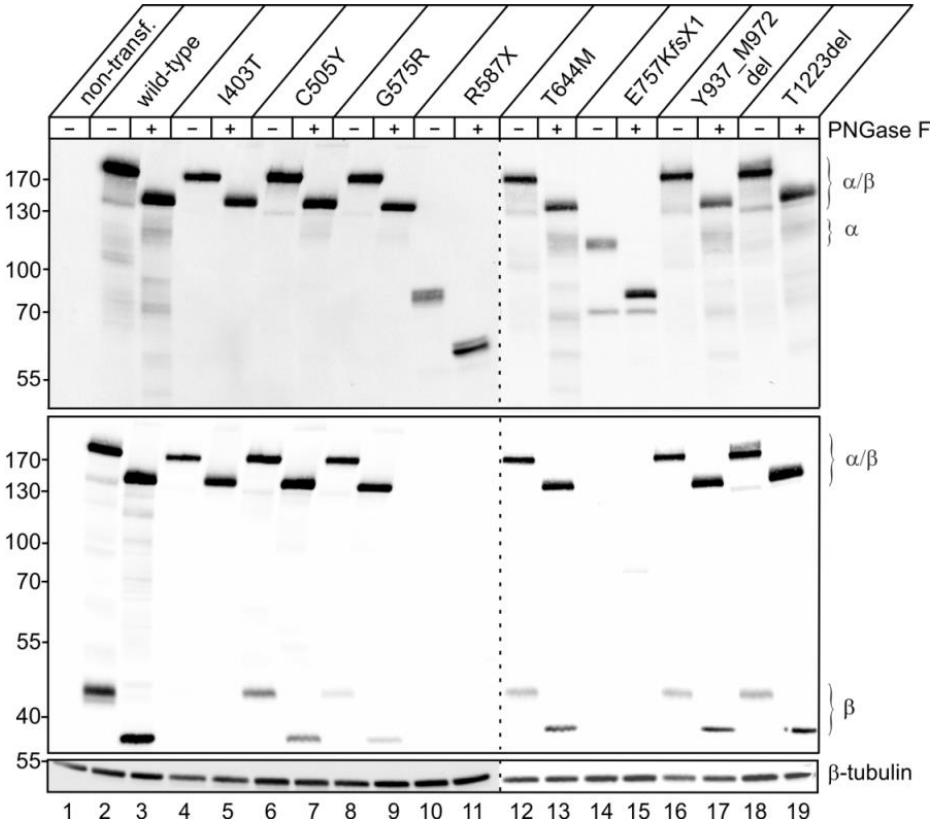

Fig. 3.21 Expression and proteolytic cleavage analysis of wild-type and mutant α/β-full length constructs. HEK cells were transfected with cDNA of wild-type and mutant α/β-subunits. Twenty four hours after transfection, cell extracts were prepared and incubated for 1 h in the presence (+) or absence (−) of PNGase F followed by SDS-PAGE (10 % acrylamide) under reducing conditions and western blotting. Immunoreactive bands were detected with monoclonal antibodies against the α-subunit or against the myc-tag. The endogenous β-tubulin was used as loading control. Extracts of non-transfected cells were used as negative control. The positions of α/β-precursor, α-, β-subunit, and molecular mass marker proteins in kDa are indicated.

The *GNPTAB* transcript levels of these overexpressed constructs were analysed by real-time PCR and the expression of wild-type *GNPTAB* was set 100 %. The mRNA levels of the overexpressed *GNPTAB* mutants I403T, C505Y, G575R, T644M, Y937_M972del, and T1223del were comparable to the wild-type *GNPTAB* mRNA level (Fig. 3.22).

In agreement with the protein level observed by western blotting (Fig. 3.20), mRNA levels of the nonsense mutants R587X and frameshift mutant E757K*fs*X1 were decreased approximately by 50 % compared to the wild-type *GNPTAB* mRNA level suggesting an impaired mRNA stability of these mutants (Fig. 3.22).

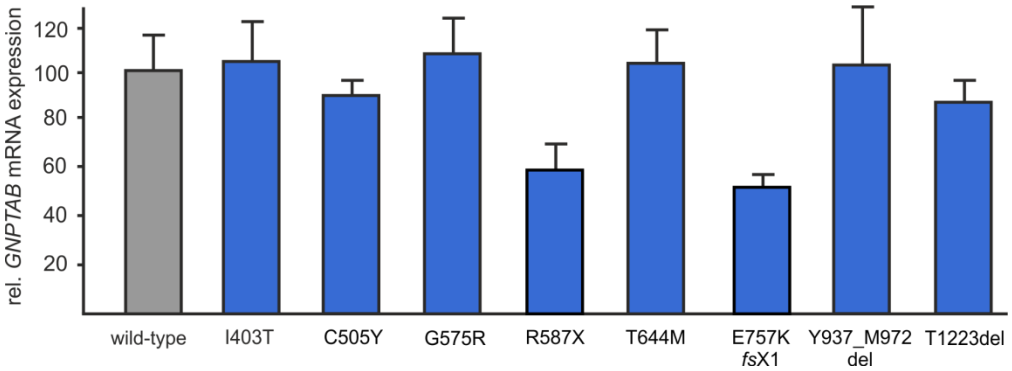

Fig. 3.22 Analysis of mRNA expression of overexpressed full length wild-type and mutants α/β-precursor in HEK cells. The relative mRNA levels of overexpressed wild-type and α/β-precursor mutants were determined 24 h post transfection by real-time PCR and normalized to actin (*ACTB*) mRNA expression (mean ± SD, n = 3). The mRNA expression of the overexpressed wild-type α/β-precursor in HEK cells was assigned as 100 %.

To analyse whether mutations in *GNPTAB* affect the intracellular localization, HeLa cells overexpressing the wild-type and mutant α/β-precursor constructs were analysed by immunofluorescence microscopy using an antibody against the α-subunit of GlcNAc-1-phosphotransferase. Cells were co-stained for the ER marker protein PDI or the *cis*-Golgi marker protein GM130. Wild-type α/β-subunit precursors were found to localize in the *cis*-Golgi apparatus (Fig. 3.23, see also Fig. 3.19). A complete co-localization with PDI was observed in cells overexpressing the mutant I403T accompanied by the failure of the mutant α/β-subunit precursors to be proteolytically processed (Fig. 3.21). Although the majority of the C505Y, G575R and R587X were found to co-localize with PDI, a small amount of the G575R mutant reached GM130-positive Golgi structures (Fig. 3.23) and was cleaved into mature α- and β-subunits (Fig. 3.21). As expected by the presence of cleaved α- and β-subunits, the mutant T644M (Fig. 3.21) was correctly targeted to the Golgi apparatus and showed co-localization with GM130 but not with PDI (Fig. 3.23).

The frameshift mutant E757K*fs*X1 and the deletion mutant Y937_M972del completely co-localized with PDI whereas the deletion mutant T1223del was correctly transported to the *cis*-Golgi apparatus and showed co-localization with GM130 but not with PDI.

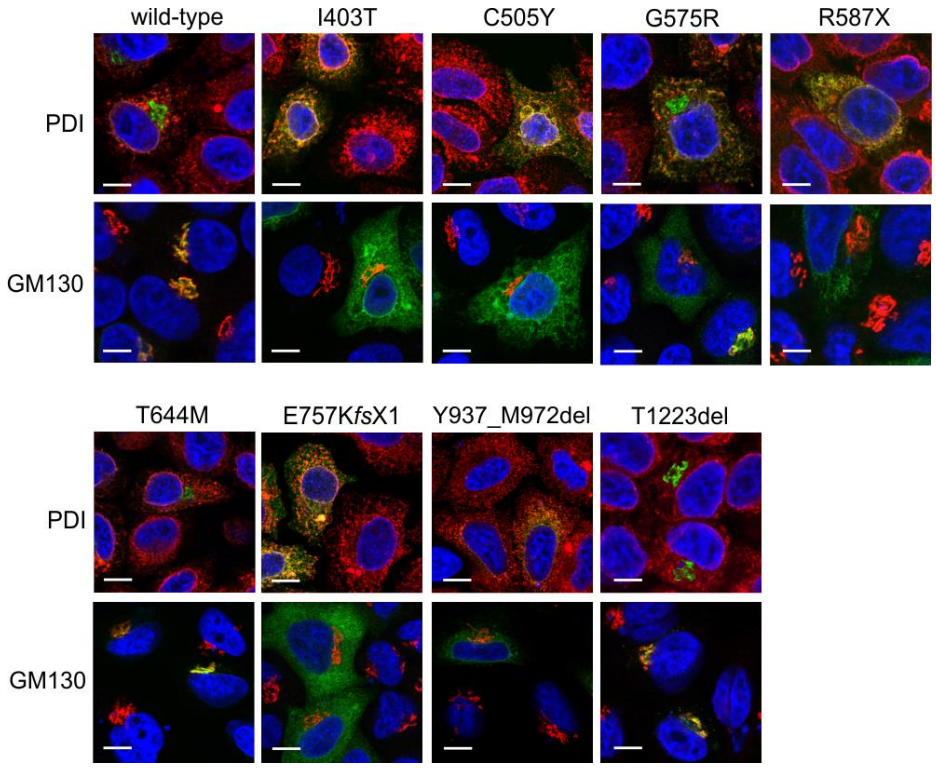

Fig. 3.23 Intracellular localization of wild-type and mutant α/β-precursor protein. HeLa cells were transfected with cDNAs encoding the wild-type or mutant α/β-precursor protein for 24 h. Cells were treated with 100 µg/ml cycloheximide for 40 min to block protein translation and release newly synthesized precursor proteins from the ER. Cells were fixed and stained with monoclonal antibodies against the α-subunit (green), the ER marker protein PDI (red) or the *cis*-Golgi marker protein GM130 (red). Nuclei were stained by DAPI (blue). Only the magnified merge images are shown. The yellow color indicates co-localization. Scale bar: 10 µm.

3.3.4 Enzymatic activity of wild-type and mutants of α/β-subunits of the GlcNAc-1-phosphotransferase

The measurement of GlcNAc-1-phosphotransferase activity *in vitro* was used to investigate which mutations in the α/β-precursor proteins affect the catalytic center directly or indirectly, e.g., by impairing the assembly of the GlcNAc-1-phosphotransferase complex.

First, the GlcNAc-1-phosphotransferase activity was determined in total extracts of HEK cells overexpressing wild-type α/β-precursor and α*/β-mini precursor proteins (Fig. 3.24). The activity of overexpressed wild-type GlcNAc-1-phosphotransferase was 13-fold increased compared to the non-transfected HEK cells, and was set to 100 %. The activity of the α*/β-mini construct in comparison with the wild-type α/β-precursor was reduced by 98 % (Fig. 3.24 B), suggesting that the α*/β-mini protein was enzymatically inactive.

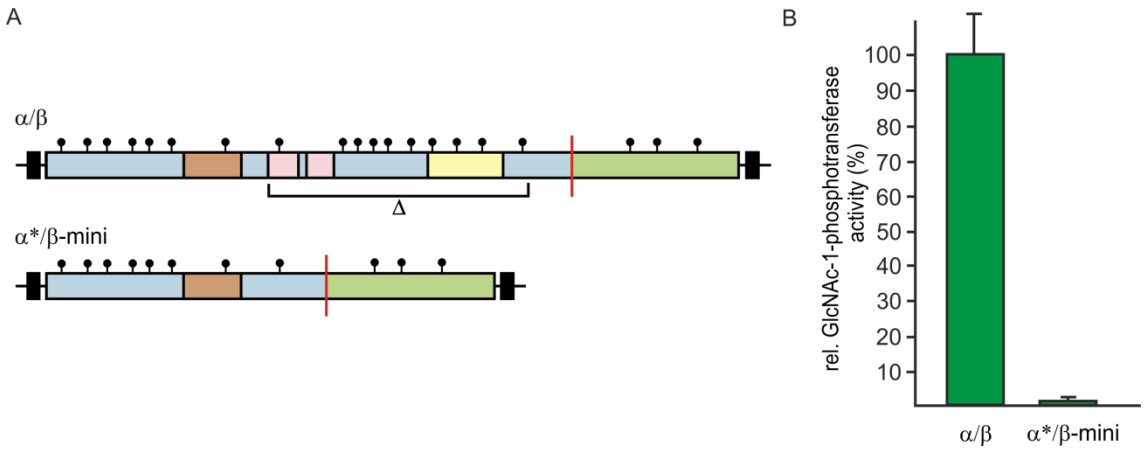

Fig. 3.24 Enzymatic activity of wild-type and α*/β-mini precursor of the GlcNAc-1-phosphotransferase. A. Schematic representation of the full length α/β-precursor and the α*/β-mini precursor lacking the amino acids 431-848 (α*/β-mini). B. The GlcNAc-1-phosphotransferase activity corresponding to 100 µg protein extracts of HEK cells overexpressing full length wild-type or α*/β-mini construct of the GlcNAc-1-phosphotransferase was measured for 60 min. Each activity value was normalised to the β-subunit immunoband intensity determined by densitometry of western blots using aliquots of the same extracts used for activity measurements. The activity of overexpressed wild-type was set to 100 % ± the calculated standard deviation.

Therefore, the full length wild-type cDNA has been used as template to introduce the patients' mutations for the analysis of GlcNAc-1-phosphotransferase (Table 3.1). The GlcNAc-1-phosphotransferase activities in extracts of HEK cells overexpressing these different mutant α/β-precursor were measured and related to the activity of the wild-type protein (Fig. 3.25). Mutations resulting in truncated α/β-subunit precursor proteins lacking the C-terminus or the second transmembrane domains are retained in the ER, and prevent the proteolytic cleavage in the Golgi apparatus.

As expected, the three frameshift mutations E757K*fs*X1, G1049R*fs*X16, L1168Q*fs*X5, as well as one nonsense mutation R587X, exhibited less than 2 % GlcNAc-1-phosphotransferase activity compared to the wild-type protein (Fig. 3.25). The activities of GlcNAc-1-phosphotransferase containing point mutations in the luminal domain of the α-subunit that are not or only partially transported to the Golgi apparatus (S399F, I403T, C505Y and G575R) are also significantly reduced by 93 – 99 %. Deletion of 30 amino acids in the β-subunit (Y937_M972del) resulted in the complete loss of GlcNAc-1-phosphotransferase activity. The mutants T644M, T1223del, and K1236M are correctly transported to the Golgi apparatus and are cleaved into mature α- and β-subunits. T1223del and K1236M exhibit comparable enzymatic activity as the wild-type protein, whereas the T644M is reduced to 36 %. Although the R986C mutant is transported to the Golgi apparatus and proteolytically cleaved, the protein is enzymatically inactive suggesting that this point mutation affect the binding sites for the UDP-GlcNAc substrate or the recognition region for the lysosomal enzymes.

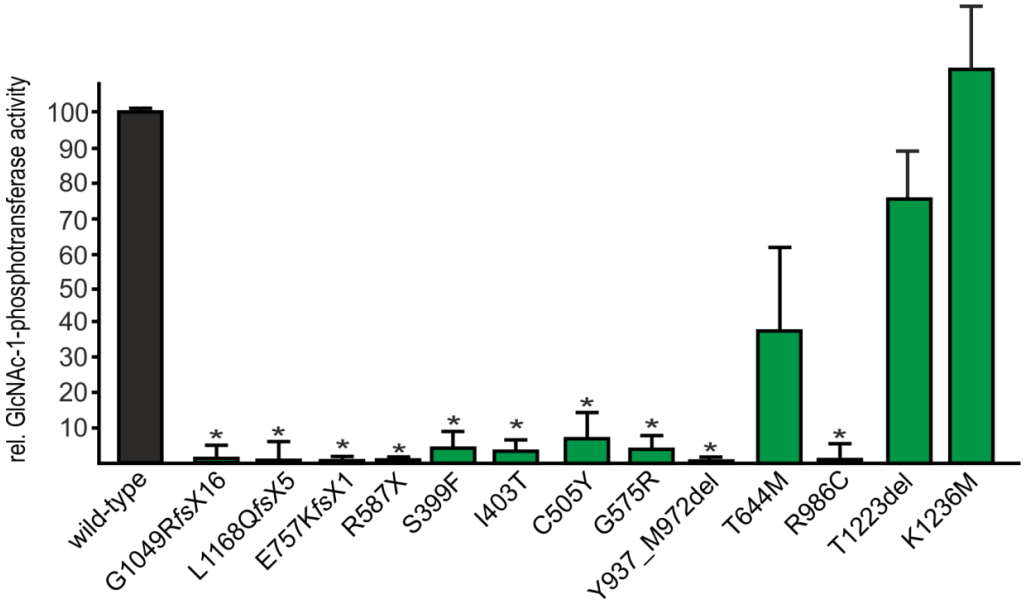

Fig. 3.25 Activity of full length wild-type and mutant α/β-precursor of the GlcNAc-1-phosphotransferase. The GlcNAc-1-phosphotransferase activity in extracts of HEK cells (100 µg) overexpressing full length wild-type or mutant constructs of the GlcNAc-1-phosphotransferase was measured for 60 min. Each activity value was normalised to the β-subunit immunoband intensities determined by densitometry of western blots using aliquots of the same extracts used for activity measurements. The activity of overexpressed wild-type was set as 100 % ± the calculated standard deviation (*P < 0.05).

Taken together, these data showed that the analysed mutants K1236M, T644M, and T1223del, that are associated with the less progressive MLIII alpha/beta disease, are correctly transported to the Golgi apparatus and proteolytically cleaved by site-1 protease (S1P) to enzymatically active GlcNAc-1-phosphotransferase subunits. These mutants may have an impaired ability to recognise lysosomal hydrolases. The nonsense and frameshift mutations (R587X, E757K*fs*X1, G1049R*fs*X16, and L1168Q*fs*X5), but also the missense mutations in the luminal domain of the α-subunit (W81L, S399F, I403T, C505Y, and G575R), cause ER retention or impaired transport to the Golgi apparatus of the mutant α/β-precursor protein preventing proteolytic activation by S1P resulting in loss of enzymatic activity of GlcNAc-1-phosphotransferase. The missense mutant R986C was correctly transported to the Golgi apparatus and S1P-mediated cleaved but exhibited no enzymatic activity, suggesting that the binding sites for the UDP-GlcNAc substrate or for the lysosomal enzymes was effected. The deletion mutant Y937_M972del is partially localized in the Golgi apparatus but is irregularly cleaved, resulting in non-active subunits. All these mutants result in the severe clinical phenotype of MLII patients.

4 Discussion

The GlcNAc-1-phosphotransferase is the key enzyme for the formation of M6P recognition marker on newly synthesized lysosomal enzymes, required for their efficient receptor-mediated transport to lysosomes (Braulke *et al*, 2013). The GlcNAc-1-phosphotransferase exists as hexameric complex composed of six subunits: two α-, two β- and two γ-subunits. The α- and β-subunits are synthesized as a common type III membrane-bound α/β-precursor protein that is signal-dependently transported from the ER to the Golgi apparatus where it is cleaved by the site-1 protease, generating the mature α- and β-subunits (Marschner *et al*, 2011).

Since the mature α- and β-subunits perform the catalytic function (Kudo & Canfield, 2006), ER export and transport to the Golgi apparatus of α/β-subunit precursor is prerequisite for the enzymatic activity of GlcNAc-1-phosphotransferase. The interactions between the different subunits of GlcNAc-1-phosphotransferase and the structural requirements for these interactions were not known.

4.1 Subunit interactions of the GlcNAc-1-phosphotransferase

To examine the interactions between membrane-bound α/β-subunit precursor as well as the membrane-bound α- and β-subunits and the soluble γ-subunit of the GlcNAc-1-phosphotransferase, different tagged constructs of the subunits were studied in HEK cells (Fig. 3.1). For most experiments GFP-Trap® beads were used to precipitate GFP-tagged subunits and their interacting proteins from cell extracts. A different pull-down was performed by precipitating the α-subunit and its interacting proteins with a novel monoclonal antibody produced in rat against the human α-subunit (De Pace *et al*, 2014). This antibody was produced by cDNA immunization using equal amounts of cDNA of α*/β-subunit mini constructs and noncleavable mutant R925A (Marschner *et al*, 2011) conjugated to gold particles, which were ballistically injected into Wistar rats. None of the generated hybridoma clones reacted with the endogenous GlcNAc-1-phosphotransferase. In the present study, the antibody clone #1 has been used and it recognizes both the overexpressed α-subunit and the α/β-precursor protein.

4.1.1 Interactions between the α-, β- and γ-subunits

In the original study to identify the α/β-subunits of GlcNAc-1-phosphotransferase, the human γ-subunit was purified from insect cells infected by a baculo-virus harboring the γ-subunit cDNA. Subsequently, detergent extracts from enriched Golgi membranes of human placenta were applied to a γ-subunit-Ni-chelate affinity matrix. The bound fractions contain, among others, peptides covering sequences of both the α- and the β-subunits (Tiede *et al*, 2005b). From these data, no conclusions on which subunit the γ-subunit binds to, and whether mature subunits can bind indirectly via the other subunits to the γ-subunit, were possible.

The *in vitro* pull-down studies have clearly shown that the soluble γ-subunit interacts directly with the isolated type II membrane-bound α-subunit of GlcNAc-1-phosphotransferase (Fig. 3.7). No direct interaction between the γ-subunit and the isolated type I membrane β-subunit was observed (Fig. 3.8 C). As expected, the γ-subunit interacted also with full length α/β-subunit precursor (Fig. 3.9 C and 3.10 C), supporting a previous report using size exclusion-chromatography (Encarnação *et al*, 2011). These results lead to the conclusion that the complex assembly of the GlcNAc-1-phosphotransferase takes place in the ER.

In precipitates containing the γ-subunit and the α/β-precursor also the mature β-subunits were found, indicating an indirect binding via direct interaction between the α- and γ-subunits. The nature of the interaction between the α- and β-subunits is not known. Preliminary *in vitro* pull-down experiments revealed no interaction between single α-subunit C-terminally fused to a myc-tag and β-subunits that were N-terminally fused to an HA-tag. Pull-down experiments using subunits without tags both under reducing and non-reducing conditions failed to show a strong interactions between α- and β-subunits. Further experiments are required to establish various conditions such as variable ion concentration or pH, as well as washing conditions of the precipitates.

4.1.2 Role of post-translational modifications for the interaction between α- and γ-subunits

The α-subunit is a highly *N*-glycosylated protein and contains 17 potential *N*-glycosylation sites. PNGase F treatment of cell extracts showed that the α-subunit was expressed in three different forms, and only the most slowly migrating form, representing the completely processed *N*-glycosylated α-subunit, was able to interact with the γ-subunit (Fig. 3.7 D). This observation indicates that *N*-glycosylations of the α-subunit play an important role for the interaction with the γ-subunit. Moreover, at present it is not clear whether the glycosylation of all 17 potential *N*-glycosylation sites occurs *in vivo* or selected oligosaccharides are sufficient for the interaction between the α- and γ-subunits. In general, *N*-glycans promote proper folding, directly by stabilizing newly synthesized polypeptide structures, but also indirectly by interacting with a variety of lectins/chaperones, glycosidases, and glycosyltransferases which have a central role in folding and retention of newly synthesized proteins in the ER (Helenius & Aebi, 2001; Morais *et al*, 2006). *N*-glycosylations have also been shown to be important for subunit interaction, for example for the heteromeric *N*-metyl-D-aspartate (NMDA) receptor (Chazot *et al*, 1995). The γ-subunit is also *N*-glycosylated at asparagine residues N88 and N115 (Encarnação *et al*, 2011). The deletion of single or combined *N*-glycosylation sites of the γ-subunit does not impair the interaction with the α-subunit (Fig. 3.12 B and D). Non-glycosylated γ-subunits, however, are unstable and rapidly degraded (Encarnação *et al*, 2011). Moreover, the interruption of the *N*-glycosylation consensus sequence at position 116 by a missense mutation in the *GNPTG* gene leads to mucolipidosis type III (Tiede *et al*, 2004), suggesting that glycosylation of N115 is rather important for GlcNAc-1-phosphotransferase activity but not for the interaction between α- and γ-subunits.

Both the α- and γ-subunits form disulfide-linked homodimers (Bao *et al*, 1996; Raas-Rothschild *et al*, 2000). The cysteine residue C245 is responsible for the dimerization of the human γ-subunit (Encarnação *et al*, 2011), whereas the cysteine residue C70 is required for the dimerization of the full length α/β-precursor and α-subunit (Fig. 3.2 D and E). The monomeric mutant C70S of the full length α/β-precursor was correctly transported to the Golgi apparatus (Fig. 3.3), cleaved into mature α- and β-subunits (Fig. 3.2 B and C), and exhibits comparable activity to the dimeric wild-type GlcNAc-1-phosphotransferase (Fig. 3.4).

These experiments suggest that the dimerization of α-subunit is neither important for the transport to the Golgi apparatus nor for the activity of GlcNAc-1-phosphotransferase. However, [^{35}S]methionine pulse-chase experiments showed that the mature monomeric α-subunit is less stable than the wild-type protein (Fig. 3.5). When the C70S mutant GlcNAc-1-phosphotransferase was expressed in cells treated with bafilomycin A1, an inhibitor of the vacuolar ATPase, the mutated α-subunits accumulated indicating that degradation occurs in acidic lysosomal compartments (Fig. 3.6). Finally, pull-down experiments clearly showed that the interaction between γ- and α-subunits occurs independently of the dimerization state of both the γ- and α-subunits (Fig. 3.13 B, C and D). In contrast, overexpressed monomeric γ-subunit failed to assemble with the endogenous α/β-subunit precursor to a high molecular mass complex (Encarnação *et al,* 2011). It is likely that the highly enriched precipitated monomeric γ-subunits used in *in vitro* pull-down experiments are sufficient to detect interactions between α- and γ-subunits.

4.1.3 Identification of the α-subunit domain required for the interaction with the γ-subunit

The luminal part of the α-subunit is composed of several modular domains with similarities to other proteins (Fig. 1.4) (Tiede *et al,* 2005b) but almost unknown function. The N-terminal luminal domain exhibits similarities to bacterial capsule biosynthesis proteins (stealth proteins) of bacteria containing GlcNAc-1-phosphate residues in their glycocalyx (Sperisen *et al,* 2005). Therefore, it has been suggested that the amino acids 60-430 comprise the UDP-GlcNAc binding site. Amino acids 433-469 as well as 500-535 show homologies with Notch-repeat like domains and the corresponding calcium binding residues of the Notch receptor (NCBI sequence viewer Q3T906 GI: 90185244). Since all twelve cysteine residues in this region are highly conserved, a functional secondary structure can be suggested. The DMAP homology domain has been recently identified to have a role in the binding of lysosomal enzymes (Qian *et al,* 2013). To define which domain of the α-subunit is responsible for the interaction with the γ-subunit, an α*/β-mini construct lacking amino acids 431-848 was used (Fig. 3.14 A).

Pull-down analyses have shown that the γ-subunit failed to interact with this polypeptide construct (Fig. 3.14 B), suggesting that the deleted domain contains the α-subunit binding site. Moreover, deletion of aa 433-535 did not affected the interaction between the α- and γ-subunits (Fig. 3.15 B). The Notch region (aa 428-539) and a longer part including the Notch region (aa 366-565) were fused to the N-acetylgalactosamine-4-O-sulfotransferase type II membrane protein (Fig. 3.16 A). These fusion proteins failed to interact with the γ-subunit (Fig. 3.16 B). These experiments exclude the Notch-repeat like domain as binding site. When the DMAP domain was deleted in the α/β-precursor protein, the interaction with γ-subunit was not disturbed (Fig. 3.15 C). Since also the DMAP domain could be excluded (Qian *et al*, 2013), the probability for the region comprising amino acids 535-698 and sharing no similarities to other proteins to represent the contact site between the α- and γ-subunits is very high. This region contains ~50 residues that are highly conserved trough different species from human to fish and are clustered in groups of 4-9 residues. The functional role of these residues in the interaction with the γ-subunit has to be investigated. In addition, this region contains five potential *N*-glycosylation sites that should be examined for their role in the interaction with the γ-subunit. Furthermore, the deletion of this region from both the α/β-subunit precursor and the α-subunit, as well as the transfer of this domain to other suitable membrane-bound proteins, are required to define the binding site between the α- and γ-subunit. In addition to pull-down assays, the yeast two hybrid system, Förster resonance energy transfer (FRET), as well as single amino acid substitutions, can be used to complete this study.

Based on previous and present findings, the following model of the human GlcNAc-1-phosphotransferase complex is proposed: the membrane-bound α-subunit interacts directly with the soluble γ-subunit, whereas the membrane-bound β-subunit fail to bind the γ-subunit directly (Fig. 4.1). *In vitro* pull-down assays of various deletion and single amino acid substitution mutants of the α-subunit with the γ-subunit resulted in the identification of a region comprising amino acids 535-698, that is likely to function as contact site between the α- and γ-subunits.
This interaction is dependent on *N*-glycosylation sites but is independent of dimerization of the α-subunit.

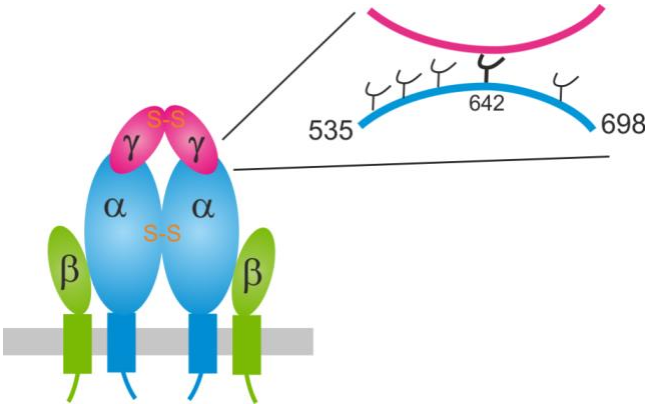

Fig. 4.1 Schematic representation of the model of the human GlcNAc-1-phosphotransferase. The membrane-bound α-subunit interacts with both soluble γ-subunit and membrane-bound β-subunit. The contact region between γ- and α-subunits (aa 535-698) is indicated in the magnification. The potential γ-subunit region involved in the α-subunit interaction is still unknown. Potential *N*-glycosylation sites that might be important for the interaction are indicated. The position of *N*-glycosylation N642 found to be mutated in an MLIII alpha/beta patient (N-X-T644M) is indicated. There is no direct interaction between the γ- and β-subunit.

4.2 Molecular and biochemical analysis of disease-related mutations in *GNPTAB*

The α/β-subunit precursor of the human GlcNAc-1-phosphotransferase is encoded by the *GNPTAB* gene (Tiede *et al*, 2005b). Mutations in *GNPTAB* lead to the autosomal recessive lysosomal storage diseases mucolipidosis (ML) type II and MLIII alpha/beta. Biochemically, MLII and MLIII alpha/beta diseases are characterized by the complete or partial loss of GlcNAc-1-phosphotransferase activity, respectively, leading to non-phosphorylated or partial phosphorylated lysosomal enzymes. The subsequent missorting and hypersecretion of multiple lysosomal proteins result in lysosomal dysfunction and lysosomal accumulation of non-degraded storage material.

MLII is a severe disease with onset of clinical signs and symptoms such as dysostosis multiplex, psychomotoric retardation, and cardiopulmonary complications in the first decade of life. In contrast, MLIII alpha/beta is a slower progressive disorder mainly affecting skeletal, joint, and connective tissues (Braulke *et al*, 2013; Spranger *et al*, 2002). To date 125 different mutations in *GNPTAB* have been described causing MLII or MLIII alpha/beta (Human Gene Mutation Database, www.hgmd.org).

Almost all MLII patients have nonsense, frameshift or splice site mutations in *GNPTAB*, and these mutations are usually associated with a severe clinical course. In contrast, missense mutations or at least one hypomorphic allele lead to residual GlcNAc-1-phosphotransferase activity and slower progression of the disease in MLIII alpha/beta patients (Braulke *et al*, 2013). MLII and MLIII alpha/beta are very rare diseases. The prevalence is variable and was documented to be 0.16 (The Netherlands), 0.22 (Czech Republic), 0.31 (Australia), 9.4 (Japan), or 0.8 (north Portugal) per 100,000 live birth for MLII and 0.06 (The Netherlands) and 1.89 (north Portugal) per 100,000 live birth for MLIII alpha/beta (Raas-Rothschild *et al*, 2012). The highest MLII frequency, estimated at 16.2/100,000, has been found in Quebec, Canada (Plante *et al*, 2008).

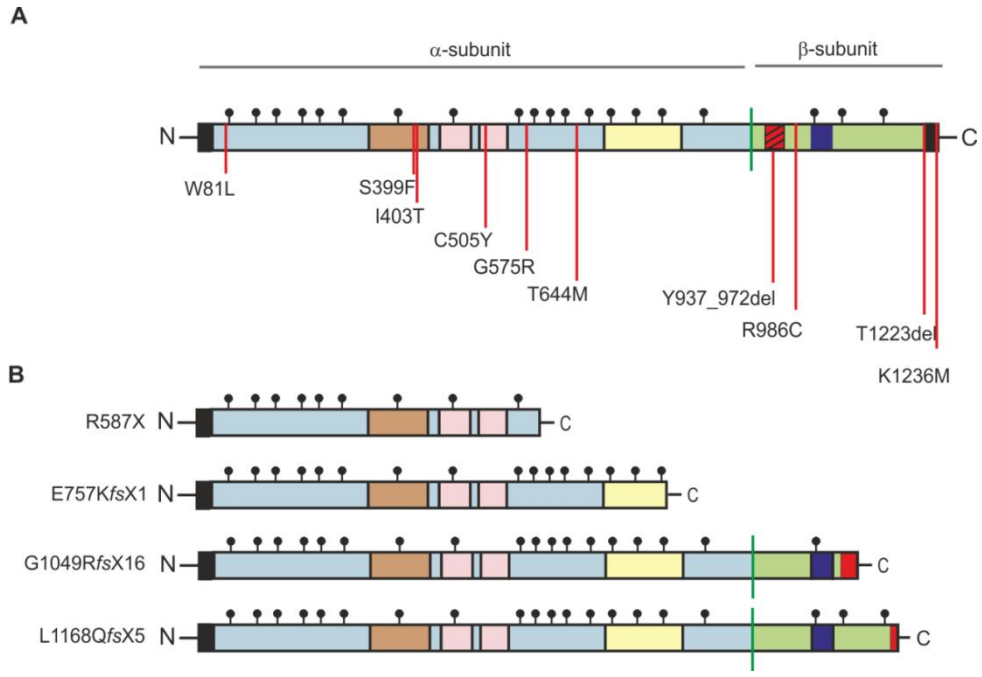

Fig. 4.2 Schematic representation of GlcNAc-1-phosphotransferase mutants examined in this thesis. A. Localization of missense and deletion mutations in the α/β-precursor protein. The positions of substituted amino acids (red line) and the deleted region (red rectangle with diagonal lines) are shown. B. Predicted translation products of *GNPTAB* nonsense and frameshift mutants. New amino acids after the frameshift mutations are indicated (red rectangles). The different homology domains are described in Fig. 1.4. The positions of potential *N*-glycosylation sites (•) and the site-1 protease cleavage site between amino acids K928 and D929 (green line) are indicated.

In this thesis the effects of 14 mutations in *GNPTAB*, that were identified in MLII and MLIII alpha/beta patients from different populations in both homozygous and heterozygous states, on the stability, subcellular localization, proteolytic cleavage and enzymatic activity of the GlcNAc-1-phosphotransferase were investigated. Among these, eight mutations result in an amino acid substitution in the α-subunit (W81L, S399F, I403T, C505Y, G575R and T644M) or in the β-subunit (R986C and K1236M) of the GlcNAc-1-phosphotransferase (Fig. 4.2). Two mutations (Y937_972del and T1223del) result in small deletions of amino acids in the β-subunit. Truncated proteins lacking C-terminal parts including the second transmembrane domain are caused by the nonsense and frameshift mutations R587X, E757K*fs*X1, G1049R*fs*X16, and L1168Q*fs*X5. These mutations were inserted in the cDNA of full length α/β-subunit precursor or α*/β-subunit precursor mini construct and used for transient transfection of HEK or HeLa cells.

4.2.1 Analysis of *GNPTAB* frameshift and nonsense mutations

The *GNPTAB* frameshift mutation L1168Q*fs*X5 (c.3503_3504delTC) is the most common MLII and MLIII alpha/beta disease-causing mutation. Among the described MLII patients from different countries and populations the mutation was observed in homozygosity and in heterozygosity with frameshift and nonsense mutations in the second allele (Bargal *et al*, 2006; Cury *et al*, 2013; Encarnação *et al*, 2009; Kudo *et al*, 2006; Plante *et al*, 2008; Tappino *et al*, 2009). All these patients show a severe course of the disease but no further clinical data have been reported. However, there are a few reports on MLIII alpha/beta patients that carry missense mutations in the second affected allele resulting in the less progressive disease (Bargal *et al*, 2006; Cury *et al*, 2013; Encarnação *et al*, 2009).

The frameshift mutation E757K*fs*X1 (c.2269_2273delGAAAC) was found in homozygosity in one Brazilian female MLII patient who was diagnosed at 2 years of age (Cury *et al*, 2013). No clinical data are available. The *GNPTAB* mutation G1049R*fs*X16 (c.3145insC) has been identified in a male MLII patient (Tiede *et al*, 2005a). He was normal at birth but showed joint contractures and claw hand deformity by the age of 4 months.

At 2 years of age he presented coarse facial features, mild corneal clouding, an enlarged tongue, hepatomegaly and a neuromotoric developmental retardation. He had a short stature and radiographs revealed typical signs of dysostosis multiplex. He was unable to walk because of the progressive skeletal manifestations. This MLII patient mutation was also introduced into the orthologous *Gnptab* gene to generate an MLII "knock-in" mouse model which shows biochemical and clinical features of the human MLII disease (Kollmann *et al*, 2012; Kollmann *et al*, 2013). The nonsense mutation R587X (c.1759C>T) was found in heterozygosity with C505Y in the second allele in two Brazilian MLIII alpha/beta patients (Cury *et al*, 2013) and with a frameshift mutation (p.V653V*fs*X1) in one MLII patient of unknown origin (Cathey *et al*, 2010). The *GNPTAB* mRNA levels of these frameshift and nonsense mutants were strongly reduced by 50 % for the E757K*fs*X1 and R587X or by 80 % for the G1049R*fs*X16 and L1168Q*fs*X5 transcripts compared to the wild-type mRNA levels (Fig. 3.18 and 3.22). These data indicate that the mutant mRNAs are most likely degraded by nonsense-mediated mRNA decay (NMD). The NMD pathway is a translation-coupled quality control system that recognizes and degrades aberrant mRNAs with truncated open reading frames due to the presence of a premature stop codon (Schweingruber *et al*, 2013). Confirmatory results were obtained by western blot analysis (Fig. 3.17 and 3.21). Due to the complete (E757K*fs*X1 and R587X) or partial (G1049R*fs*X16 and L1168Q*fs*X5) loss of the β-subunit, respectively, the mutant α-subunit-immunoreactive polypeptides were smaller than the wild-type α/β-subunit precursor but unable to be cleaved into the mature α-subunit (Fig. 4.2 B). This can be explained by the combinatorial sorting motif in both the N- and C-terminal cytoplasmic tails for ER-Golgi transport (Franke *et al*, 2013) which is missing in the truncated α/β-subunit precursor mutants and lead to their retention in the ER (Fig. 3.19 and 3.23). Subsequently the truncated mutant proteins failed to be proteolytically activated which is associated with the loss of GlcNAc-1-phosphotransferase activity (Fig. 3.25).

4.2.2 Analysis of MLIII alpha/beta-associated *GNPTAB* missense and deletion mutations

In a male Brazilian patient (Fig. 4.3) the deletion mutation T1223del (c.3668_3670delCTA) and the missense mutation T644M (c.1931_1932CA>TG) were found in heterozygosity in the *GNPTAB* gene (Genetics Department, UFRGS, Brazil). Clinically and biochemically, the diagnosis of MLIII alpha/beta have been confirmed. He is now 9 years old and attends to a regular school without difficulties and had no cognitive impairment.

Fig. 4.3 Male patient with MLIII alpha/beta. The boy, aged 9 years old, presents mild coarse facial features, joint contractures in shoulders, claw hands, hindering arm elevation above the head. He had no organomegaly but prominent abdomen.

The mutated amino acid T644M is located in a luminal part of the α-subunit that might be part of the interaction contact site of the α- and γ-subunits (see 4.1). The mutation disrupts the potential *N*-glycosylation motif ^{642}NST^{644} which might contribute to the glycosylation-dependent interaction between the α- and the γ-subunit. The second deletion in this patient (T1223del) leads to the removal of one amino acid in the transmembrane domain of the β-subunit (Fig. 4.2 A). Both missense and deletion mutations results in comparable mRNA and protein level as the wild-type control (Fig. 3.21 and 3.22). Although the mutants were correctly transported to the Golgi apparatus and proteolytically cleaved into α- and β-subunits (Fig. 3.21 and 3.23), the enzymatic activity of the T1223del and T644M GlcNAc-1-phosphotransferase mutants were 80 % and 40 %, respectively, of the wild-type enzyme (Fig. 3.25).

Since the activity assay uses α-methylmannoside (α-MM) as phosphate acceptor instead of lysosomal enzymes, mutations in the binding site for lysosomal enzymes cannot be detected enzymatically. Further investigations are required to differentiate whether T644M impair the interaction between α- and γ-subunit or the binding pocket for lysosomal enzymes. In contrast, the T1223del mutation affects the length of the second transmembrane domain of the α/β-subunit precursor protein. It has been shown for the ERGIC-53 membrane protein that the length and polar residues of transmembrane domains influence the oligomerization and ER export (Nufer *et al*, 2003). As the ER exit of T1223del mutant results normal, the conformational changes induced by this mutation may affect the recognition of lysosomal hydrolases.

The *GNPTAB* missense mutation S399F (c.1196C>T) was found in homozygosity in a Portuguese (Encarnação *et al*, 2009) and in heterozygosity in French and Brazilian MLIII alpha/beta patients (Bargal *et al*, 2006; Cury *et al*, 2013). The onset of symptoms in the Portuguese patient has been reported at 9 years of age, whereas the male Brazilian patient and female French patient were diagnosed at 5 and 3.5 years, respectively. The French patient developed mild gingival hypertrophy, macroglossia, contractures of the large articulation, mild coarse facial feature, aortic valve regurgitation, hearing loss, and mild cognitive delay (Bargal *et al*, 2006). The missense mutation I403T (c.1208T>C) was found in heterozygosity with the G575R mutation on the second allele in Brazilian and in homozygosity in Italian and Portuguese MLIII alpha/beta patients (Encarnação *et al*, 2009; Tappino *et al*, 2009). No clinical data of these patients are available. The protein expression level of the S399F and I403T mutants were decreased by approximatelly 50 % compared to the wild-type protein (Fig. 3.17 and 3.21). Surprisingly, immunofluorescence microscopy and western blot analysis showed that both mutant proteins were retained in the ER, which prevent proteolytic activation in the Golgi apparatus (Fig. 3.17, 3.19, 3.21 and 3.23). As expected, the activity of the GlcNAc-1-phosphotransferase mutants were decreased by 90-95 % compared to the wild-type protein (Fig. 3.25). Therefore, the mild clinical phenotype of patients carrying the S399F and I403T mutations is not clear. However, these results indicate that the export and proteolytic cleavage of the α/β-subunit precursor is essential for the enzyme complex activity and raise the question how mutations in the luminal part of α/β-subunit precursor can affect the transport of GlcNAc-1-phosphotransferase.

There are other examples in literature such as the lysosomal integrated membrane protein 2 (LIMP-2), a type II membrane protein, where missense mutations in the luminal part cause misfolding of the mutant protein and retention in the ER (Blanz *et al*, 2010). Furthermore, the most common F508 mutation in the cystic fibrosis transmembrane conductance regulator (CTFR) protein causing cystic fibrosis impair the exit from the ER due to misfolding (Farinha *et al*, 2013). The decreased protein expression level of S399F and I403T of the GlcNAc-1-phosphotransferase mutants in comparison to the wild-type protein suggests that misfolded-induced degradation processes are likely. Alternatively, the highly conserved region surrounding S399 and I403 might be a binding site for luminal ER proteins required for ER exit.

The missense C505Y (c.1514G>A) mutation was found in heterozygosity in three patients clinically diagnosed for MLIII alpha/beta (Cathey *et al*, 2010; Cury *et al*, 2013). No additional clinical data of these patients are available. The mRNA level of the overexpressed C505Y mutant was comparable to the wild-type mRNA levels (Fig. 3.22). The mutant protein C505Y was incompletely proteolytically cleaved compared to the wild-type protein (Fig. 3.21) and exhibit 7 % of residual GlcNAc-1-phosphotransferase activity (Fig. 3.25). The immunofluorescence microscopy analysis indicate that C505Y may impair the efficient transport to the Golgi apparatus since a significant part of the mutant protein was found in the ER (Fig. 3.23). It is likely that this substituted residue may affect the catalytic center of the GlcNAc-1-phosphotransferase. This hypothesis is supported by analysis of the GlcNAc-1-phosphotransferase α*/β-mini construct lacking amino acids 431 to 848 and showing 2 % of the full length wild-type enzyme activity (Fig. 3.24), suggesting that the catalytic residues within this region are responsible for the activity of GlcNAc-1-phosphotransferase. The C505 residue is localized in the Notch-like repeat domain of the α-subunit, that contain many cysteine residues and might determine a secondary structure via intramolecular disulfide bridges. The interruption of disulfide pattern by this mutation may impair the structure of the GlcNAc-1-phosphotransferase complex.

The missense mutation G575R (c.1723G>A) was found in heterozygosity with the I403T mutant in a male Brazilian MLIII alpha/beta patient at an age of 14 years. No clinical data are available. The mRNA level of the overexpressed G575R mutant was comparable to the wild-type *GNPTAB* mRNA level (Fig. 3.22).

Similarly to the mutant C505Y, the mutant G575R protein was partially found in the Golgi compartment (Fig. 3.23). Although it was cleaved, the mutant exhibit only 3 % of wild-type GlcNAc-1-phosphotransferase activity (Fig. 3.25). Whether the G575 residue is part of the contact site between the α- and γ-subunits has to be studied further. These residues are also missing in the α*/β-mini construct that shows complete loss of GlcNAc-1-phosphotransferase activity (Fig. 3.24).

The missense mutation K1236M (c.3707A>T) was described in a German male patient clinically classified as MLIII alpha/beta (Tiede *et al*, 2006). The protein expression level of the mutant K1236M precursor was reduced by approximately 60 % (Fig. 3.17) accompanied by reduced transcript levels (Fig. 3.18). The mutation neither affect the transport of the α/β-subunit precursor to the Golgi compartment (Fig. 3.19) nor the cleavage of the protein into mature α- and β-subunits (Fig. 3.17) or its activity (Fig. 3.25). So far it is not clear how this mutation leads to a pathogenic phenotype in patients.

4.2.3. Analysis of MLII-associated *GNPTAB* missense and deletion mutations

Although missense mutations have been described to cause a milder phenotype and a later onset of the disease, the homozygous missense mutation R986C (c.2956C>T) was identified in a male Indian patient who was clinically classified as MLII (Coutinho *et al*, 2012). The expression level of the mutant R986C precursor was moderately decreased by 20 %, the remaining polypeptide was cleaved into mature α- and β-subunits (Fig. 3.17 and 3.18), which were localized in the Golgi apparatus (Fig. 3.19). Moreover, almost no enzymatic activity of the mutant R986C GlcNAc-1-phosphotransferase was observed (Fig. 3.25), which explains the severe phenotype of the affected patient. The R986C mutation is localized in the luminal part of the β-subunit, and the strong loss of enzymatic activity can be caused either indirectly by inhibition of the substrate binding site or directly by affecting the catalytic center of the enzyme.

The missense mutation W81L (c.242G>T), detected in homozygosity in two male patients of two non-consanguineous Portuguese families, resulted in the severe MLII disease with first symptoms at the age of 3 or 4 months (Encarnação *et al*, 2009).

Both presented psychomotor retardation, multiple malformations, gingival hypertrophy, hypertonia, respiratory difficulties, and delayed growth leading to death of one of the patient at 23 months of age (Encarnação *et al*, 2009). The W81L mutation is localized in the luminal part of the α-subunit. By immunofluorescence microscopic analysis the mutant W81L seems to be mainly retained in the ER and only partially transported to the Golgi apparatus (Fig. 3.19). As consequence, very small amounts of cleaved α- and β-subunits were detectable (Fig. 3.17). The tryptophan residue 81 is close to the cysteine residue 70, which is responsible for the dimerization of the α-subunit. Most of the C70S as well as the W81L mutant α/β-precursor proteins are found in the monomeric state, demonstrating impaired dimer formation of the mutants (Fig. 3.20). In contrast to the W81L mutant, the C70S mutant is correctly transported to the Golgi apparatus and cleaved into the mature α- and β-subunits (Fig. 3.2 and 3.3), demonstrating that the dimer formation is not required for ER export and subsequent S1P-mediated cleavage in the Golgi apparatus. Therefore, it is unlikely that the impaired dimerization of the W81L mutant causes the transport defect. However, W81 is part of a potential conserved coiled-coil domain comprising amino acids 80 - 120 in the luminal domain of the α-subunit. Coiled-coil domains have been shown in other proteins to be involved in protein-protein interactions (Lupas *et al,* 1991). Therefore, it is possible that still unknown proteins may bind in the ER lumen to the coiled-coil domain and facilitate the ER export which may be interrupted by the W81L mutation.

The *GNPTAB* deletion mutation Y937_M972del (c.2808A>G) was found in heterozygosity with the most common L1168Q*fs*X5 frameshift mutation on the second allele in one Brazilian MLII patient (Cury *et al*, 2013). The boy was diagnosed at 3 years of age and died at the age of 7 years. In the mutant protein, 36 amino acids of the highly conserved β-subunit downstream to the cleavage site are deleted. Surprisingly, the mutant mRNA and protein level were comparable to the wild-type controls (Fig. 3.21 and Fig. 3.22). Immunofluorescence microscopy analysis of overexpressing Y937_M972del mutant HeLa cells revealed complete ER localization (Fig. 3.23), whereas in overexpressing HEK cells the mutant was partially localized in the Golgi apparatus (not shown), which support the finding of proteolitycally cleaved α- and β-subunits in HEK cells (Fig. 3.21). The cleaved β-subunit, moreover, did not exhibit a lower molecular mass as expected by the lack of 36 amino acids indicating an unusual cleavage process (Fig. 3.21).

In S1P-deficient CHO cells, the overexpressed mutant was not cleaved, demonstrating that the S1P is responsible for the alternative cleavage (not shown). The irregular cleaved α- and β-subunits are shown to be enzymatically inactive (Fig. 3.25).

The biogenesis of lysosomes depends on the formation of M6P targeting signals on acid hydrolases catalysed by the α/β-subunits of GlcNAc-1-phosphotransferase complex. From these results we conclude that mutations in the α/β-subunit precursor encoded by *GNPTAB* may impair different steps of this process, including: i) transport of the newly synthesized α/β-subunit precursor protein from the ER to the Golgi apparatus, ii) proteolytic activation by site-1 protease, or iii) the ability to transfer GlcNAc-1-phosphate residues on the high mannose-type oligosaccharides. For all the investigated mutations the three possibilities were analysed and discussed. For the GlcNAc-1-phosphotransferase activity measurement we used α-methylmannoside as an acceptor substrate, which is a small sugar and allowed the reaction even if the binding region for lysosomal enzymes was affected, and provided information exclusively about the effective functionality of the GlcNAc-1-phosphotransferase catalytic center. An MLII causing missense mutation in the DMAP domain, for example, exhibited full activity toward the simple sugar α-methylmannoside but impaired phosphorylation of lysosomal enzymes (Qian *et al*, 2013). Therefore, the specific recognition of different lysosomal enzymes remains to be investigated.

4.3 Degradation of GlcNAc-1-phosphotransferase

Although the C70S mutant of the Golgi-resident GlcNAc-1-phosphotransferase is correctly transported to the Golgi apparatus and cleaved by S1P into the mature α- and β-subunits (Fig. 3.3 and 3.2), the monomeric C70 α-subunit was found to be less stable than the wild-type α-subunit.

Not much is known about the quality control occurring in the Golgi apparatus and how Golgi-resident proteins are degraded. A defective protein that passes the ER quality control and reaches the Golgi apparatus may undergo three different mechanisms, it may i) undergo retrograde transport to the ER for ERAD, ii) be targeted to endosomal system for lysosomal degradation or iii) be transported via the plasma membrane to lysosomes (Arvan *et al*, 2002).

A recent work has reported that secretion or shedding at the plasma membrane contribute to the rapid loss of a soluble α-subunit of the mutant GlcNAc-1-phosphotransferase. Other portions of the mutant GlcNAc-1-phosphotransferase are delivered to lysosomes for final degradation (van Meel *et al*, 2014).

Our group could not confirm that wild-type or mutant GlcNAc-1-phosphotransferase subunits are secreted into the medium (data not shown). In currently running experiments the lysosomal degradation of the C70S monomeric mutant could be blocked by bafilomycin A treatment. Additionally, bafilomycin treatment allows the immunofluorescence microscopic detection of accumulated α-subunit-immunoreactive C70S material in lysosomal compartments (Fig. 3.6). The signal structures for Golgi exit and interacting proteins recognising mutant α/β-subunits of the GlcNAc-1-phosphotransferase in the Golgi apparatus are not known yet.

5 Summary

GlcNAc-1-phosphotransferase plays a key role in the generation of mannose 6-phosphate residues, a recognition marker essential for efficient transport of lysosomal enzymes to lysosomes. Mutations in the genes encoding the hexameric GlcNAc-1-phosphotransferase complex ($\alpha_2\beta_2\gamma_2$) lead to the lysosomal storage disorders MLII and MLIII. The aim of the study was focused on the analysis of structural requirements for the transport, subunit assembly, and activity of the GlcNAc-1-phosphotransferase complex.

• Cysteine residue 70 has been identified to be responsible for the disulfide-mediated dimerization of the α-subunits. Expression and [^{35}S]methionine pulse-chase analysis showed that dimerization is neither required for ER export nor for proteolytic activation of the α/β-subunit precursor of GlcNAc-1-phosphotransferase. The reduced half life of the monomeric α-subunit was found to be caused by lysosomal degradation.

• Pull-down experiments with different GlcNAc-1-phosphotransferase subunit fusion proteins provided evidence that the γ-subunit interacts directly with the α/β-precursor subunit and with the mature α-subunit, but not with the β-subunit. Analysis of various deletion mutants of the α-subunit and α/β-precursor protein suggested that the amino acid residues 535 to 698 comprise the binding site for the γ-subunit. The interaction between α- and γ-subunits does not depend on the dimerization state of the subunits. *N*-linked oligosaccharides of the α-subunits are required for efficient interaction between α- and γ-subunits.

• Frameshift and nonsense mutations of GlcNAc-1-phosphotransferase failed to reach the Golgi apparatus due to the interrupted cooperative ER export signals localized both in the N- and C-terminal cytosolic tails and lacked proteolytic activation of the α/β-subunit precursor. In addition, luminal missense mutations of the GlcNAc-1-phosphotransferase can also impair the transport to the Golgi apparatus, suggesting the presence of a protein contact site required for efficient ER export. The establishment of a radioactive assay to measure the enzymatic activity of the GlcNAc-1-phosphotransferase confirmed that the transport to the Golgi and proteolytic cleavage into mature α- and β-subunits is prerequisite for enzymatic activity.

Analysis of mutants that are transported and cleaved in the Golgi apparatus, but lack GlcNAc-1-phosphotransferase activity, suggest that the catalytic center is constituted by a complex structure involving amino acids 431-848 of the α-subunit and residues 937-986 in the β-subunit.

The present data provide new insight into structural requirements for localization and activity of GlcNAc-1-phosphotransferase that may help explaining the variability in the clinical phenotypes of MLII and MLIII patients.

6 References

Arvan P, Zhao X, Ramos-Castaneda J, Chang A (2002) Secretory pathway quality control operating in Golgi, plasmalemmal, and endosomal systems. *Traffic* **3:** 771-780

Bao M, Booth JL, Elmendorf BJ, Canfield WM (1996) Bovine UDP-N-acetylglucosamine:lysosomal-enzyme N-acetylglucosamine-1-phosphotransferase. I. Purification and subunit structure. *J Biol Chem* **271:** 31437-31445

Bargal R, Zeigler M, Abu-Libdeh B, Zuri V, Mandel H, Ben Neriah Z, Stewart F, Elcioglu N, Hindi T, Le Merrer M, Bach G, Raas-Rothschild A (2006) When Mucolipidosis III meets Mucolipidosis II: GNPTA gene mutations in 24 patients. *Mol Genet Metab* **88:** 359-363

Barlowe C (2003) Signals for COPII-dependent export from the ER: what's the ticket out? *Trends Cell Biol* **13:** 295-300

Ben-Yoseph Y, Baylerian MS, Nadler HL (1984) Radiometric assays of N-acetylglucosaminylphosphotransferase and alpha-N-acetylglucosaminyl phosphodiesterase with substrates labeled in the glucosamine moiety. *Anal Biochem* **142:** 297-304

Blanz J, Groth J, Zachos C, Wehling C, Saftig P, Schwake M (2010) Disease-causing mutations within the lysosomal integral membrane protein type 2 (LIMP-2) reveal the nature of binding to its ligand beta-glucocerebrosidase. *Hum Mol Genet* **19:** 563-572

Bonifacino JS, Glick BS (2004) The mechanisms of vesicle budding and fusion. *Cell* **116:** 153-166

Bonifacino JS, Traub LM (2003) Signals for sorting of transmembrane proteins to endosomes and lysosomes. *Annu Rev Biochem* **72:** 395-447

Bonner WM, Laskey RA (1974) A film detection method for tritium-labelled proteins and nucleic acids in polyacrylamide gels. *Eur J Biochem* **46:** 83-88

Braulke T, Bonifacino JS (2009) Sorting of lysosomal proteins. *Biochim Biophys Acta* **1793:** 605-614

Braulke T, Raas-Rothschild A, Kornfeld S (2013) I-cell disease and pseudo-Hurler polydystrophy: Disorders of lysosomal enzyme phosphorylation and localization. In *The online metabolic and molecular basis of inherited diseases*, Valle D BA, Vogelstein B, Kinzler KW, Antonarakis SE, Ballabio A, Scriver CR, Sly WS, Bunz F, Gibson KM, Mitchell G (ed).

Brown MS, Goldstein JL (1999) A proteolytic pathway that controls the cholesterol content of membranes, cells, and blood. *Proc Natl Acad Sci U S A* **96:** 11041-11048

Caramelo JJ, Parodi AJ (2008) Getting in and out from calnexin/calreticulin cycles. *J Biol Chem* **283:** 10221-10225

Castonguay AC, Olson LJ, Dahms NM (2011) Mannose 6-phosphate receptor homology (MRH) domain-containing lectins in the secretory pathway. *Biochim Biophys Acta* **1810:** 815-826

Cathey SS, Leroy JG, Wood T, Eaves K, Simensen RJ, Kudo M, Stevenson RE, Friez MJ (2010) Phenotype and genotype in mucolipidoses II and III alpha/beta: a study of 61 probands. *J Med Genet* **47:** 38-48

Chazot PL, Cik M, Stephenson FA (1995) An investigation into the role of N-glycosylation in the functional expression of a recombinant heteromeric NMDA receptor. *Mol Membr Biol* **12:** 331-337

Couso R, Lang L, Roberts RM, Kornfeld S (1986) Phosphorylation of the oligosaccharide of uteroferrin by UDP-GlcNAc:glycoprotein N-acetylglucosamine-1-phosphotransferases from rat liver, Acanthamoeba castellani, and Dictyostelium discoideum requires alpha 1,2-linked mannose residues. *J Biol Chem* **261:** 6326-6331

Coutinho MF, Santos Lda S, Girisha KM, Satyamoorthy K, Lacerda L, Prata MJ, Alves S (2012) Mucolipidosis type II alpha/beta with a homozygous missense mutation in the GNPTAB gene. *Am J Med Genet A* **158A:** 1225-1228

Cury GK, Matte U, Artigalas O, Alegra T, Velho RV, Sperb F, Burin MG, Ribeiro EM, Lourenco CM, Kim CA, Valadares ER, Galera MF, Acosta AX, Schwartz IV (2013) Mucolipidosis II and III alpha/beta in Brazil: Analysis of the GNPTAB gene. *Gene* **524:** 59-64

De Pace R, Coutinho MF, Koch-Nolte F, Haag F, Prata MJ, Alves S, Braulke T, Pohl S (2014) Mucolipidosis II-related mutations inhibit the exit from the endoplasmic reticulum and proteolytic cleavage of GlcNAc-1-phosphotransferase precursor protein (GNPTAB). *Hum Mutat* **35:** 368-376

Encarnação M, Kollmann K, Trusch M, Braulke T, Pohl S (2011) Post-translational modifications of the gamma-subunit affect intracellular trafficking and complex assembly of GlcNAc-1-phosphotransferase. *J Biol Chem* **286:** 5311-5318

Encarnação M, Lacerda L, R. C, Prata MJ, Coutinho MF, Ribeiro H, Lopes L, Pineda M, Ignatius J, Galvez H, Mustonen A, Lima MR, Alves S (2009) Molecular analysis of the GNPTAB and GNPTG genes in 13 patients with mucolipidosis type II or type III - identification of eight novel mutations. *Clin Genet* **76:** 76-84

Farinha CM, King-Underwood J, Sousa M, Correia AR, Henriques BJ, Roxo-Rosa M, Da Paula AC, Williams J, Hirst S, Gomes CM, Amaral MD (2013) Revertants, low temperature, and correctors reveal the mechanism of F508del-CFTR rescue by VX-809 and suggest multiple agents for full correction. *Chem Biol* **20:** 943-955

Franke M, Braulke T, Storch S (2013) Transport of the GlcNAc-1-phosphotransferase alpha/beta-subunit precursor protein to the Golgi apparatus requires a combinatorial sorting motif. *J Biol Chem* **288:** 1238-1249

Ghosh P, Dahms NM, Kornfeld S (2003) Mannose 6-phosphate receptors: new twists in the tale. *Nat Rev Mol Cell Biol* **4:** 202-212

Giraudo CG, Maccioni HJ (2003) Endoplasmic reticulum export of glycosyltransferases depends on interaction of a cytoplasmic dibasic motif with Sar1. *Mol Biol Cell* **14:** 3753-3766

Guruharsha KG, Kankel MW, Artavanis-Tsakonas S (2012) The Notch signalling system: recent insights into the complexity of a conserved pathway. *Nat Rev Genet* **13:** 654-666

Helenius A, Aebi M (2001) Intracellular functions of N-linked glycans. *Science* **291:** 2364-2369

Kollmann K, Damme M, Markmann S, Morelle W, Schweizer M, Hermans-Borgmeyer I, Röchert AK, Pohl S, Lübke T, Michalski JC, Kakela R, Walkley SU, Braulke T (2012) Lysosomal dysfunction causes neurodegeneration in mucolipidosis II 'knock-in' mice. *Brain* **135:** 2661-2675

Kollmann K, Pestka JM, Kuhn SC, Schone E, Schweizer M, Karkmann K, Otomo T, Catala-Lehnen P, Failla AV, Marshall RP, Krause M, Santer R, Amling M, Braulke T, Schinke T (2013) Decreased bone formation and increased osteoclastogenesis cause bone loss in mucolipidosis II. *EMBO Mol Med* **5:** 1871-1886

Kollmann K, Pohl S, Marschner K, Encarnação M, Sakwa I, Tiede S, Poorthuis BJ, Lübke T, Müller-Loennies S, Storch S, Braulke T (2010) Mannose phosphorylation in health and disease. *Eur J Cell Biol* **89:** 117-123

Kornfeld S, Reitman ML, Varki A, Goldberg D, Gabel CA (1982) Steps in the phosphorylation of the high mannose oligosaccharides of lysosomal enzymes. *Ciba Found Symp***:** 138-156

Kudo M, Brem MS, Canfield WM (2006) Mucolipidosis II (I-cell disease) and mucolipidosis IIIA (classical pseudo-hurler polydystrophy) are caused by mutations in the GlcNAc-phosphotransferase alpha / beta -subunit precursor gene. *Am J Hum Genet* **78:** 451-463

Kudo M, Canfield WM (2006) Structural requirements for efficient processing and activation of recombinant human UDP-N-acetylglucosamine:lysosomal-enzyme-N-acetylglucosamine-1-phosphotransferase. *J Biol Chem* **281:** 11761-11768

Lang L, Couso R, Kornfeld S (1986) Glycoprotein phosphorylation in simple eucaryotic organisms. Identification of UDP-GlcNAc:glycoprotein N-acetylglucosamine-1-phosphotransferase activity and analysis of substrate specificity. *J Biol Chem* **261:** 6320-6325

Lazzarino DA, Gabel CA (1989) Mannose processing is an important determinant in the assembly of phosphorylated high mannose-type oligosaccharides. *J Biol Chem* **264:** 5015-5023

Leach MR, Cohen-Doyle MF, Thomas DY, Williams DB (2002) Localization of the lectin, ERp57 binding, and polypeptide binding sites of calnexin and calreticulin. *J Biol Chem* **277:** 29686-29697

Lee MC, Miller EA, Goldberg J, Orci L, Schekman R (2004) Bi-directional protein transport between the ER and Golgi. *Annu Rev Cell Dev Biol* **20:** 87-123

Lee WS, Payne BJ, Gelfman CM, Vogel P, Kornfeld S (2007) Murine UDP-GlcNAc:lysosomal enzyme N-acetylglucosamine-1-phosphotransferase lacking the gamma-subunit retains substantial activity toward acid hydrolases. *J Biol Chem* **282:** 27198-27203

Lübke T, Lobel P, Sleat DE (2009) Proteomics of the lysosome. *Biochim Biophys Acta* **1793:** 625-635

Lupas A, Van Dyke M, Stock J (1991) Predicting coiled coils from protein sequences. *Science* **252:** 1162-1164

Makrypidi G, Damme M, Muller-Loennies S, Trusch M, Schmidt B, Schluter H, Heeren J, Lubke T, Saftig P, Braulke T (2012) Mannose 6 dephosphorylation of lysosomal proteins mediated by acid phosphatases Acp2 and Acp5. *Mol Cell Biol* **32:** 774-782

Marschner K, Kollmann K, Schweizer M, Braulke T, Pohl S (2011) A key enzyme in the biogenesis of lysosomes is a protease that regulates cholesterol metabolism. *Science* **333:** 87-90

Molinari M, Helenius A (1999) Glycoproteins form mixed disulphides with oxidoreductases during folding in living cells. *Nature* **402:** 90-93

Morais VA, Brito C, Pijak DS, Crystal AS, Fortna RR, Li T, Wong PC, Doms RW, Costa J (2006) N-glycosylation of human nicastrin is required for interaction with the lectins from the secretory pathway calnexin and ERGIC-53. *Biochim Biophys Acta* **1762:** 802-810

Müller-Loennies S, Galliciotti G, Kollmann K, Glatzel M, Braulke T (2010) A novel single chain antibody fragment for detection of mannose 6-phosphate-containing proteins: Application in mucolipidosis type II patients and mice. *Am J Pathol* **177:** 240-247

Nufer O, Kappeler F, Guldbrandsen S, Hauri HP (2003) ER export of ERGIC-53 is controlled by cooperation of targeting determinants in all three of its domains. *J Cell Sci* **116:** 4429-4440

Nyathi Y, Wilkinson BM, Pool MR (2013) Co-translational targeting and translocation of proteins to the endoplasmic reticulum. *Biochim Biophys Acta* **1833:** 2392-2402

Oliver JD, Roderick HL, Llewellyn DH, High S (1999) ERp57 functions as a subunit of specific complexes formed with the ER lectins calreticulin and calnexin. *Mol Biol Cell* **10:** 2573-2582

Parodi AJ (2000) Role of N-oligosaccharide endoplasmic reticulum processing reactions in glycoprotein folding and degradation. *Biochem J* **348 Pt 1:** 1-13

Pichler G, Leonhardt H, Rothbauer U (2012) Fluorescent protein specific Nanotraps to study protein-protein interactions and histone-tail peptide binding. *Methods Mol Biol* **911:** 475-483

Plante M, Claveau S, Lepage P, Lavoie EM, Brunet S, Roquis D, Morin C, Vezina H, Laprise C (2008) Mucolipidosis II: a single causal mutation in the N-acetylglucosamine-1-phosphotransferase gene (GNPTAB) in a French Canadian founder population. *Clin Genet* **73:** 236-244

Pohl S, Tiede S, Castrichini M, Cantz M, Gieselmann V, Braulke T (2009) Compensatory expression of human N-Acetylglucosaminyl-1-phosphotransferase subunits in mucolipidosis type III gamma. *Biochim Biophys Acta* **1792:** 221-225

Qian Y, Flanagan-Steet H, van Meel E, Steet R, Kornfeld SA (2013) The DMAP interaction domain of UDP-GlcNAc:lysosomal enzyme N-acetylglucosamine-1-phosphotransferase is a substrate recognition module. *Proc Natl Acad Sci U S A* **110:** 10246-10251

Qian Y, Lee I, Lee WS, Qian M, Kudo M, Canfield WM, Lobel P, Kornfeld S (2010) Functions of the alpha, beta, and gamma subunits of UDP-GlcNAc:lysosomal enzyme N-acetylglucosamine-1-phosphotransferase. *J Biol Chem* **285:** 3360-3370

Raas-Rothschild A, Cormier-Daire V, Bao M, Genin E, Salomon R, Brewer K, Zeigler M, Mandel H, Toth S, Roe B, Munnich A, Canfield WM (2000) Molecular basis of variant pseudo-hurler polydystrophy (mucolipidosis IIIC). *J Clin Invest* **105:** 673-681

Raas-Rothschild A, Pohl S, Braulke T (2012) Multiple enzyme deficiencies: Defects in transport: Mucolipidosis II alpha/beta; mucolipidosis III alpha/beta and mucolipidosis III gamma. In *Lysosomal storage diseases: A practical guide*, Mehta AB, Winchester B (eds), pp 121-126. Oxford: WILEY-BLACKWELL

Reitman ML, Kornfeld S (1981) UDP-N-acetylglucosamine:glycoprotein N-acetylglucosamine-1-phosphotransferase. Proposed enzyme for the phosphorylation of the high mannose oligosaccharide units of lysosomal enzymes. *J Biol Chem* **256:** 4275-4281

Robinson MS (2004) Adaptable adaptors for coated vesicles. *Trends Cell Biol* **14:** 167-174

Ruddock LW, Molinari M (2006) N-glycan processing in ER quality control. *J Cell Sci* **119:** 4373-4380

Sakai J, Nohturfft A, Goldstein JL, Brown MS (1998) Cleavage of sterol regulatory element-binding proteins (SREBPs) at site-1 requires interaction with SREBP cleavage-activating protein. Evidence from in vivo competition studies. *J Biol Chem* **273:** 5785-5793

Sato K, Nakano A (2007) Mechanisms of COPII vesicle formation and protein sorting. *FEBS Lett* **581:** 2076-2082

Schmid SL (1997) Clathrin-coated vesicle formation and protein sorting: an integrated process. *Annu Rev Biochem* **66:** 511-548

Schmittgen TD, Livak KJ (2008) Analyzing real-time PCR data by the comparative C(T) method. *Nat Protoc* **3:** 1101-1108

Schweingruber C, Rufener SC, Zund D, Yamashita A, Muhlemann O (2013) Nonsense-mediated mRNA decay - mechanisms of substrate mRNA recognition and degradation in mammalian cells. *Biochim Biophys Acta* **1829:** 612-623

Seidah NG, Mowla SJ, Hamelin J, Mamarbachi AM, Benjannet S, Toure BB, Basak A, Munzer JS, Marcinkiewicz J, Zhong M, Barale JC, Lazure C, Murphy RA, Chretien M, Marcinkiewicz M (1999) Mammalian subtilisin/kexin isozyme SKI-1: A widely expressed proprotein convertase with a unique cleavage specificity and cellular localization. *Proc Natl Acad Sci U S A* **96:** 1321-1326

Soderberg M, Lang MA (2006) Megaprimer-based methodology for deletion of a large fragment within a repetitive polypyrimidine-rich DNA. *Mol Biotechnol* **32:** 65-71

Sperisen P, Schmid CD, Bucher P, Zilian O (2005) Stealth proteins: in silico identification of a novel protein family rendering bacterial pathogens invisible to host immune defense. *PLoS Comput Biol* **1:** e63

Spranger J, Brill P, Poznanski A (2002) Bone dysplasias: an atlas of genetic disorders of the skeletal development. pp 57-79. Oxford University Press, New York

Tappino B, Chuzhanova NA, Regis S, Dardis A, Corsolini F, Stroppiano M, Tonoli E, Beccari T, Rosano C, Mucha J, Blanco M, Szlago M, Di Rocco M, Cooper DN, Filocamo M (2009) Molecular characterization of 22 novel UDP-N-acetylglucosamine-1-phosphate transferase alpha- and beta-subunit (GNPTAB) gene mutations causing mucolipidosis types IIalpha/beta and IIIalpha/beta in 46 patients. *Hum Mutat* **30:** E956-973

Tiede S, Cantz M, Raas-Rothschild A, Muschol N, Bürger F, Ullrich K, Braulke T (2004) A novel mutation in UDP-N-acetylglucosamine-1-phosphotransferase gamma subunit (GNPTAG) in two siblings with mucolipidosis type III alters a used glycosylation site. *Hum Mutat* **24:** 535

Tiede S, Cantz M, Spranger J, Braulke T (2006) Missense mutation in the N-acetylglucosamine-1-phosphotransferase gene (GNPTA) in a patient with mucolipidosis II induces changes in the size and cellular distribution of GNPTG. *Hum Mutat* **27:** 830-831

Tiede S, Muschol N, Reutter G, Cantz M, Ullrich K, Braulke T (2005a) Missense mutations in N-acetylglucosamine-1-phosphotransferase alpha/beta subunit gene in a patient with mucolipidosis III and a mild clinical phenotype. *Am J Med Genet A* **137A:** 235-240

Tiede S, Storch S, Lübke T, Henrissat B, Bargal R, Raas-Rothschild A, Braulke T (2005b) Mucolipidosis II is caused by mutations in GNPTA encoding the alpha/beta GlcNAc-1-phosphotransferase. *Nat Med* **11:** 1109-1112

Tzeng YL, Noble C, Stephens DS (2003) Genetic basis for biosynthesis of the (alpha 1-->4)-linked N-acetyl-D-glucosamine 1-phosphate capsule of Neisseria meningitidis serogroup X. *Infect Immun* **71:** 6712-6720

van Meel E, Qian Y, Kornfeld SA (2014) Mislocalization of phosphotransferase as a cause of mucolipidosis III alphabeta. *Proc Natl Acad Sci U S A* **111:** 3532-3537

Voeltz GK, Rolls MM, Rapoport TA (2002) Structural organization of the endoplasmic reticulum. *EMBO Rep* **3:** 944-950

Votsmeier C, Gallwitz D (2001) An acidic sequence of a putative yeast Golgi membrane protein binds COPII and facilitates ER export. *EMBO J* **20:** 6742-6750

Walter P, Gilmore R, Blobel G (1984) Protein translocation across the endoplasmic reticulum. *Cell* **38:** 5-8

Yoshimori T, Yamamoto A, Moriyama Y, Futai M, Tashiro Y (1991) Bafilomycin A1, a specific inhibitor of vacuolar-type H(+)-ATPase, inhibits acidification and protein degradation in lysosomes of cultured cells. *J Biol Chem* **266:** 17707-17712

Zanetti G, Pahuja KB, Studer S, Shim S, Schekman R (2012) COPII and the regulation of protein sorting in mammals. *Nat Cell Biol* **14:** 20-28

7 Publications and conference contributions

7.1 Publications

Abstract:

- Schwartz IVD, Velho RV, Sperb-Ludwig F, **De Pace R**, Taciane A, Ludwig NF, Lourenc CM, Braulke T, Pohl S (2014) Genotype-phenotype correlation in mucolipidosis III alpha/beta: A comprehensive study of a Brazilian patient exhibiting novel *GNPTAB* mutations. *Journal of Inborn Errors of Metabolism & Screening* 2, 1158, p.45

Research article:

- **De Pace R**, Coutinho MF, Koch-Nolte F, Haag F, Prata MJ, Alves S, Braulke T, Pohl S (2014) Mucolipidosis II-related mutations inhibit the exit from the endoplasmic reticulum and proteolytic cleavage of GlcNAc-1-phosphotransferase precursor protein (GNPTAB). *Human Mutation* 35: 368-376

7.2 Conference contributions

7.2.1 Oral presentations

- **De Pace R.** Subunit interactions of the Golgi-resident GlcNAc-1-phosphotransferase,
  Retreat of the Research Training Group 1459, 25.-27.10.2012, Wedel, Germany
- **De Pace R.** Interactions between subunits of the Golgi-resident GlcNAc-1-phosphotransferase complex and analysis of mucolipidosis type II patient mutations, ESGLD (European Study Group on Lysosomal Diseases) workshop, 25.-29.09.2013, Leibnitz, Austria
- **De Pace R.** Mucolipidosis Type II- and III-related mutations: New findings about the localization and proteolytic activation of mutant GlcNAc-1-phosphotransferase precursor protein (GNPTAB), Annual Conference of the Working Group for Paediatric disturbances, 05.-07.03.2014, Fulda, Germany (Young Scientist's Award)

- **De Pace R**. Structural requirements of the Golgi-resident GlcNAc-1-phosphotransferase complex for subunits assembly and analysis of mucolipidosis type II patient mutations, Retreat of the Research Training Group 1459, 09.-11.10.2014, Hohwacht, Germany

7.2.2 Poster presentations

- Encarnação M, **De Pace R**, Braulke T, Pohl S. Structural requirements of the γ-subunit for assembly and intracellular transport of the GlcNAc-1-phosphotransferase,
  Renewal Proposal for the Research Training Group 1459, 16.-17.11.2011, Hamburg, Germany
- **De Pace R**, Braulke T, Pohl S. Subunit interactions of the Golgi-resident GlcNAc-1-phosphotransferase,
  2nd International Symposium of the Research Training Group 1459 "Protein trafficking in health and disease", 26.-28.09.2012, Hamburg, Germany
- **De Pace R**, Braulke T, Pohl S. Interactions between subunits of the Golgi-resident GlcNAc-1-phosphotransferase complex,
  International Joint Meeting of the German Society for Cell Biology (DGZ) and the German Society for Developmental Biology (GfE), 20.-23.03.2013, Heidelberg, Germany
- **De Pace R**, Franke M, Pohl S, Storch S, Braulke T. Structural requirements for the ER export of the GlcNAc-1-phosphotransferase alpha/beta precursor protein,
  2nd UKE Microscopy (UMIF) Symposium, 23.-24.04.2014, Hamburg, Germany
- **De Pace R**, Velho RV, Braulke T, Pohl S. Structural requirements of the Golgi-resident GlcNAc-1-phosphotransferase complex for subunits assembly and analysis of mucolipidosis type II patient mutations,
  3rd International Symposium of the Research Training Group 1459 "Protein trafficking in health and disease", 10.-12.09.2014, Hamburg, Germany
- Franke M, **De Pace R**, Storch S, Pohl S, Braulke T. Turnover of the Golgi-resident GlcNAc-1-phosphotransferase
  3rd International Symposium of the Research Training Group 1459 "Protein trafficking in health and disease", 10.-12.09.2014, Hamburg, Germany

7.2.3 Conference (attendance only)

- International Symposium “Lysosomes“, 29.09.- 01.10.2011, Hamburg, Germany
- ESGLD (European Study Group on Lysosomal Diseases) graduate course, 25.-29.09.2013, Leibnitz, Austria

8 Abbreviations

× g	times gravity
aa	amino acid
Acp2	acid phosphatase 2
Acp5	acid phosphatase 5
ACTB	β-actin gene
APS	ammonium peroxydisulfate
ATP	adenosine triphosphate
BafA1	bafilomycin A1
BIP	binding immunoglobulin protein
bp	base pairs
BSA	bovine serum albumin
cDNA	complementary DNA
CNX	calnexin
COP	coat protein
CRT	calreticulin
C-terminal	carboxy-terminal
DAPI	4',6-diamidino-2-phenylindole
dH_2O	destillated water
DMAP	DNA methyltransferase 1 associated protein 1
DMEM	Dulbecco's modified Eagle's medium
DMSO	dimethylsulfoxide
DNA	deoxyribonucleic acid
dNTP	deoxynucleoside triphosphate
DTT	dithiothreitol
DUF3184	domain of unknown function 3184
E. coli	*Escherichia coli*
e.g.	for example
ECL	enhanced chemiluminescence
EDTA	ethylenediaminetetraacetic acid
ER	endoplasmic reticulum
ERAD	ER-associated degradation
ERGIC	ER-Golgi intermediate compartment
Erp57	ER protein 57
et al	and others
FCS	fetal calf serum
Fig	figure
for	forward
GFP	green fluorescent protein
Glc	glucose
GlcNAc	N-acetylglucosamin
GM130	Golgi matrix protein 130
GNPTAB	GlcNAc-1-phosphotransferase, α/β-subunit precursor gene
GNPTG	GlcNAc-1-phosphate transferase, γ-subunit gene
HA	hemagglutinin
HEK293	human embryonic kidney cell line 293

HeLa	human cell line from cervical cancer (Henrietta Lacks)
HRP	horseradish peroxidase
IF	immunofluorescence microscopy
IgG	immunoglobulin G
IP	immunoprecipitation
LAMP1	lysosomal-associated membrane protein 1
LB	lysogeny broth
LIMP-2	lysosome membrane protein 2
M6P	mannose 6-phosphate
Man	mannose
MIM	mendelian inheritance in man
ML	mucolipidosis
MPR	mannose 6-phosphate receptor
mRNA	messenger RNA
N-terminal	amino-terminal
OD	optical density
PAGE	polyacrylamide gelelectrophoresis
PBS	Phosphate-buffered saline
PCR	polymerase chain reaction
PDI	protein disulfide isomerase
PFA	paraformaldehyde
PNGase F	peptide *N*-glycosidase F
PPO	2,5-diphenyloxazole
PT	GlcNAc-1-phosphotransferase
rev	reverse
RNA	ribonucleic acid
RT	room temperature
S1P	site-1 protease
SDS	sodium dodecyl sulfate
siRNA	small interfering RNA
SRP	signal recognition particle
TAE	tris-acetate-ethylenediaminetetraacetic acid
Taq	*Thermus aquaticus*
TBS	tris-buffered saline
TBST	tris-buffered saline/tween 20
TEMED	NNN'N'-tetramethylethylenediamine
TGN	trans-Golgi network
TM	transmembrane
Tris	tris-hydroxymethyl-aminomethane
U	units
UCE	uncovering enzyme
UDP	uridine diphosphate
UKE	University Medical Center Hamburg-Eppendorf
UV	ultraviolet
WB	western blotting
WT	wild-type
β-hex	β-hexosaminidase

One and three letter symbols for amino acids		
Alanine	A	Ala
Arginine	R	Arg
Asparagine	N	Asn
Aspartate	D	Asp
Cysteine	C	Cys
Glutamate	E	Gln
Glutamine	Q	Glu
Glycine	G	Gly
Histidine	H	His
Isoleucine	I	Ile
Leucine	L	Leu
Lysine	K	Lys
Methionine	M	Met
Phenylalanine	F	Phe
Proline	P	Pro
Serine	S	Ser
Threonine	T	Thr
Tryptophan	W	Trp
Tyrosine	Y	Tyr
Valine	V	Val

9 Acknowledgement

This doctoral thesis is based upon studies conducted during October 2011 to December 2014 at the Department of Biochemistry, Children's Hospital, UKE, Germany. I would like to thank Prof. Dr. Thomas Braulke and Prof. Dr. Matthias Kneussel for evaluating this dissertation.

During my time spent at the laboratory of Thomas Braulke, I've grown enormously as a person and as a scientist. I am grateful to my thesis advisor for his guidance and support: Thomas, your suggestions and advice improved my research skills and prepared me for future challenges. Your supervision of the Research Training Group gave me many opportunities to interact with top class researchers in the field of protein trafficking from all over the world, professionally, with our special students' talks, but also informally with our afterwards sudents' dinners. Thank you for pushing to never be lazy ("run, don't walk") an "please make questions!". Thank to this I grew a more mature attitude.

I would like to express my sincere gratitude to Dr. Sandra Pohl: Sandra, your advice and support are priceless, you always have time for my questions an give me great help in each single step of this PhD period. Without this I would have get lost many times. Your experienced and practical point of view always brings me to satisfying results. Thanks to the GRK1459 and DFG for the funding support and to all PIs and colleagues for the useful retreats, lectures and practical courses. I'm thankful to Prof. Dr. Peter Walter for my internship period in his lab for three months at the UCSF, California.

I am very thankful to Dr. Mine Franke for the important suggestions and contribution for the phosphotransferase degradation part of this thesis. A special thank goes to Renata Voltolini Velho, she cloned and analysed the Brazilian patients mutations and helped me to establish the phosphotransferase activity assay. I would like to thank also Francisca Coutinho for collaborating in the analysis of some patient mutations. The discussions with PD Dr. Stephan Storch were also of great benefit to my studies. Thank you Johannes for your constant help, Georgia for your suggestions (grazie!), thank to (piccola) Sarah, Jessica, Carolin, Laura, Sandra M. You have been my colleagues during this period, but most important you have been my friends.

It is important to thank my beloved family and husband Francesco, your personal support especially in the "moody" moments was extremely helpful.

Declaration on oath

I hereby declare, on oath, that I have written the present dissertation by my own and have not used other than the acknowledged resources and aids.

De Pace Raffaella

City and date

HAMBURG
12.3.15

Signature

Me, Harry Byers , born in London, United Kingdom , native English speaker, after reading the present thesis with the title "Structural requirements for transport and subunit interactions of the GlcNAc-1-phosphotransferase complex" hereby confirm the linguistic accuracy of the present dissertation.

Signature: 

Date: 29. 09. 2014